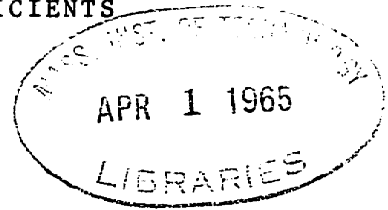


GENERALIZED INTERACTION COEFFICIENTS

by

CLAUDE HENRI PAUL LUPIS



Licencié ès Sciences, University of Paris (1959)
Diplomé de l'Institut d'Administration des Entreprises, Paris (1960)
Ingenieur Civil des Mines,
Ecole Nationale Supérieure des Mines de Paris (1961)

Submitted in partial fulfillment of the requirements

for the degree of

DOCTOR OF SCIENCE

at the

Massachusetts Institute of Technology

January, 1965

Signature of Author
Department of Metallurgy

Signature of Professor
in Charge of Research

Signature of Chairman of
Departmental Committee
on Graduate Students

ABSTRACT

GENERALIZED INTERACTION COEFFICIENTS

by

CLAUDE HENRI PAUL LUPIS

Submitted to the Department of Metallurgy on January 11, 1965 in partial fulfillment of the requirements for the degree of Doctor of Science.

The concept of interaction coefficients is generalized to apply to the enthalpy and entropy functions, as well as to the free energy function, and to cover terms of different orders in the expansion of these functions in Taylor's series. The use of a second order free energy interaction coefficient is particularly emphasized. Relationships between various interaction coefficients are developed, and a method to combine activity data in a multi-component system is proposed.

The application of the "quasi-chemical" model to liquid metallic solutions is critically reviewed, and the second order free energy interaction coefficient calculated and compared with experimental data. A new model is outlined. Its simplest form introduces the "first quasi-regular" solution, a one parameter model (for a binary system) which takes into account the contribution of the vibrational entropy. The model also explains some discrepancies in the predictions of the quasi-chemical theory.

The solubility of oxygen in liquid silver is determined as a function of temperature and pressure, and a small deviation from Sievert's law observed. The solubility is increased by copper and decreased by gold, platinum and palladium. Free energy, enthalpy and entropy interaction coefficients are calculated and correlated with the statistical models.

Thesis Supervisor:

John F. Elliott
Professor of Metallurgy

TABLE OF CONTENTS

<u>Chapter Number</u>		<u>Page Number</u>
	ABSTRACT	ii
	TABLE OF CONTENTS	iii
	LIST OF FIGURES	vii
	LIST OF TABLES	ix
	ACKNOWLEDGMENTS	xi
I	INTRODUCTION	1
II	OUTLINE OF THE THEORETICAL STUDY	2
III	GENERALIZED INTERACTION COEFFICIENTS	4
	1. Definition of the Generalized Free Energy Interaction Coefficients	4
	2. Relations between Interaction Coeffi- cients; Application to a Ternary System ..	5
	3. The Second Order Free Energy Interaction Coefficient	8
	4. Discussion of Sherman and Chipman's Method; Presentation of an Alternate Method	17
	5. Definition of the Generalized Enthalpy and Entropy Interaction Coefficients	24
	6. Conclusions	30
IV	THE QUASI-CHEMICAL MODEL	31
	1. Introduction	31
	2. Assumptions	31
	3. Binary System	33
	3.1 Regular Solution	35
	3.2 Quasi-Chemical Solution	36
	4. Ternary System	45
	4.1 Regular Solution	45
	4.2 Quasi-Chemical Solution	46
	5. First Order Free Energy Interaction Coefficient	46
	6. Second Order Free Energy Interaction Coefficient	49
	6.1 The Quasi-Chemical Expression	49
	6.2 Comparison with Experimental Results	53
	6.2.1 Sulfur in liquid iron alloys .	54
	6.2.2 Oxygen in liquid iron alloys .	56
	6.2.3 Nitrogen in liquid iron alloys	56

<u>Chapter Number</u>		<u>Page Number</u>
	6.2.4 Carbon in liquid iron alloys	57
	6.2.5 Hydrogen in liquid Iron alloys	57
	6.3 Conclusions	58
7.	Summary and Conclusions	58
V	THE CELL MODEL	60
	1. Introduction	60
	2. Partition Function of a Binary Solution	61
	3. Free Volume	62
	4. Probabilities Associated with Different Configurations	64
	5. Excess Enthalpy and Vibrational Entropy	66
	5.1 Excess Enthalpy	66
	5.2 The Excess Vibrational Entropy ...	67
	6. Quasi-Regular Solutions	69
	7. Correlation between Excess Enthalpy and Excess Entropy	73
	8. The Proportionality Constant τ	80
	9. Conclusions	83
VI	CONCLUSIONS ON THE THEORETICAL WORK	85
VII	OUTLINE OF EXPERIMENTAL WORK	87
VIII	LITERATURE SURVEY	88
	1. Solubility of Oxygen in Solid Silver ...	88
	2. Solubility of Oxygen in Liquid Silver ..	89
IX	APPARATUS, MATERIALS AND EXPERIMENTAL PROCEDURE	92
	1. Sieverts' Apparatus	92
	1.1 Gas Purification Trains	92
	1.2 Vacuum System	92
	1.3 Measuring Instruments	95
	1.4 Heating Unit	96
	1.5 Reaction Chamber	96
	1.6 Refractories	96
	1.7 Device for Dropping Alloying Additions	98
	2. Materials	98
	3. Experimental Procedure	101
X	THERMODYNAMICS OF GAS SOLUBILITIES AND CALCULATIONS	104
	1. Thermodynamics of Gas Solubilities	104
	2. Practical Method of Calculation	108

<u>Chapter Number</u>		<u>Page Number</u>
XI	PRESENTATION AND ANALYSIS OF RESULTS	110
	1. Determination of the Origin for the Oxygen Concentration in the Melt	110
	1.1 Experimental Difficulties	110
	1.2 Theoretical Determination of Y_0	112
	2. Solubility of Oxygen in Liquid Silver ...	116
	2.1 The Self-Interaction Coefficient of Oxygen	116
	2.2 Free Energy, Enthalpy and Entropy ..	120
	2.3 Self-Interaction Enthalpy and Entropy Coefficients of Oxygen	122
	2.4 Summary of the Thermodynamic Properties of the Solubility of Oxygen in Liquid Silver	123
	3. Solubility of Oxygen in Liquid Silver- Gold Alloys	124
	4. Solubility of Oxygen in Liquid Silver- Platinum Alloys	126
	5. Solubility of Oxygen in Liquid Silver- Palladium Alloys	128
	6. Solubility of Oxygen in Liquid Silver- Copper Alloys	128
XII	DISCUSSION OF ERRORS AND CONCLUSIONS ON EXPERIMENTAL WORK	136
	1. Systematic Errors	136
	1.1 Hot Volume	136
	1.2 Vaporization of the Silver	138
	1.3 Impurities in the Melt	138
	2. Random Errors	139
	3. Conclusions on Experimental Work	141
XIII	CORRELATION BETWEEN THE EXPERIMENTAL RESULTS AND THE THEORETICAL MODELS	144
XIV	SUMMARY AND CONCLUSIONS	148
XV	SUGGESTIONS FOR FURTHER WORK	150
	REFERENCES	151

<u>Appendix Number</u>		<u>Page Number</u>
A	GENERALIZED INTERACTION COEFFICIENTS - SUMMARY	154
B	RECIPROCAL RELATIONSHIPS BETWEEN GENERAL- IZED INTERACTION COEFFICIENTS	158
C	CONVERSION RELATIONSHIP BETWEEN THE INTERACTION COEFFICIENTS ϵ , ρ AND e , r	161
D	CALCULATIONS OF THE QUASI-CHEMICAL MODEL ..	169
E	IDENTIFICATION OF THE EXPERIMENTAL POINTS IN FIG. IV.1	176
F	CALCULATION OF THE "FREE VOLUME"	178
G	IDENTIFICATION OF THE EXPERIMENTAL POINTS IN FIG. V.1	182
H	EXPERIMENTAL DATA	185
	BIOGRAPHICAL NOTE	215

LIST OF FIGURES

<u>FIGURE NUMBER</u>		<u>PAGE NUMBER</u>
III.1	First and Second Order Free Energy Interaction Coefficients	10
III.2	Evaluation of the Second Order Interaction Coefficient $\rho_2^{(2,3)}$	13
III.3	Possible Estimates of the Second Order Interaction Coefficients $\rho_3^{(2,4)}$ and $\rho_2^{(3,4)}$	15
III.4	Sherman and Chipman's Method	18
III.5	Construction of the Term $\rho_2^{(i,j)} X_i X_j$ in the Alternate Method	22
IV.1	Test of the Quasi-Chemical Model on Various Binary Alloys	38
IV.2	Test of the Quasi-Chemical Model for the Sn-Cd System at 500°C	44
IV.3	Curvatures Predicted by the Quasi-Chemical Model	51
V.1	Correlation between Excess Enthalpy and Entropy	81
IX.1	The Sieverts' Apparatus	93
IX.2	The Reaction Chamber	97
IX.3	Additions Reservoir	99
XI.1	Self-Interaction of Oxygen in Silver ...	113
XI.2	Determination of the Origin for the Oxygen Concentration in the Melt	115
XI.3	The Silver-Oxygen System	121
XI.4	Effect of Gold on the Activity Coefficient of Oxygen in Silver	125
XI.5	Effect of Platinum on the Activity Coeffi- cient of Oxygen in Liquid Silver	127

List of Figures, Continued..

<u>FIGURE NUMBER</u>		<u>PAGE NUMBER</u>
XI.6	Effect of Palladium on the Activity Coefficient of Oxygen in Silver	129
XI.7	Effect of Copper on the Activity Coefficient of Oxygen in Liquid Silver	130
XI.8	Effect of Copper on Oxygen in Liquid Silver-Palladium Alloys	132
XI.9	Effect of Copper on Oxygen in Liquid Silver-Platinum Alloys	133
XII.1	"Hot Volume" Study	137
XII.2	Effect of Alloying Elements on the Activity Coefficient of Oxygen in Liquid Silver at 1060°C	143
F.1	Cell Geometry for the "Free Volume" Model	179

LIST OF TABLES

<u>Table Number</u>		<u>Page Number</u>
IV.1	Theoretical Explanation of Some Discrepancies Observed in the Application of Eq. IV.19.....	42
IV.2	Calculated and Experimental Values of the First Order Interaction Coefficient ϵ	48
IV.3	Predicted Values of $\rho_2^{(3)}$ by the Quasi-Chemical Model	52
IV.4	Experimental and Calculated Values of the Second Order Interaction Coefficient ρ_2^3 in Liquid Iron Alloys	55
V.1	Calculated Values of τ in Some Ternary Alloys	83
VIII.1	Sieverts and Hagenacker's Data for The Solubility of Oxygen in Liquid Silver	90
IX.1	Materials Characteristics	100
XI.1	Self-Interaction Coefficient of Oxygen $e_0^{(0)}$ in Liquid Silver	117
XI.2	Dissolution of Oxygen in Liquid Silver: The Reaction Constant K' and the Enthalpy ΔH	118
XI.3	Interaction Coefficients of Gold on Oxygen in Liquid Silver	124
XI.4	Interaction Coefficients of Platinum on Oxygen in Liquid Silver	126
XI.5	Interaction Coefficients of Palladium on Oxygen in Liquid Silver	128
XI.6	Experimental Data on the First Order Free Energy and Enthalpy Interaction Coefficients	134
XI.7	Interaction Coefficients of Copper on Oxygen in Liquid Silver	135

<u>Table Number</u>		<u>Page Number</u>
XII.1	Interaction Coefficients of Various Elements on Oxygen in Liquid Silver	142
XIII.1	Comparison of the Effects of Gold and Platinum on Sulfur in Copper and Oxygen in Silver	144
C.1	Conversion Relationship between the Interaction Coefficients ϵ , ρ and e , r	161
C.2	Interaction Coefficients $\epsilon_i^{(j)}$ for Dilute Solutions of Elements Dissolved in Liquid Iron at 1600°C	165
	Interaction Coefficients $e_i^{(j)} \times 10^2$ for Dilute Solutions of Elements Dissolved in Liquid Iron at 1600°C	167
E.1	Identification of the Experimental Points in Fig. IV.1	176
G.1	Identification of the Experimental Points in Fig. V.1	178

ACKNOWLEDGMENTS

The author wishes to express his sincere appreciation
to:

Professor John F. Elliott for his invaluable guidance
and support throughout this program;

Professor Harold Freeman for his precious advice;

Professor John Chipman for his fruitful discussions
and interest in this work;

To other members of the faculty at the Massachusetts
Institute of Technology, particularly to Professors V. Ramakrishna
and T.R. Meadowcroft for their encouragement;

To Mr. Donald L. Guernsey and his assistants for the
chemical analyses;

To Mr. George Prince, Glassblower, and Mr. Walter
Correia for numerous friendly services;

To Mr. Frank Woolley for many valuable suggestions and
his ever-present help;

To the graduate students and members of the staff at
the Massachusetts Institute of Technology, in particular to Mr.
Alain Boyer, Mr. Albert Solbes and Dr. Michel Turpin;

To Miss Cathy Walsh for her unselfish help in the
preparation of this manuscript, and the introduction of many
commas;

To the members of the M.I.T. Computation Center for
their assistance in carrying out the computations;

To the National Science Foundation for their support,
under Contract GP-2294 and G-2294;

To the Atomic Energy Commission for their support,
under Contract At(30-1)-1888.

CHAPTER I INTRODUCTION

To progress in the understanding of the properties of liquid metallic solutions, our aim should be to obtain more experimental data, as well as to develop better theoretical models to satisfactorily explain these data. In the pursuit of these goals, classical thermodynamics constitute the unifying and convenient language. A good vocabulary is needed and, in this study, a modest attempt is made to improve it.

Among the many statistical mechanics models which may describe liquid metallic solutions, a special preference is shown for those which have the most general applications and introduce the minimum number of parameters, so that, in the comparison between experimental and statistical results, no artificial agreement may hide a theoretical inadequacy.

Finally, the lack of really precise data on oxygen in liquid silver, and the experimental possibility of determining the effects of various alloying elements on the free energy, enthalpy and entropy of this system, have prompted an investigation of the solubility of oxygen in liquid silver alloys.

CHAPTER II
OUTLINE OF THE THEORETICAL STUDY

The concept of activity and activity coefficient has proved its usefulness. In a multicomponent system, the study of an activity coefficient is a complex problem, and Wagner's⁽¹⁾ definition of the interaction coefficient ϵ is, in the next Chapter, the starting point of a possible treatment of this problem. And, as statistical thermodynamics is the natural associate of classical thermodynamics, the development of a statistical model to describe the thermodynamic properties of liquid metallic solutions is, at present, attempted mainly by two distinct approaches. The first is based on the free electron theory of metals and describes the thermodynamic properties of a solution in terms of changes occurring in the energies of the conduction electrons.^(2,3) The second refers to the chemical theory and describes these properties in terms of atomic bonding energies.

The use of an electron theory has lead Himmler,⁽⁴⁾ for example, to show that data on the solubility of hydrogen in solid copper alloys can be qualitatively accounted for in terms of the chemical potential of the free electrons alone. However, neglect of the interaction of the ion cores has already been shown by Wagner⁽³⁾ to be unacceptable, in the case of some ternary systems, and it is believed⁽⁵⁾ that, as the theory becomes more refined, it will resemble the chemical theory more and more.

The main advantage of the chemical theory is that it offers a simple description and appreciation of the thermodynamic

properties of a system. It has been used with fair success for dilute metallic solutions by Alcock and Richardson⁽⁶⁾ and Durand.⁽⁷⁾ However, some notable breakdowns⁽⁸⁾ point out the serious discrepancies brought to the model by two assumptions: the neglect of non-configurational factors and the consideration that the bonding energy between two neighboring atoms is independent of their surroundings. Yet, it should be emphasized that the very inadequacy of a model to a particular system often brings light to the physical phenomenon which is responsible for this inadequacy. Chapter IV explores the possibilities and limitations of the chemical models, whereas Chapter V presents the cell model,^(9,10) and a possible adaptation of this model to retain the advantages of the chemical theory while removing its most critical assumptions.

CHAPTER III
GENERALIZED INTERACTION COEFFICIENTS

Classical thermodynamics offers a convenient way to set on a rigorous foundation and to express precisely many empirical notions and experimental data. For instance, the effect of a solute (2) on another solute (3) in a dilute ternary system has advantageously been represented by the interaction coefficient $\epsilon_3^{(2)} = \left(\frac{\partial \ln \gamma_3}{\partial X_2} \right)_{X_1 \rightarrow 1}$ and a formal thermodynamic treatment allowed Wagner⁽¹⁾ to show that $\epsilon_3^{(2)} = \epsilon_2^{(3)}$. In this discussion, the relevant relationships are developed for multicomponent systems.

1. Definition of the Generalized Free Energy Interaction Coefficients

Given a solution where (1) is the solvent, and (2), ... (j), ... (m), the solutes, the excess free energy is expanded in a Taylor's series with respect to the mole fractions of the solute $X_2, \dots, X_j, \dots, X_m$... near the state of infinite dilution ($X_2, \dots, X_j, \dots, X_m \rightarrow 0$).

$$F^E = RT \sum_{n_2} \dots \sum_{n_j} \dots \sum_{n_m} \phi_{n_2 \dots n_j \dots n_m} X_2^{n_2} \dots X_j^{n_j} \dots X_m^{n_m} \quad (\text{III.1})$$

where the index j can take any value from 2 to m, and the subscript n_j any positive integer value including 0. By the very nature of a Taylor's series, the coefficient ϕ is defined as follows:

$$RT \phi_{n_2 \dots n_j \dots n_m} = \frac{1}{n_2! \dots n_j! \dots n_m!} \left(\frac{\partial^{n_2 + \dots + n_j + \dots + n_m} F^E}{\partial X_2^{n_2} \dots \partial X_j^{n_j} \dots \partial X_m^{n_m}} \right)_{X_1 \rightarrow 1} \quad (\text{III.2})$$

Similarly the natural logarithm of the activity coefficient of element

(1) is expressed as:

$$\ln \gamma_1 = \sum_{n_2} \dots \sum_{n_j} \dots \sum_{n_m} K_{n_2 \dots n_j \dots n_m}^{(1)} X_2^{n_2} \dots X_j^{n_j} \dots X_m^{n_m} \quad (\text{III.3})$$

where

$$K_{n_2 \dots n_j \dots n_m}^{(1)} = \frac{1}{n_2! \dots n_j! \dots n_m!} \left(\frac{\partial^{n_2 + \dots + n_j + \dots + n_m} \ln \gamma_1}{\partial X_2^{n_2} \dots \partial X_j^{n_j} \dots \partial X_m^{n_m}} \right)_{X_1 \rightarrow 1} \quad (\text{III.4})$$

We propose to call $K_{n_2 \dots n_j \dots n_m}^{(1)}$ with $n = \sum_{j=2}^m n_j$ a free energy

interaction coefficient of order n. The interest of this definition will hopefully become clearer as we proceed to the following sections.

2. Relations Between Interactions Coefficients. Application to a Ternary System

The excess free energy is equal to:

$$F^E = RT (X_1 \ln \gamma_1 + X_2 \ln \gamma_2 + \dots + X_j \ln \gamma_j + \dots + X_m \ln \gamma_m) \quad (\text{III.5})$$

The Gibbs-Duhem differential equation yields a system of (m-1) equations:

$$(1 - X_2 - \dots - X_j - \dots - X_m) \frac{\partial \ln \gamma_1}{\partial X_k} + X_2 \frac{\partial \ln \gamma_2}{\partial X_k} + \dots + X_j \frac{\partial \ln \gamma_j}{\partial X_k} + \dots + X_m \frac{\partial \ln \gamma_m}{\partial X_k} = 0 \quad (k = 2, \dots, j, \dots, m) \quad (\text{III.6})$$

Since $X_2, \dots, X_j, \dots, X_m$ are independent variables, and the (m-1) Equations (III.6) above are identities, the factor multiplying the general term in $X_2^{n_2} \dots X_j^{n_j} \dots X_m^{n_m}$ must be null in each equation. The details of the calculations are given in Appendix B. The results are summarized in the following two general formulae:

$$e_{n_2 \dots n_j \dots n_m} = - \frac{K_{n_2 \dots n_j \dots n_m}^{(1)}}{\binom{m}{\sum_{j=2}^m n_j} - 1} \quad (\text{III.7})$$

and

$$K_{n_2 \dots n_i \dots n_m}^{(1)} = K_{n_2 \dots n_1 \dots n_m}^{(1)} - \frac{n_i + 1}{\sum_{j=2}^m n_j} K_{n_2 \dots, n_i+1, \dots n_m}^{(1)} \quad (\text{III.8})$$

from which are derived many familiar results.

For convenience, Equation (III.8) is rewritten for a ternary solution:

$$K_{n_2, n_3}^{(2)} = K_{n_2, n_3}^{(1)} - \frac{n_2+1}{n_2+n_3} K_{n_2+1, n_3}^{(1)} \quad (\text{III.8a})$$

$$K_{n_2, n_3}^{(3)} = K_{n_2, n_3}^{(1)} - \frac{n_3+1}{n_2+n_3} K_{n_2, n_3+1}^{(1)} \quad (\text{III.8b})$$

For $n_2 = 0, n_3 = 0$, Equation (III.8a) yields: $K_{0,0}^{(2)} = K_{0,0}^{(1)} - \frac{1}{0} K_{1,0}^{(1)}$

The first two terms are finite: $K_{0,0}^{(2)} = \ln v_2^0$ and $K_{0,0}^{(1)} = 0$

since $\ln v_1 = 0$ at $X_1 = 1$.

Thus $K_{1,0}^{(1)} = 0$. Similarly $K_{0,1}^{(1)} = 0$ (by Equation (III.8b)).

Consequently, there is no term of the first order in X_2 or X_3 alone, in the expansion of $\ln v_1$

$$\ln v_1 = K_{2,0}^{(1)} X_2^2 + K_{0,2}^{(1)} X_3^2 + K_{1,1}^{(1)} X_2 X_3 + \dots \quad (\text{III.9})$$

For $n_2 = 1, n_3 = 0$, Equation (III.8a) yields:

$$K_{1,0}^{(2)} = K_{1,0}^{(1)} - 2 K_{2,0}^{(1)} = -2 K_{2,0}^{(1)}$$

(relation which involves only terms of the binary 1, 2).

But

$$K_{1,0}^{(2)} = \left(\frac{\partial \ln v_2}{\partial X_2} \right)_{X_1=1} = e_2^{(2)}$$

and $K_{2,0}^{(1)}$ is the first term in the expansion of the α_1 function: $\frac{\ln \gamma_1}{X_2^2}$ or $\frac{\ln \gamma_1}{(1-X_1)^2}$, in a binary solution. Hence:

$$\epsilon_2^{(2)} = -2(\alpha_1)_{X_2 \rightarrow 0} \quad (\text{III.10})$$

It is also useful to note that in any multicomponent system, the function

$\alpha_2 = \frac{\ln \gamma_2}{(1-X_2)^2}$ yields:

$$(\alpha_2)_{X_1 \rightarrow 1} = \ln \gamma_2^0 \quad (\text{III.11})$$

and as

$$\frac{\partial \alpha_2}{\partial X_2} = \frac{1}{(1-X_2)^2} \left\{ \frac{\partial \ln \gamma_2}{\partial X_2} + \frac{2}{1-X_2} \ln \gamma_2 \right\}$$

Then

$$\left(\frac{\partial \alpha_2}{\partial X_2} \right)_{X_1 \rightarrow 1} = \epsilon_{2,2} + 2 \ln \gamma_2^0$$

or:

$$\epsilon_{2,2} = \left(\frac{\partial \alpha_2}{\partial X_2} - 2 \alpha_2 \right)_{X_1 \rightarrow 1} \quad (\text{III.12a})$$

In a binary, this may be rewritten:

$$\left(\frac{\partial \alpha_2}{\partial X_2} \right)_{X_2 \rightarrow 0} = 2(\alpha_2 - \alpha_1)_{X_2 \rightarrow 0} \quad (\text{III.12b})$$

For $n_2 = 0$, $n_3 = 1$, Equations (III.8a) and (III.7) yield:

$$K_{0,1}^{(2)} = -K_{1,1}^{(1)} = \phi_{1,1}$$

or

$$\epsilon_2^{(3)} = \left(\frac{\partial \ln \gamma_2}{\partial X_3} \right)_{X_1 \rightarrow 1} = - \left(\frac{\partial^2 \ln \gamma_1}{\partial X_2 \partial X_3} \right)_{X_1 \rightarrow 1} = \frac{1}{RT} \left(\frac{\partial^2 F^E}{\partial X_2 \partial X_3} \right)_{X_1 \rightarrow 1} \quad (\text{III.13})$$

Because of the symmetry of the result (or through Equation (III.8) with $n_2 = 1$, $n_3 = 0$), Wagner's relation⁽¹⁾ is established: $\epsilon_2^{(3)} = \epsilon_3^{(2)}$

It seems often desirable to keep the symmetry of the result by rewriting $\epsilon_2^{(3)}$ and $\epsilon_3^{(2)}$ as $\epsilon_{2,3}$. Similarly, we shall set $\epsilon_2^{(2)} = \epsilon_{2,2}$ and $\epsilon_3^{(3)} = \epsilon_{3,3}$.

At this point, a few of the above results are summarized by rewriting Equations (III.1 and III.3) for a ternary:

$$\frac{F^E}{RT} = X_2 \ln \gamma_2^0 + X_3 \ln \gamma_3^0 + \frac{1}{2} \epsilon_{2,2} X_2^2 + \frac{1}{2} \epsilon_{3,3} X_3^2 + \epsilon_{2,3} X_2 X_3 + \dots$$

$$- \frac{K_{n_2, n_3}^{(1)}}{(n_2 + n_3 - 1)} X_2^{n_2} X_3^{n_3} + \dots \quad (\text{III.14})$$

$$\ln \gamma_i = -\frac{1}{2} \epsilon_{2,2} X_2^2 - \frac{1}{2} \epsilon_{3,3} X_3^2 - \epsilon_{2,3} X_2 X_3 + \dots + K_{n_2, n_3}^{(1)} X_2^{n_2} X_3^{n_3} + \dots \quad (\text{III.15a})$$

$$\ln \gamma_2 = \ln \gamma_2^0 + \epsilon_{2,2} X_2 + \epsilon_{2,3} X_3 + \dots$$

$$+ \left\{ K_{n_2, n_3}^{(1)} - \frac{n_2 + 1}{n_2 + n_3} K_{n_2 + 1, n_3}^{(1)} \right\} X_2^{n_2} X_3^{n_3} + \dots \quad (\text{III.15b})$$

$$\ln \gamma_3 = \ln \gamma_3^0 + \epsilon_{2,3} X_2 + \epsilon_{3,3} X_3 + \dots$$

$$+ \left\{ K_{n_2, n_3}^{(1)} - \frac{n_3 + 1}{n_2 + n_3} K_{n_2, n_3 + 1}^{(1)} \right\} X_2^{n_2} X_3^{n_3} + \dots \quad (\text{III.15c})$$

3. The Second Order Free Energy Interaction Coefficient

In the literature, all the emphasis, understandingly, has been put on the first order coefficients (ϵ), but as our needs for greater accuracy grow rapidly, the second order coefficients become increasingly important. We shall give the general symbol of ρ to these second order coefficients. They involve only binary, ternary, or quaternary systems. In the binary, $K_{2,0}^{(2)}$ becomes $\rho_2^{(2)}$; in the ternary $K_{0,2}^{(2)} = \rho_2^{(3)}$ and $K_{1,1}^{(2)} = \rho_2^{(2,3)}$; in the quaternary $K_{0,1,1}^{(2)} = \rho_2^{(3,4)}$.

Consider a system in which one component (2) remains very dilute. We are interested in knowing how small additions of another component (3) changes its behavior in the solvent (1). This is for instance the problem of the effect of alloying elements (Al, Si, C, Cr, Mn ..) on the solubility of gases (H₂, N₂, O₂) or on the activity of other metalloids (S, P, C ..) in iron. In these cases, the reference state is usually infinite dilution and $\ln(\gamma_2/\gamma_2^0)$ is of more interest than $\ln\gamma_2$. For gases, as X₂ is usually very small (order of magnitude: 10⁻³), the terms in X₂ are also small and can often be neglected. It is then said that the gas follows "Sieverts' law."

Again for convenience, let $\psi_2 = \gamma_2/\gamma_2^0$. Then:

$$\left(\ln\psi_2\right)_{X_2 \rightarrow 0} = \varepsilon_2^{(3)} X_3 + \rho_2^{(3)} X_3^2 + O(X_3^3)$$

where $O(X_3^3)$ means other terms of order at least equal to 3.

$\varepsilon_2^{(3)}$ measures the slope of the curve $\ln\psi_2$ vs X₃ at the origin (Figure III.1a), or in other words, describes the straight line which best fits the data near the origin. In a very dilute solution, it gives us sufficient information as to the effect of one component on another, but in a less dilute solution, or for a greater accuracy, it is necessary to analyze the deviations from the straight line. This may be conveniently done by the coefficient $\rho_2^{(3)}$ which measures the curvature at the origin, or describes what parabola best fits the data at the origin. In many cases of practical interest, these two coefficients are sufficient to describe the data well.

In the case of a system of m components, Equation (III.3) is rewritten in the following way:

$$\begin{aligned} \ln\psi_2 = & \sum_{i=2}^m \varepsilon_2^{(i)} X_i + \rho_2^{(1)} X_i^2 + \dots + K_{0\dots n_1\dots}^{(2)} X_i^{n_1} + \dots \\ & + \sum_{\substack{i=2 \\ i \neq j}}^m \sum_{j=2}^m (\rho_2^{(i,j)} X_i X_j + \dots + K_{0\dots n_1\dots n_j\dots 0}^{(2)} X_i^{n_1} X_j^{n_j} + \dots) \\ & + \sum_{\substack{i=2 \\ i \neq j \neq k}}^m \sum_{j=2}^m \sum_{k=2}^m (\text{terms in } X_i^{n_i} X_j^{n_j} X_k^{n_k}) + \dots \end{aligned} \quad (\text{III.16})$$

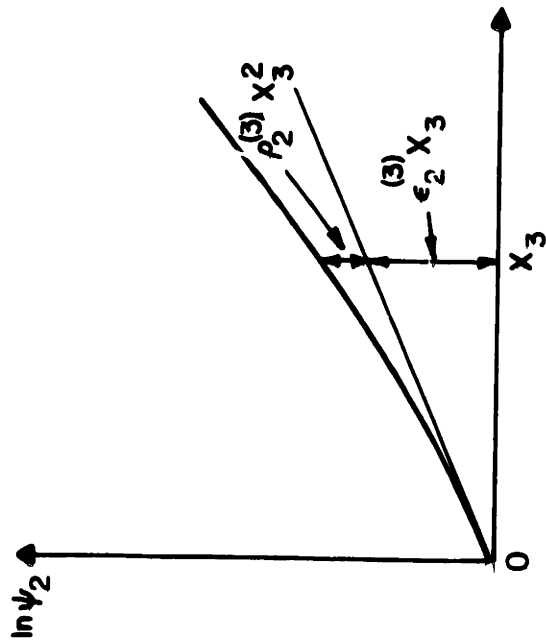


FIG. III 1 a

composition coordinate: mole fraction

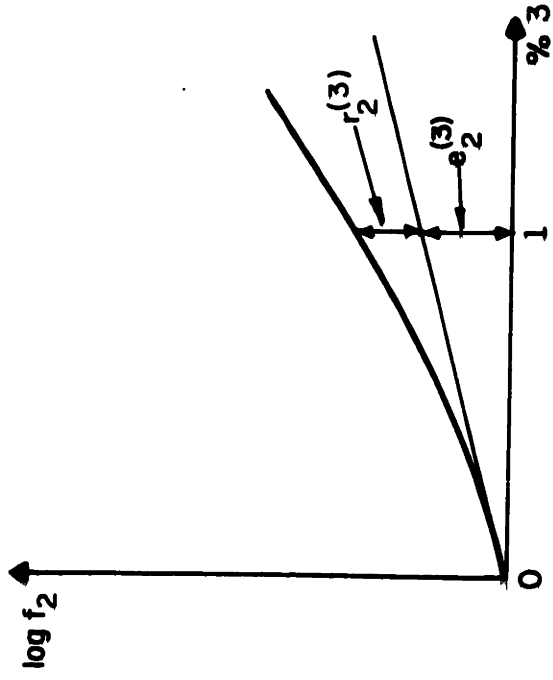


FIG. III 1 b

composition coordinate: weight percent

FIG. III. 1. FIRST AND SECOND ORDER FREE ENERGY INTERACTION COEFFICIENTS

Retaining only the terms of the first summation in the expansion gives

$$\ln \psi_2 \approx (\ln \psi_2)^{(2)} + (\ln \psi_2)^{(1)} + \dots + (\ln \psi_2)^{(j)} \quad (\text{III.17})$$

where $(\ln \psi_2)^{(1)}$ stands for $(\ln \psi_2)_{X_1 \neq 0, X_2 = X_3 = \dots = X_j}$ and involves either the binary 1-2 (for $i = 2$), or the ternary 1-2-1 at infinite dilution of (2). Data on these systems are usually much more readily available in the literature than data on ternaries where X_2 is not very dilute, or on systems of more than 3 components, and Equation (III.17), which neglects the cross product terms, is widely applied. However, even in the dilute range, the application of Equation (III.17) is often subject to criticism, the terms in $\rho_2^{(i,j)} X_i X_j$ being a priori as important as those in $\rho_2^{(1)} X_1^2$. This may account for many discrepancies between experimental and calculated values.

For instance, Ramachandran, Walsh and Fulton⁽¹¹⁾ reported that, on a weight percent basis, the value used for $e_0^{(Si)}$ in stainless steels is much smaller than the $e_0^{(Si)}$ value of -0.16 in the ternary Fe-Si-O. At above 2 percent silicon, they adjust $e_0^{(Si)}$ to -0.02. This difference is undoubtedly mostly due to the interaction of chromium and silicon and an estimation of $\rho_0^{(Si,Cr)}$ (or the corresponding coefficient for a weight percent coordinate) would conveniently and more rigorously account for this effect.

Of course, it must be admitted that accurate measurements of these ρ coefficients will be quite difficult, but even a rough estimate, a reasonable guess, is preferable to setting them arbitrarily equal to zero. Equation (III.17) should then be improved by rewriting it as:

$$\ln \psi_2 = (\ln \psi_2)^{(2)} + (\ln \psi_2)^{(1)} + \dots + (\ln \psi_2)^{(j)} + \rho_2^{(2,1)} X_2 X_1 + \dots + \rho_2^{(2,j)} X_2 X_j + \dots + \rho_2^{(1,j)} X_1 X_j \quad (\text{III.18})$$

The difficulties associated with the last terms of this equation were early recognized however, and in 1952, Sherman and Chipman⁽¹²⁾ devised a semi-empirical method to combine the data. Its discussion is delayed to the following section. Nevertheless, our conclusions are anticipated in saying that a reasonable direct estimate of these second order coefficients ρ seems more desirable. It is thus extremely important to fully utilize all the information which may be indirectly provided. The following considerations illustrate this point.

Dealing with a ternary system, assume the available data are the experimental curves shown in Figure III.2: $\ln\psi_2$ versus X_2 at infinite dilution of component 3, versus X_3 at infinite dilution of component 2 and $\ln\psi_3$ versus X_2 at infinite dilution of component 3. We seek the value of $\ln\psi_2$ at the point (X_2, X_3) . Equation (III.18) yields:

$$\ln\psi_2 = (\ln\psi_2)^{(2)} + (\ln\psi_2)^{(3)} + \rho_2^{(2,3)} X_2 X_3 \quad (\text{III.18a})$$

$(\ln\psi_2)^{(2)}$ and $(\ln\psi_2)^{(3)}$ are readily found. The following relation is used to calculate $\rho_2^{(2,3)}$. It is obtained from Equation (III.8a) with $n_2 = 1$, $n_3 = 1$ and Equation (III.8b) with $n_2 = 2$ and $n_3 = 0$:

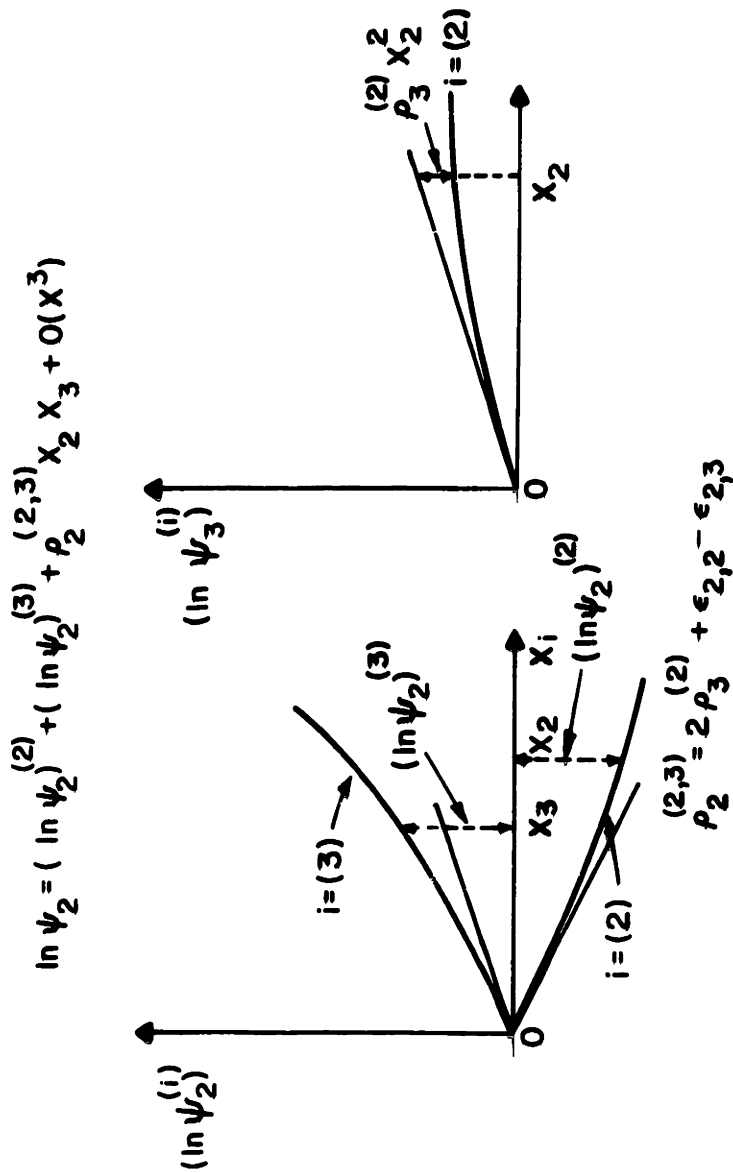
$$\rho_2^{(2,3)} + \epsilon_{2,3} = 2\rho_3^{(2)} + \epsilon_{2,2} = -K_{2,1}^{(1)} \quad (\text{III.19})$$

or

$$\rho_2^{(2,3)} = 2\rho_3^{(2)} + \epsilon_{2,2} - \epsilon_{2,3} \quad (\text{III.19a})$$

All of the terms on the right are obtained experimentally.

Most often, however, the curve $(\ln\psi_3)^{(2)}$ is not known. What is known is the slope at the origin since $\epsilon_3^{(2)} = \epsilon_2^{(3)}$. But obviously should any information as to the deviation from the straight line be available, it should be



$\epsilon_{2,i}$ measures the slope of the curves $(\ln \psi_2)^{(i)}$ or $(\ln \psi_i)^{(2)}$ at the origin

FIG. III. 2. EVALUATION OF THE SECOND ORDER INTERACTION COEFFICIENT $\rho_2^{(2,3)}$

used. For the case of Figure III.2, the neglect of $\rho_2^{(2,3)}$ would lead to an overestimate of $\ln\psi_2$, since the three quantities in the second member of Equation (III.19a) are negative.

Another example of a possible way to estimate ρ may be given for a quaternary system (4 is the maximum number of components which can be involved in the definition of ρ). The following information on the ternaries are assumed to be given (Figure III.3): $(\ln\psi_2)^{(3)}$, $(\ln\psi_2)^{(4)}$, $(\ln\psi_1)^{(2)}$, $(\ln\psi_3)^{(4)}$. We seek the value of $\ln\psi_2$ at infinite dilution of X_2 , and at concentrations X_3 and X_4 of components (3) and (4). Equation (III.16) can be then rewritten as:

$$\ln\psi_2 = (\ln\psi_2)^{(3)} + (\ln\psi_2)^{(4)} + \rho_2^{(3,4)} X_3 X_4 \quad (\text{III.18b})$$

Relations similar to Equation (III.18) may again be of considerable help in the estimate of $\rho_2^{(3,4)}$. Equation (III.8) leads to:

$$\rho_2^{(3,4)} + \epsilon_{2,-} = \rho_3^{(2,4)} + \epsilon_{2,-} = \rho_4^{(2,3)} + \epsilon_{2,3} = -\frac{1}{2} K_{i,i,i}^{(1)} \quad (\text{III.20})$$

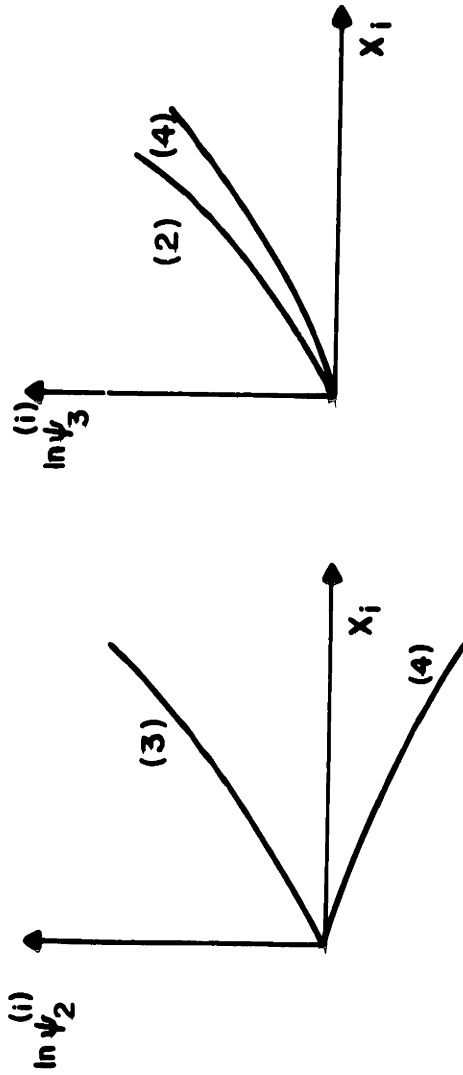
If components (2) and (4) have rather similar effects on (3), one may then venture to take $\rho_3^{(2,4)}$ as the geometric mean of the two ternary curvature coefficients:

$$\rho_3^{(2,4)} = \left(\frac{\partial^2 \ln\gamma_3}{\partial X_2 \partial X_4} \right)_{X_1 \rightarrow 1} \cdot \left(\frac{\partial^2 \ln\gamma_3}{\partial X_2^2} \right)_{X_1 \rightarrow 1}^{1/2} \cdot \left(\frac{\partial^2 \ln\gamma_3}{\partial X_4^2} \right)_{X_1 \rightarrow 1}^{1/2} = 2 \left(\rho_3^{(2)} \rho_3^{(4)} \right)^{1/2} \quad (\text{III.21})$$

or the arithmetic mean:

$$\rho_3^{(2,4)} = \frac{1}{2} \left(\frac{\partial^2 \ln\gamma_3}{\partial X_2^2} \right)_{X_1 \rightarrow 1} + \frac{1}{2} \left(\frac{\partial^2 \ln\gamma_3}{\partial X_4^2} \right)_{X_1 \rightarrow 1} = \rho_3^{(2)} + \rho_3^{(4)} \quad (\text{III.22})$$

$$\rho_2^{(3,4)} + \epsilon_{3,4} = \rho_3^{(2,4)} + \epsilon_{2,4} = \rho_4^{(2,3)} + \epsilon_{2,3}$$



$$\rho_3^{(2,4)} = \left(\frac{\partial^2 \ln \gamma_3}{\partial x_2 \partial x_4} \right)_{x_1 \rightarrow 1} \approx \left(\frac{\partial^2 \ln \gamma_3}{\partial x_2^2} \right)_{x_1 \rightarrow 1}^{1/2} \cdot \left(\frac{\partial^2 \ln \gamma_3}{\partial x_4^2} \right)_{x_1 \rightarrow 1}^{1/2} = 2 \left[\rho_3^{(2)} \rho_3^{(4)} \right]^{1/2}$$

or:

$$\rho_3^{(2,4)} \approx \frac{1}{2} \left\{ \left(\frac{\partial^2 \ln \gamma_3}{\partial x_2^2} \right)_{x_1 \rightarrow 1} + \left(\frac{\partial^2 \ln \gamma_3}{\partial x_4^2} \right)_{x_1 \rightarrow 1} \right\} = \rho_3^{(2)} + \rho_3^{(4)}$$

FIG. III.3. POSSIBLE ESTIMATES OF THE SECOND ORDER INTERACTION COEFFICIENTS $\rho_3^{(2,4)}$ AND $\rho_2^{(3,4)}$

For practical reasons that will become more evident in the following section, the arithmetic mean is preferable. With either estimate of $\rho_3^{(2,4)}$, the value of $\rho_2^{(3,4)}$ is calculated by Equation (III.20)

It is often convenient to choose weight percent rather than mole fraction as composition coordinate. Taylor's series expansions can be rewritten in a strictly parallel form to those in Equation (III.1) and (III.3). The coefficient:

$$e_i^{(j)} = \left(\frac{\partial \log f_i}{\partial \%j} \right)_{X_1 \rightarrow 100} \quad \text{(III.23)}$$

corresponds to the first order interaction coefficient ϵ , and we shall designate by r the parallel coefficient to ρ (Figure III.16). Thus:

$$\rho_i^{(j,k)} = \left(\frac{\partial^2 \ln \gamma_i}{\partial X_j \partial X_k} \right)_{X_1 \rightarrow 1} \quad \text{and} \quad \rho_i^{(j)} = \frac{1}{2} \left(\frac{\partial^2 \ln \gamma_i}{\partial X_j^2} \right)_{X_1 \rightarrow 1}$$

would correspond respectively to

$$r_i^{(j,k)} = \left(\frac{\partial^2 \log f_i}{\partial \%j \partial \%k} \right)_{\%1 \rightarrow 100} \quad \text{and} \quad r_i^{(j)} = \frac{1}{2} \left(\frac{\partial^2 \log f_i}{\partial \%j^2} \right)_{\%1 \rightarrow 100} \quad \text{(III.24)}$$

It is recalled, however, that a Gibbs-Duhem integration in terms of weight percents cannot be carried directly under the form of Equation (III.6).

The conversion relation between the coefficients on a molar basis and those on a weight basis becomes increasingly cumbersome with the order. Indeed, some care is required at the level of the first order (ϵ and e), and as pointed out by Lupis and Elliott (Reference (13) and Appendix (B)), an incorrect relationship has been widely used in the literature. But for the coefficients we are most interested in, namely first and second order ones, the complication is still quite minor.

The derivation is outlined in Appendix C. The results are:

$$e_i^{(j)} = \frac{0.434 \times 10^{-2}}{M_j} \left\{ M_1 \epsilon_i^{(j)} - (M_1 - M_j) \right\} \quad (\text{III.25})$$

$$r_i^{(j,K)} = \frac{0.434 \times 10^{-4}}{M_j M_K} \left\{ M_1^2 \rho_i^{(j,K)} - M_1(M_1 - M_K) \epsilon_i^{(j)} - M_1(M_1 - M_j) \epsilon_i^{(K)} \right. \\ \left. + (M_1 - M_j)(M_1 - M_K) \right\} \quad (\text{III.26a})$$

$$r_i^{(j)} = \frac{0.434 \times 10^{-4}}{M_j^2} \left\{ M_1^2 \rho_i^{(j)} - M_1(M_1 - M_j) \epsilon_i^{(j)} + \frac{1}{2} (M_1 - M_j)^2 \right\} \quad (\text{III.26b})$$

4. Discussion of Sherman and Chipman's Method. Presentation of an Alternate Method.

Sherman and Chipman's semi-empirical method^(1,2) of calculating activities in a multicomponent system may be reconsidered in view of the above treatment. The method and its analysis are applied to the particular case of a ternary illustrated in Figure (III.4). We seek the value of $\ln \psi_2$ at the point (X_2, X_3) . Assume X_2 and X_3 can be treated as infinitesimal quantities of the same order. Then to an approximation of the third order:

$$\ln \psi_2 \approx \epsilon_{2,2} X_2 + \rho_2^{(2)} X_2^2 + \epsilon_{2,3} X_3 + \rho_2^{(3)} X_3^2 + \rho_2^{(2,3)} X_2 X_3 \quad (\text{III.27})$$

It is also possible to write:

$$(\ln \psi_2)^{(2)} = \epsilon_{2,2} X_2 + \rho_2^{(2)} X_2^2 + \epsilon_{2,3} X_3 + \rho_2^{(3)} X_3^2 \quad (\text{III.28})$$

where X_3^1 is the concentration of (3) which would yield: $(\ln \psi_2)^{(2)} = (\ln \psi_2)^{(3)}$.

To this virtual concentration X_3^1 , Sherman and Chipman add the actual one, such that the effective concentration of (3) becomes now:

$$X_3'' = X_3 + X_3^1 \quad (\text{III.29})$$

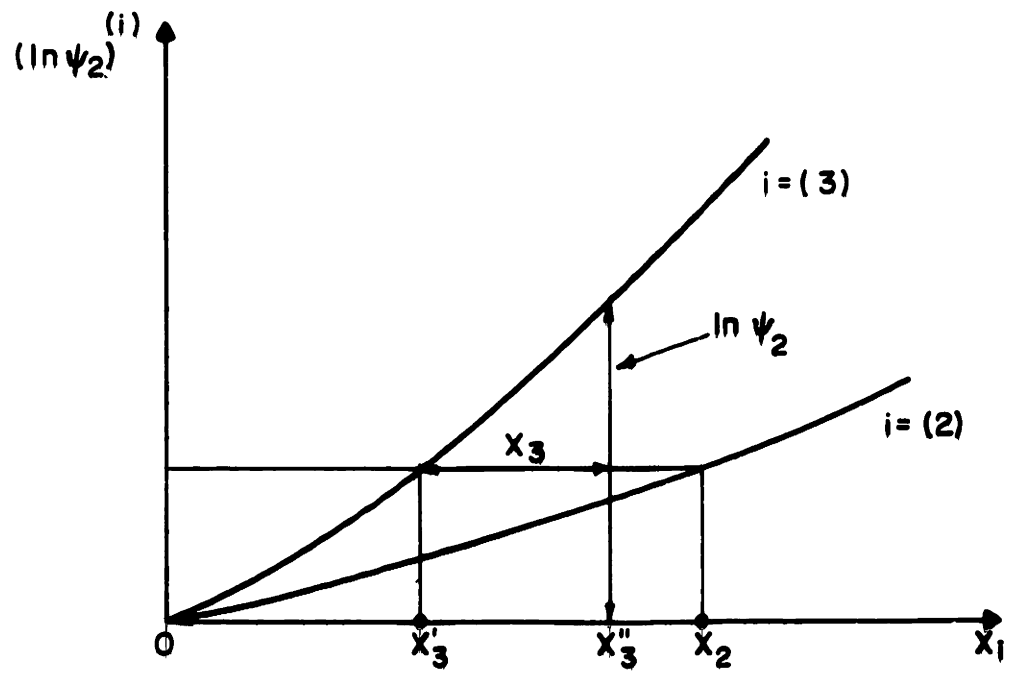


FIG. III. 4. SHERMAN AND CHIPMAN'S METHOD

Their calculated value is then:

$$\ln\psi_{2(\text{calc.})} = \epsilon_{2,3} (X_3 + X_3') + \rho_2^{(3)} (X_3 + X_3')^2 \quad (\text{III.30})$$

Or through Equation (III.28):

$$\ln\psi_{2(\text{calc.})} = \epsilon_{2,3} X_3 + \rho_2^{(3)} X_3^2 + \epsilon_{2,2} X_2 + \rho_2^{(2)} X_2^2 + 2\rho_2^{(3)} X_3 X_2' \quad (\text{III.31})$$

Hence:

$$\ln\psi_2 - \ln\psi_{2(\text{calc.})} = X_3 (\rho_2^{(2,3)} X_2 - 2\rho_2^{(3)} X_2') \quad (\text{III.32})$$

This difference is null for:

$$\rho_2^{(2,3)} X_2 = 2\rho_2^{(3)} X_2'$$

or

$$X_2 \left(\frac{\partial^2 \ln\psi_2}{\partial X_2 \partial X_3} \right)_{X_3 \rightarrow 1} = X_2' \left(\frac{\partial^2 \ln\psi_2}{\partial X_3^2} \right)_{X_2 \rightarrow 1} \quad (\text{III.33})$$

which is satisfied only by two values (possibly imaginary) of X_2 : the roots of the equation obtained by elimination of X_3' in Equations (III.28) and (III.33).

In the case represented in Figure III.4, it is reasonable to hope

that:

$$\left(\frac{\partial^2 \ln\psi_2}{\partial X_2^2} \right)_{X_3 \rightarrow 1} < \left(\frac{\partial^2 \ln\psi_2}{\partial X_2 \partial X_3} \right)_{X_2 \rightarrow 1} < \left(\frac{\partial^2 \ln\psi_2}{\partial X_3^2} \right)_{X_2 \rightarrow 1} \quad (\text{III.34})$$

or

$$2\rho_2^{(2)} < \rho_2^{(2,3)} < 2\rho_2^{(3)}$$

and as

$$X_2 > X_2' \quad (\text{III.35})$$

the above difference is expected to be small. It is noted that at least theoretically, it makes little difference if instead of going from lines of low curvatures to lines of higher curvatures, one chooses the opposite way (from lines of high curvature to lines of lower curvature). Then:

$$\ln \psi_2 - \ln \psi_{2(\text{calc.})} = X_2 (\rho_2^{(2,3)} X_3 - 2\rho_2^{(2)} X_2^2) \quad (\text{III.36})$$

and as

$$X_3 < X_2^2 \quad (\text{III.37})$$

in the above particular case just as good an agreement is expected. The only case where the difference in Equation (III.32) is of the third order (thus assumed negligible) is when:

$$\rho_2^{(2,3)} \epsilon_{2,2} = 2\rho_2^{(3)} \epsilon_{2,3} \quad \left(\text{since } \frac{X_2}{X_3} = \frac{\epsilon_{2,2}}{\epsilon_{2,3}} \right) \quad (\text{III.38})$$

and in Equation (III.36) when:

$$\rho_2^{(2,3)} \epsilon_{2,3} = 2\rho_2^{(2)} \epsilon_{2,2} \quad \left(\text{since } \frac{X_3}{X_2} = \frac{\epsilon_{2,3}}{\epsilon_{2,2}} \right) \quad (\text{III.39})$$

independently of the actual values of X_2 and X_3 . These are particular cases, indeed.

Generalizing this analysis to the multicomponent case is simple: the method is identical and has only to be reiterated.

Two important points must be noted. First, Sherman and Chipman's method just adds algebraically the total positive and total negative contributions and thus neglects all terms in $\rho_2^{(i,j)}$ where (i) and (j) are components giving rise to interactions of opposite signs. Second, the calculated values

of the activity coefficient are different when calculated on a weight percent basis or on a mole fraction basis.

The simplicity of Sherman and Chipman's method is extremely attractive; we feel, however, that an educated guess of the values of $\rho_2^{(i,j)}$ would prove valuable for more accurate results.

Presently though, little knowledge is available on the experimental values of these coefficients and a certain experience in predicting them is yet to be developed. It should be emphasized, however, that each time a value for $\rho_3^{(2)}$ or $\rho_2^{(3,4)}$ is experimentally obtained, the exact values of other coefficients $\rho_2^{(2,3)}$ or $\rho_3^{(2,4)}$ and $\rho_4^{(2,3)}$ are also automatically obtained (Equations III.19 and III.20). In cases where no experimental data are available, the following approximation may be used for $\rho_2^{(i,j)}$:

$$\rho_2^{(i,j)} = \left(\frac{\partial^2 \ln Y_2}{\partial X_1 \partial X_j} \right)_{X_1 \rightarrow 1} - \frac{1}{2} \left\{ \left(\frac{\partial^2 \ln Y_2}{\partial X_1^2} \right)_{X_1 \rightarrow 1} + \left(\frac{\partial^2 \ln Y_2}{\partial X_j^2} \right)_{X_1 \rightarrow 1} \right\} = \rho_2^{(i)} + \rho_2^{(j)} \quad (\text{III.40})$$

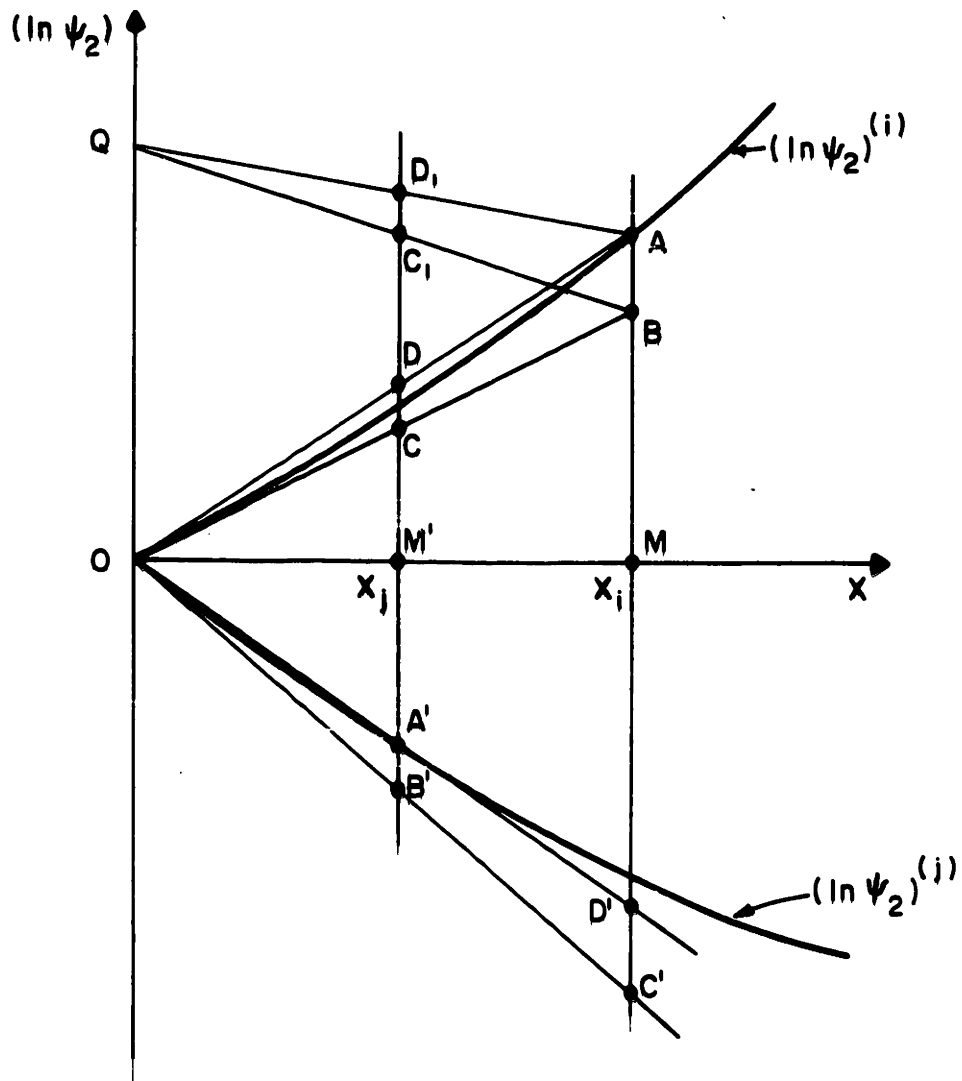
A geometrical mean instead of an algebraical one could be used, but the latter has the advantage of not being complicated by a problem of sign and also offers a simple geometric construction.

Consider Figure III.5. To evaluate $\ln \psi_2$, one adds first:

$$\overline{MA} + \overline{M'A'} = (\ln \psi_2)^{(i)} + (\ln \psi_2)^{(j)} \quad (\text{III.41})$$

To calculate $\rho_2^{(i,j)} X_1 X_j$, Equation (III.40) is used in the following way:

$$\rho_2^{(i,j)} X_1 X_j = (\rho_2^{(i)} X_1^2) \frac{X_j}{X_1} + (\rho_2^{(j)} X_j^2) \frac{X_1}{X_j}$$



Q is any point on the ordinate axis: $\overline{C_1 D_1} = \overline{C D}$

$$\overline{C D} + \overline{C' D'} = \rho_2^{(i,j)} x_i x_j$$

FIG. III.5. CONSTRUCTION OF THE TERM $\rho_2^{(i,j)} x_i x_j$ IN THE ALTERNATE METHOD.

or:

$$\rho_2^{(i,j)} X_1 X_j = \overline{BA} \frac{X_j}{X_1} + \overline{B'A'} \frac{X_1}{X_j} = \overline{CD} + \overline{C'D'} \quad (\text{III.42})$$

and:

$$(\ln \psi_2)^{(i)} + (\ln \psi_2)^{(j)} + \rho_2^{(i,j)} X_1 X_j = \overline{MA} + \overline{M'A'} + \overline{CD} + \overline{C'D'} \quad (\text{III.43})$$

The sign of each quantity \overline{CD} is the sign of the corresponding curvature $\rho_2^{(i)}$ and all contributions are added algebraically. In a solution of $(m + 1)$ components, there are $m(m - 1)/2$ terms in $\rho_2^{(i,j)}$ and $m(m-1)$ terms of the CD type. Of course, in many instances, the deviation CD from the tangent at the origin OB may be very small; then the magnified (or reduced) deviation CD may also be negligible and the construction permits one to visualize it.

One of the advantages of the method is its flexibility. When $\rho_2^{(i,j)}$ is known or when a good estimate of its value is possible, one calculates directly the term $\rho_2^{(i,j)} X_1 X_j$ and omits the two corresponding CD terms.

Another advantage is the fact that whether the procedure is carried in terms of mole fraction or weight percent, the results are identical. This is due to the fact that the conversion relationship between the second order interaction coefficients is linear (Equations III.25 and III.26).

Of course, these advantages should not hide our basic ignorance in using the approximation of Equation (III.40). As often as possible, we must try to replace in this geometric method, approximately constructed coefficients by better estimated ones. These better estimated values can be provided by models of statistical thermodynamics. We shall analyze one of these models in the following chapter.

5. Definition of the Generalized Enthalpy and Entropy Interaction Coefficients

Thus far, through interaction coefficients of adequate orders, only the excess free energy of a solution has been described. As recently proposed by Lupis and Elliott⁽¹⁴⁾, this treatment is now extended to the excess enthalpy and entropy functions.

In accordance with Equation (III.3), the partial molar enthalpy of component (i) may be written:

$$H_i^E = \sum_{n_2} \dots \sum_{n_j} \sum_{n_m} I_{n_2 \dots n_j \dots n_m}^{(i)} X_2^{n_2} \dots X_j^{n_j} \dots X_m^{n_m} \quad (\text{III.44})$$

and the partial molar entropy:

$$S_i^E = \sum_{n_2} \dots \sum_{n_j} \sum_{n_m} J_{n_2 \dots n_j \dots n_m}^{(i)} X_2^{n_2} \dots X_j^{n_j} \dots X_m^{n_m} \quad (\text{III.45})$$

where the index j can take any value from 2 to m , and the subscript n_j any positive integer value including 0.

We propose to call $I_{n_2 \dots n_j \dots n_m}^{(i)}$ with $n = \sum_{j=2}^m n_j$ an enthalpy interaction coefficient of order n and $J_{n_2 \dots n_j \dots n_m}^{(i)}$ with $n = \sum_{j=2}^m n_j$, an entropy interaction coefficient of order n .

$$\text{Since } F_i^E = H_i^E - TS_i^E$$

it follows immediately that:

$$K_{n_2 \dots n_j \dots n_m}^{(i)} = \frac{I_{n_2 \dots n_j \dots n_m}^{(i)}}{RT} - \frac{J_{n_2 \dots n_j \dots n_m}^{(i)}}{R} \quad (\text{III.46})$$

Inasmuch as the enthalpy and entropy functions are practically independent of temperature, the free energy interaction coefficients vary linearly with $1/T$.

Moreover, as enthalpy and entropy are extensive properties, the Gibbs-Duhem differential equation applies to the excess enthalpy and entropy functions. In a manner parallel to that of Section 2, the following relations are obtained between the enthalpy interaction coefficients.

$$I_{n_2 \dots n_i \dots n_m}^{(1)} = I_{n_2 \dots n_i \dots n_m}^{(1)} - \frac{n_i + 1}{\sum_{j=2}^m n_j} I_{n_2 \dots, n_i+1, \dots, n_m}^{(1)} \quad (\text{III.47})$$

and between the entropy interaction coefficients

$$J_{n_2 \dots n_i \dots n_m}^{(1)} = J_{n_2 \dots n_i \dots n_m}^{(1)} - \frac{n_i + 1}{\sum_{j=2}^m n_j} J_{n_2 \dots, n_i+1, \dots, n_m}^{(1)} \quad (\text{III.48})$$

These definitions and relations are now illustrated by applying them to a ternary system.

Obviously, the first order interaction coefficients will be the most useful and to emphasize this, a different notation is adopted, just as the symbol ϵ instead of K was adopted for the free energy interaction coefficient.

Thus:

$$\eta_i^{(j)} = \left(\frac{\partial H_i^E}{\partial X_j} \right)_{X_i \rightarrow 1} \quad (\text{III.49})$$

and:

$$\sigma_i^{(j)} = \left(\frac{\partial S_i^E}{\partial X_j} \right)_{X_i \rightarrow 1} \quad (\text{III.50})$$

The Equation (III.46) then yields:

$$\epsilon_i^{(j)} = \frac{\eta_i^{(j)}}{RT} - \frac{\sigma_i^{(j)}}{R} \quad (\text{III.51})$$

The reciprocity relations:

$$\eta_i^{(j)} = \eta_j^{(i)} \quad (\text{III.52})$$

and

$$\sigma_i^{(j)} = \sigma_j^{(i)} \quad (\text{III.53})$$

can be deduced from Equations (III.47) and (III.48).

A few of the above results for a ternary system are summarized by the following equations:

$$H_1^E = X_2 H_2^{E^\circ} + X_3 H_3^{E^\circ} + \frac{1}{2} \eta_{2,2} X_2^2 + \frac{1}{2} \eta_{3,3} X_3^2 + \eta_{2,3} X_2 X_3 + \dots - \frac{I_{n_2, n_3}^{(1)} n_2 n_3}{n_2 + n_3 - 1} X_2 X_3 + \dots \quad (\text{III.54})$$

$$H_1^E = -\frac{1}{2} \eta_{2,2} X_2^2 - \frac{1}{2} \eta_{3,3} X_3^2 - \frac{1}{2} \eta_{2,3} X_2 X_3 + \dots + I_{n_2, n_3}^{(1)} X_2 X_3 + \dots \quad (\text{III.55a})$$

$$H_2^E = H_2^{E^\circ} + \eta_{2,2} X_2 + \eta_{2,3} X_3 + \dots + \left\{ I_{n_2, n_3}^{(1)} - \frac{n_2 + 1}{n_2 + n_3} I_{n_2 + 1, n_3}^{(1)} \right\} X_2 X_3 + \dots \quad (\text{III.55b})$$

$$H_3^E = H_3^{E^\circ} + \eta_{2,3} X_2 + \eta_{3,3} X_3 + \dots + \left\{ I_{n_2, n_3}^{(1)} - \frac{n_3 + 1}{n_2 + n_3} I_{n_2, n_3 + 1}^{(1)} \right\} X_2 X_3 + \dots \quad (\text{III.55c})$$

Similar equations can be written for the entropy functions.

In connection with the partial molar excess enthalpy of a component, the β function is often used. It is defined as:

$$\beta_1 = \frac{H_1^E}{(1 - X_1)^2} \quad (\text{III.56})$$

Note that:

$$\left(\beta_1 \right)_{X_1 \rightarrow 1} = H_1^{E^o} \quad (\text{III.57})$$

and as:

$$\frac{\partial \beta_1}{\partial X_1} = \frac{1}{(1-X_1)^2} \left\{ \frac{\partial H_1^E}{\partial X_1} + \frac{2H_1^E}{1-X_1} \right\} \quad (\text{III.58})$$

at infinite dilution:

$$\left(\frac{\partial \beta_1}{\partial X_1} \right)_{X_1 \rightarrow 1} = \eta_{1,1} + 2H_1^{E^o} \quad (\text{III.59})$$

or:

$$\eta_{1,1} = \left(\frac{\partial \beta_1}{\partial X_1} - 2\beta_1 \right)_{X_1 \rightarrow 1} \quad (\text{III.60})$$

For a binary solution, Equation (III.55a) shows that:

$$\left(\beta_1 \right)_{X_2 \rightarrow 0} = -\frac{1}{2} \eta_{2,2} \quad (\text{III.61})$$

and we may rewrite Equation (III.60) as:

$$\left(\frac{\partial \beta_2}{\partial X_2} \right)_{X_2 \rightarrow 0} = \frac{2(\beta_2 - \beta_1)}{X_2 \rightarrow 0} \quad (\text{III.62})$$

Similar considerations can readily be repeated for the excess entropy.

As mentioned before, for practical applications, the use of weight percent instead of mole fraction is often convenient. With this composition coordinate, f_1 is the activity coefficient which plays an equivalent role to

γ_i , and $e_i^{(j)}$ is the free energy interaction coefficient equivalent to $\epsilon_i^{(j)}$.

$$e_i^{(j)} \equiv \left(\frac{\partial \log f_i}{\partial z_j} \right)_{z_1 \rightarrow 100}$$

Expressing a free energy term as the sum of entropy and enthalpy contributions, we may write:

$$2.3 RT \log f_i \equiv \mathcal{H}_i^E - T \mathcal{S}_i^E \quad (\text{III.63})$$

and

$$h_i^{(j)} \equiv \left(\frac{\partial \mathcal{H}_i^E}{\partial z_j} \right)_{z_1 \rightarrow 100} \quad (\text{III.64})$$

$$s_i^{(j)} \equiv \left(\frac{\partial \mathcal{S}_i^E}{\partial z_j} \right)_{z_1 \rightarrow 100} \quad (\text{III.65})$$

Consequently:

$$e_i^{(j)} = \frac{h_i^{(j)}}{2.3RT} - \frac{s_i^{(j)}}{2.3R} \quad (\text{III.66})$$

Combining Equations (III.25), (III.51) and (III.66), it can be shown that:

$$\eta_i^{(j)} = 100 \frac{M_j}{M_1} h_i^{(j)} \quad (\text{III.67})$$

but that:

$$\sigma_i^{(j)} = 100 \frac{M_j}{M_1} s_i^{(j)} - R \frac{M_1 - M_j}{M_1} \quad (\text{III.68})$$

The relationships corresponding to (III.52) and (III.53) for the h and s coefficients can also be readily established:

$$h_j^{(i)} = \frac{M_j}{M_i} h_i^{(j)} \quad (\text{III.69})$$

and

$$s_j^{(i)} = \frac{M_j}{M_i} s_i^{(j)} + \frac{R}{100} \frac{(M_j - M_i)}{M_i} \quad (\text{III.70})$$

Note also that the quantities \mathcal{H}_i^E and \mathcal{S}_i^E are defined in Equation (III.63) and their relationship to H_i^E and S_i^E must be developed. At infinite dilution, $f_i \rightarrow 1$ and $\gamma_i \rightarrow \gamma_i^\circ$, and since at a fixed temperature the ratio of two activities based on different reference states and compositions coordinates is a constant, therefore:

$$\ln \gamma_i X_i = \ln f_i \gamma_i + \ln \frac{\gamma_i^\circ M_i}{100 M_i} \quad (\text{III.71})$$

Subtracting Equation (III.63) from its equivalent on a mole fraction basis yields:

$$(H_i^E - \mathcal{H}_i^E) - T (S_i^E - \mathcal{S}_i^E) = RT (\ln \gamma_i - \ln f_i) \quad (\text{III.72})$$

then by substitution of Equation (III.71) into Equation (III.72)

$$(H_i^E - \mathcal{H}_i^E) - T (S_i^E - \mathcal{S}_i^E) = RT \ln \frac{\gamma_i \gamma_i^\circ M_i}{X_i 100 M_i} \quad (\text{III.73})$$

Thus for any selected temperature and metal composition:

$$\mathcal{K}_i^E = H_i^E - H_i^{E^\circ} \quad (\text{III.74})$$

and

$$\mathcal{S}_i^E = S_i^E - 2.3R \log \frac{100 M_i X_i}{M_i \%_i} - S_i^{E^\circ} \quad (\text{III.75})$$

6. Conclusions

The widespread use of the first order free energy interaction coefficient ϵ has already proved its convenience. We believe that the present data warrant the use of first order enthalpy and entropy coefficients as well as the use of second order free energy coefficients. Under the unifying concept of generalized interaction coefficients, many experimental results and empirical notions may be rigorously and concisely expressed.

Reciprocal relationships between generalized interaction coefficients (Equations (III.8), (III.43) and (III.44)) may be used, either as a method of Gibbs-Duhem integration in a multicomponent system, or, in some instances, as guides to the estimation of these coefficients. The next two chapters develop other means of estimation based on statistical thermodynamic models, and further illustrate the use of these coefficients.

CHAPTER IV
THE QUASI-CHEMICAL MODEL

1. Introduction

Among the many statistical models currently in the literature, the "regular solution" model probably has been the most widely used. It can be viewed as a simplified version of the "quasi-chemical" model, which was introduced by Guggenheim⁽¹⁵⁾ with considerable success. The quasi-chemical theory was developed for binary solutions, but recently^(6,7) attempts have been made to adopt the model to ternary solutions. The system of equations involved does not admit an analytical solution. However, an analytical expansion of the excess free energy, with respect to the mole fractions of the solutes, seems to be a most useful approach, as it yields quite directly the generalized interaction coefficients previously analyzed.

No attempt will be made here to present the model in great detail. However, the reader is referred to Guggenheim's original work⁽¹⁵⁾ or to the excellent review of Prigogine.⁽¹⁰⁾ Nevertheless, the essential features of the model are presented in this Chapter and in Appendix (D), and this study focuses more particularly on the prediction of the interaction coefficients.

2. Assumptions

The assumptions of the quasi-chemical model, which are either essential to its construction or essential to our technique of computation, are as follows:

a. The quasi-chemical assumes the existence of a rigid lattice. Thus, it is assumed that the motion of the atoms reduces merely to oscillations about some equilibrium positions. This is a rather questionable approximation for liquids.

b. The lattice is treated as rigid. Changes in the inter-atomic distances, due to changes in composition, are neglected.

$${}_v^M = {}_v^E = 0$$

c. In the excess functions only the configurational energy is taken into account. The vibrational energy, due to the change in the frequency spectrum of the atom (i) in an environment different from the one it would have in the pure component (i), is neglected. Consequently, the main source of excess entropy is the configurational one and, as it is by definition a deviation from complete randomness, its sign will always be negative. The second source of excess entropy usually taken into account is the "thermal" one; it is due to the effect of a temperature change on the bonding energies. This contribution seems, however, small enough to be safely neglected in most cases of practical interest.

d. Only the influence of nearest neighbors is taken into account, and pair-wise interactions are assumed.

e. This study is restricted to dilute solutions, and the number of nearest neighbors to any atom is assumed to equal the coordination number of the pure solvent.

3. Binary System.

It is rather traditional, and very convenient, in statistical thermodynamics to designate components of a solution by A, B, C,M, while in classical thermodynamics, and especially when using interaction coefficients, the symbols 1, 2, 3, ..., are adopted. Here, it is simpler to retain this duality in the notation, with A corresponding to 1, B to 2, C to 3, etc.

Consider a binary mixture of N_A atoms A, N_B atoms B, where N_{AA} , N_{BB} and N_{AB} are the number of pairs AA, BB and AB, and u_{AA} , u_{BB} and u_{AB} their respective energy. Z is the coordination number for A and B.

Summing all neighbors of the N_A and N_B atoms,

$$Z N_A = 2 N_{AA} + N_{AB} \quad (\text{IV.1})$$

$$Z N_B = 2 N_{BB} + N_{AB} \quad (\text{IV.2})$$

The energy of the lattice is:

$$E_{\text{latt}} = N_{AA} u_{AA} + N_{AB} u_{AB} + N_{BB} u_{BB}$$

or

$$E_{\text{latt}} = \frac{1}{2} Z N_A u_{AA} + \frac{1}{2} Z N_B u_{BB} + N_{AB} \omega_{AB} \quad (\text{IV.3})$$

where

$$\omega_{AB} = u_{AB} - \frac{u_{AA} + u_{BB}}{2} \quad (\text{IV.4})$$

At this point, another assumption is introduced. It may be considered that, if A is the solvent, $\frac{1}{2} Z N_A u_{AA}$ represents very closely the lattice energy E_{AA} for pure A, but the same cannot be said of $\frac{1}{2} Z N_B u_{BB}$, since u_{BB} in the solvent may differ greatly from u_{BB} in pure B. Nevertheless, for purposes of simplicity, E_{BB} is taken as equal to $\frac{1}{2} Z N_B u_{BB}$. This assumption will be removed later. Thus:

$$E_{\text{latt}} = E_{AA} + E_{BB} + N_{AB} \omega_{AB} \quad (\text{IV.5})$$

The configurational partition function is:

$$Q_{\text{conf}} = \sum_{N_{AB}} g(N_A, N_B, N_{AB}) e^{-\beta E_{\text{latt}}} \quad (\text{IV.6})$$

where g is the number of arrangements of the N_A atoms A and N_B atoms B, so that there are, altogether, N_{AB} pairs of nearest neighbors AB. The contribution of the lattice partition function to the free energy of the mixture is:

$$-kT \ln Q_{\text{conf}} = E_{AA} + E_{BB} - kT \ln \left(\sum_{N_{AB}} g e^{-\beta N_{AB} \omega_{AB}} \right) \quad (\text{IV.7})$$

and subtracting the corresponding contributions for the pure components:

$$F^M = -kT \ln(\sum_{N_{AB}} g e^{-\beta N_{AB} \omega_{AB}}) \quad (\text{IV.8})$$

No rigorous mathematical formula is available for $g(N_A, N_B, N_{AB})$; its value must be approximated.

3.1 Regular Solution

The distribution of the atoms is assumed to be completely random; g becomes the classical permutation expression:

$$g = \frac{(N_A + N_B)!}{N_A! N_B!} \quad (\text{IV.9})$$

and it may be shown also (see Appendix D) that the number N_{AB} of AB pairs is then:

$$N_{AB} = \frac{Z N_A N_B}{(N_A + N_B)} \quad (\text{IV.10})$$

Replacing, in equation IV.8, g and N_{AB} by their values and using Sterling's formula ($\ln p! \approx p \ln p - p$), it is readily found that:

$$F^M = RT(X_A \ln X_A + X_B \ln X_B) + Z X_A X_B \omega_{AB} \quad (\text{IV.11})$$

or, with the correspondence in the notation previously mentioned:

$$F^E = Z X_A X_B \omega_{AB} = Z X_1 X_2 \omega_{1,2} \quad (\text{IV.12})$$

3.2 Quasi-Chemical Solution

It is now assumed that the number of configurations corresponding to a given value of N_{AB} may be calculated as if the various types of pairs do not interfere with one another. The resulting expression of g and subsequent calculations are given in Appendix (D).

Ultimately, the model yields:

$$\frac{F}{RT} = \frac{Z}{2} X_2 \ln(1+\lambda) - \frac{Z}{2} \lambda X_2^2 + \frac{Z}{2} \lambda^2 X_2^3 - Z \lambda^2 \left(\frac{1}{4} + \frac{5}{3} \lambda\right) X_2^4 + O(X_2^5) \quad (\text{IV.13})$$

where

$$\lambda = e^{2\beta\omega_{12}} - 1 \quad (\text{IV.14})$$

Using equation (III.7), these results can be expressed also in terms of the activity coefficients:

$$\ln \gamma_1 = \frac{Z}{2} \lambda X_2^2 - Z \lambda^2 X_2^3 + \frac{3Z}{4} \left(1 + \frac{20\lambda}{3}\right) X_2^4 + O(X_2^5) \quad (\text{IV.15})$$

$$\ln \gamma_2 = \frac{Z}{2} \ln(1+\lambda) - Z \lambda X_2 + \frac{Z}{2} \lambda (1+3\lambda) X_2^2 - 2Z \lambda^2 \left(1 + \frac{10\lambda}{3}\right) X_2^3 + O(X_2^4) \quad (\text{IV.16})$$

The terms $\ln \gamma_2^s$ and $\epsilon_{2,2}$ in equation (IV.15) are readily identified:

$$\ln \gamma_2^s = \frac{Z}{2} \ln(1+\lambda) \quad (\text{IV.17})$$

$$\epsilon_{2,2} = -Z \lambda \quad (\text{IV.18})$$

and eliminating λ between these two relations:

$$\ln \gamma_2^j = \frac{Z}{2} \ln \left(1 - \frac{\epsilon_{2,2}}{Z} \right) \quad (\text{IV.19})$$

Equation (IV.19) is tested in Fig. IV.1 for a wide variety of alloys. In the calculations, a coordination number of 10 was assumed. This is a good average for liquids and, moreover, the curve is very slightly changed by a different value. The agreement between the experimental values and the theoretical curve is satisfactory. The fact that many of the corresponding alloys exhibit positive excess entropies does not seem to affect, in any marked way, this agreement. This is surprising, because the excess entropy of a quasi-chemical solution must, in all cases, be negative.

The same test could have been carried out in terms of the α function. Calculations yield:

$$\alpha_2 = \frac{\ln \gamma_2^j}{(1-X_2)} = \frac{Z}{2} \ln(1+\lambda) + Z \{ \ln(1+\lambda) - \lambda \} X_2 + 3 \frac{Z}{2} \{ \ln(1+\lambda) + \lambda(\lambda-1) \} X_2^2 + \frac{Z}{2} \{ \ln(1+\lambda) - \lambda \left(1 - \frac{\lambda}{2} + \frac{10\lambda^2}{3} \right) \} X_2^3 + o(X_2^4) \quad (\text{IV.20})$$

and, recalling equation (III.12a):

$$\left(\frac{d\alpha_2}{dX_2} \right)_{X_2 \rightarrow 0} = \epsilon_{2,2} + 2 \ln \gamma_2^j = Z \{ \ln(1+\lambda) - \lambda \} \quad (\text{IV.21})$$

The quantity in brackets is always negative and of the second order in λ . Thus the slope of α_2 vs X_2 should be almost null and

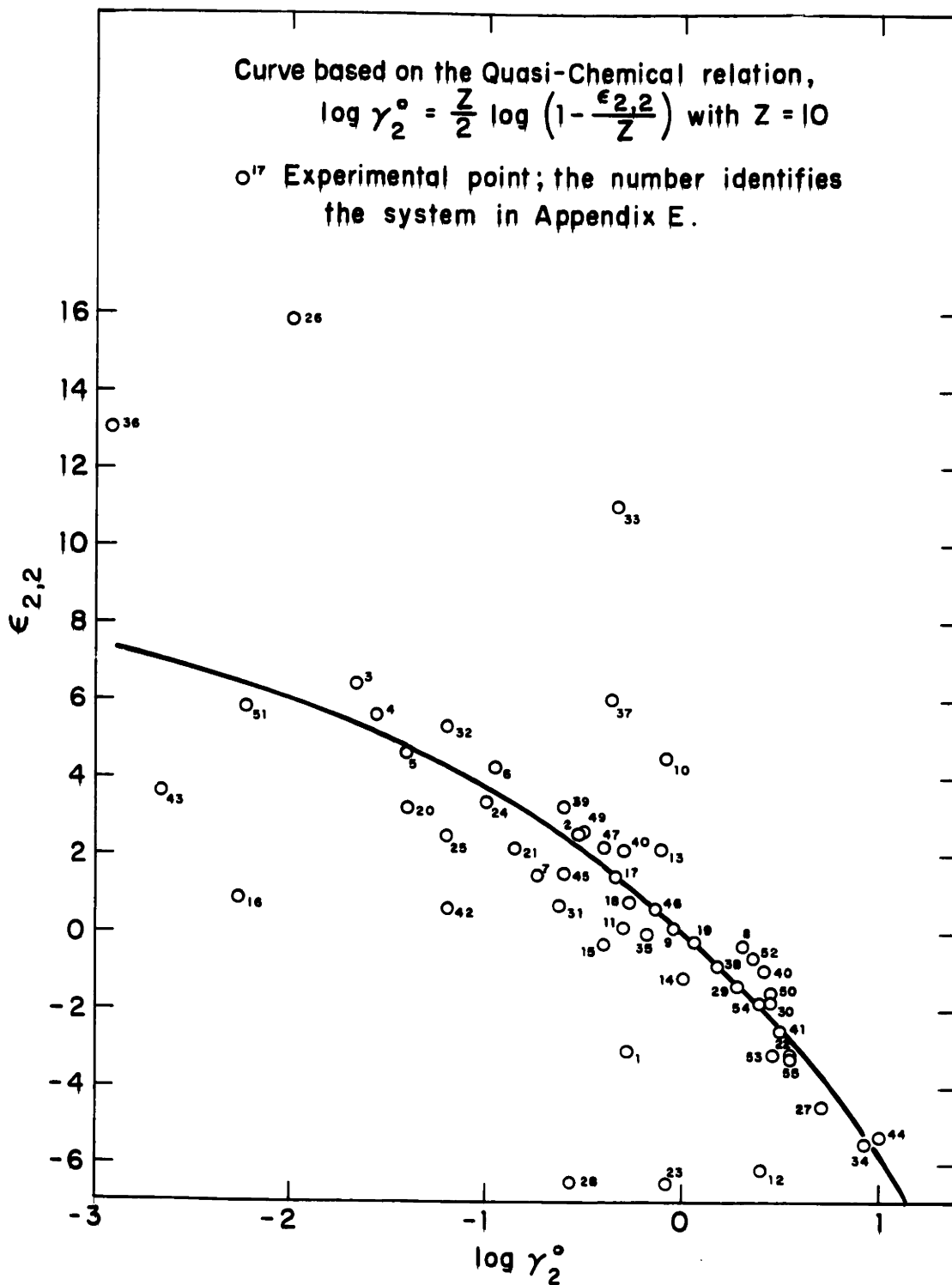


FIG. IV 1. TEST OF THE QUASI-CHEMICAL MODEL
ON VARIOUS BINARY ALLOYS.

negative for cases of solutions with small deviations from ideality.

It is to be emphasized that the bonding energy between two given atoms is assumed independent of the surroundings; in other words, ω (or λ) is assumed independent of concentration. The assumption is at its worst for $\ln \gamma_2^\circ$ in which $u_{2,2}$ is treated as equal in the solvent and solute, a quite drastic change, indeed, in the environment. It will be seen that the possible error arising from this assumption can explain many of the departures from relation (IV.19). By distinguishing between the energy u_{BB} of the pair BB in the solvent, and the energy u_{BB}° of this pair in the pure component B, some of the impact of this assumption may be removed. It is necessary, then, to carry the term:

$$\frac{1}{2} Z_A N_A u_{BB} - E_{BB} \quad \text{or} \quad \frac{1}{2} Z_A N_B \left(u_{BB} - \frac{Z_B}{Z_A} u_{BB}^\circ \right)$$

in equation (IV.5) and, consequently, in the expansion of F^E/RT .

Let:

$$\omega_{AB}^\circ = u_{BB} - \frac{1}{2} \left(u_{AA} + \frac{Z_B}{Z_A} u_{BB}^\circ \right) \quad (\text{IV.22})$$

and

$$\lambda^\circ = e^{2\beta \omega_{AB}^\circ} - 1 \quad (\text{IV.23})$$

Replacing only $\ln(1+\lambda)$ by $\ln(1+\lambda^\circ)$ in equations (IV.13), (IV.16) and (IV.17), takes this effect into account.

The difference between the corrected value of $\ln \gamma_2^\circ$ and the previous value reported by the curve in Fig. IV.1 is:

$$\ln \gamma_2^{\circ}(\text{corr}) - \ln \gamma_2^{\circ}(\text{curve}) = \frac{\beta}{2} [Z_2 u_{2,2} - Z_1 u_{2,2}^{\circ}] \quad (\text{IV.24})$$

Examination of this equation may qualitatively explain some of the departures in Fig. IV.1. In Region I above the curve:

$$\ln \gamma_2^{\circ}(\text{corr}) > \ln \gamma_2^{\circ}(\text{curve})$$

or, considering the coordination number of the solute and solvent as nearly equal:

$$u_{2,2} > u_{2,2}^{\circ}$$

and, since the sign of the energy is negative (the zero of the energy is taken for atoms infinitely distant from each other):

$$|u_{2,2}| < |u_{2,2}^{\circ}| \quad (\text{IV.25})$$

In Region II, below the curve, the opposite result is obtained:

$$|u_{2,2}| > |u_{2,2}^{\circ}|$$

It is possible to make a rough estimate of the value of $u_{2,2}^{\circ}$ from the heat of atomization of element (2) at 298.15°K, assuming that the bonding energy does not change very much with temperature.

$$\frac{1}{2} Z_2 u_{2,2}^{\circ} = \Delta H_2$$

It is not possible to make a similar evaluation of the energy of bonding $u_{2,2}$ in solvent 1. But, since it is desired only to compare $u_{2,2}$ and $u_{2,2}^{\circ}$, the following qualitative argument may be given:

The cohesive energy of an element is a function of the number of its bonding electrons. If element (2) enters into solution in the lattice of solvent 1 of smaller cohesive energy (thus, with fewer bonding electrons), a part of the bonding electrons of 2 will be lost to the atoms 1, consequently reducing the strength of the bonding between two atoms 2. Therefore, if

$$\Delta H_1 - \Delta H_2 < 0$$

then

$$|u_{2,2}| < |u_{2,2}^3|$$

and the representative point of the system should be in Region I. Similar reasoning applies to Region II.

Table IV.1 lists some of the systems for which representative points in Fig. IV.1 lay significantly apart from the theoretical curve. At least qualitatively, the result is satisfactory, since the correspondence between the region and the sign of $\Delta H_1 - \Delta H_2$ is established.

The reason why, in some instances, the cohesive energy of silver and gold is divided by three must be explained. It is believed⁽¹⁶⁾ that copper, silver and gold have a valence of 3, by promotion of electrons from the d shell to the p shell. They keep this valence when dissolved in transition metals, such as platinum, which provide an environment of d electrons available for bonding, and thus stabilize this electronic configuration. However, they tend to lose it and acquire a valence of 1 when dissolved in non-transition metals, such as aluminum, where

TABLE IV.1

Theoretical Explanation of some Discrepancies Observed
in The Application of Equation IV.19

<u>Region*</u>	<u>Identification^o</u> <u>Number</u>	<u>Solvent</u> <u>Solute</u> <u>1</u> <u>2</u>	<u>ΔH_1</u> [†]	<u>ΔH_2</u> [†]	<u>$\Delta H_1 - \Delta H_2$</u>
I	10	Au - Pb	87.3/3	46.8	-
	13	Bi - Au	49.5	87.3	-
	26	Cd - Na	26.8	25.9	+
	37	Hg - Tl	15.3	43.0	-
	33	Fe - C	99.5	170.9	-
	36	Fe - Si	99.5	108	-
II	7	Ag - Cd	68.4	26.8	+
	1	Al - Ag	77.5	68.4/3	+
	12	Bi - Ag	49.5	68.4/3	+
	15	Bi - Hg	49.5	15.3	+
	16	Bi - Mg	49.5	35.6	+
	20	Bi - Tl	49.5	43	+
	23	Cd - Bi	26.8	49.5	-
	25	Cd - Hg	26.8	15.3	+
	28	Cd - Sb	26.8	52	-
	42	Pb - Mg	46.8	35.6	+
43	Pb - Na	46.8	25.9	+	

* Regions I and II correspond, respectively, to the regions above and below the curve in Fig. (IV.1).

^o Each system is identified by a number in Fig. IV.1 and in Table E.1 in Appendix E.

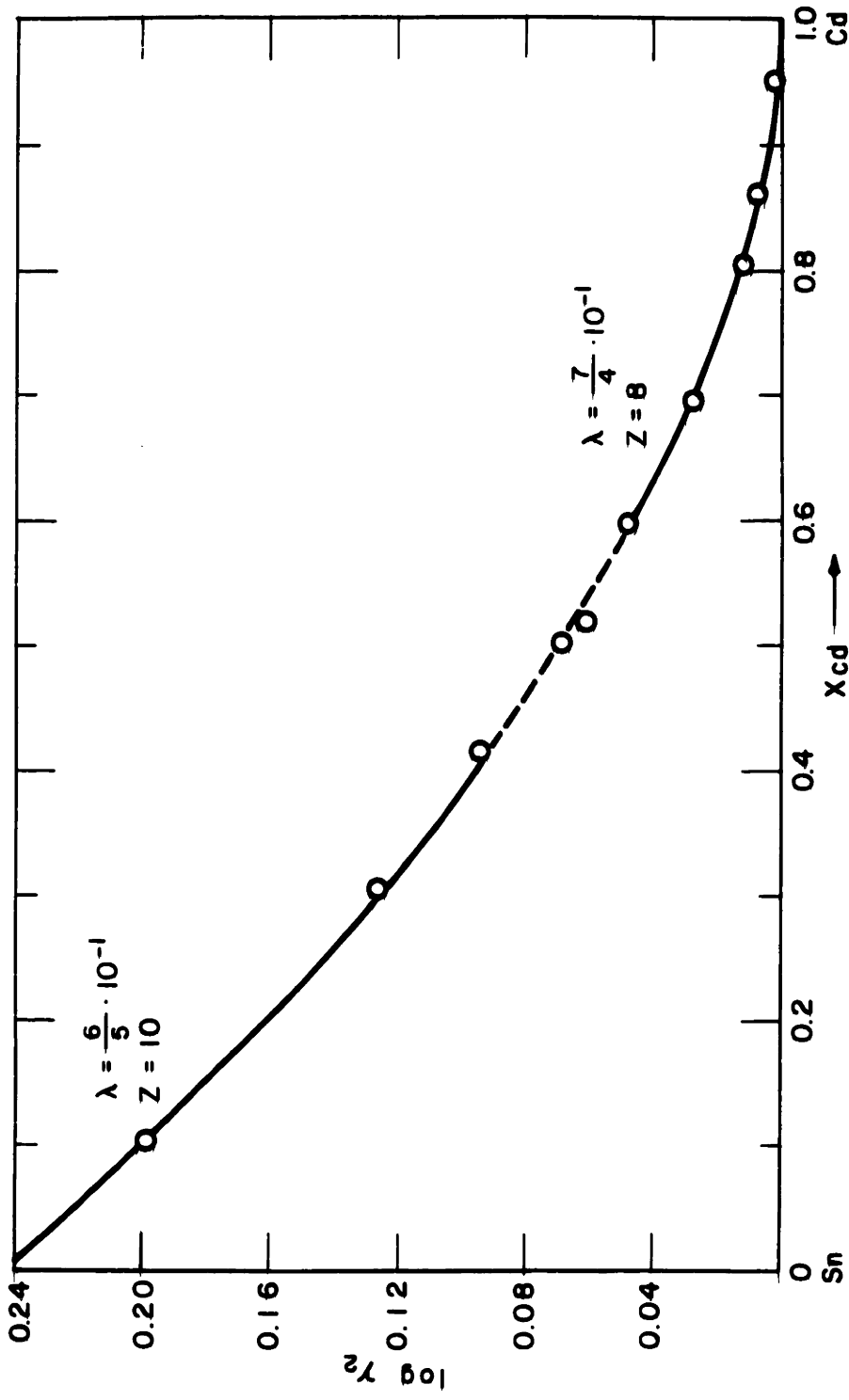
[†] ΔH is the heat of atomization of the solid elements in Kcal/g-atoms at 298.15°K, or at the melting point, whichever is lower.

no unpaired d electrons are available for bonding. In this last state, only this single valence electron is available for bonding, and comparison with the cohesive energies of the "one electron" metals, such as potassium or rubidium, then suggests cohesive energies, for copper, silver and gold, of one-third of their values, when these elements are pure

The same reasoning perhaps may explain why the dilute solution of aluminum in silver (both of valence 3) is much better approximated by the quasi-chemical model than the dilute solution of silver in aluminum

It must be emphasized, however, that the difference between the values of the bonding energies $u_{2,2}$ and $u_{2,2}^{\circ}$ is believed to be only one of the reasons for the inadequacy of the model in many systems. Some of the other reasons are discussed later in this chapter.

In view of the difference between λ and λ° , it may be more significant to compare the results over a whole region than at a point. It is recalled, however, that the above expansions are applicable only to dilute solutions (1) in (2) or (2) in (1). A typical case is offered by the Sn-Cd system⁽¹⁷⁾ in Fig. IV.2. The values of $\lambda = \frac{6}{5} \times 10^{-1}$ and $\frac{7}{4} \times 10^{-1}$ are chosen to give the best fit in the dilute ranges. The agreement is excellent and, in fact, rather surprising in view of the sizeable positive excess entropy which cannot be accounted for by the quasi-chemical theory.



O experimental values

— theoretical curve; calculations based on equations IV.15 and IV.16

The values of λ are chosen to give the best fit

FIG. IV.2 TEST OF THE QUASI-CHEMICAL MODEL FOR THE Sn-Cd SYSTEM AT 500°C

4. Ternary System

Keeping the same notation used in the binary system and, following the same procedure for a ternary system, the model yields:

$$F^M = -kT \ln \left\{ N_{AB} N_{AC} N_{BC} g e^{- (N_{AB} \omega_{AB} + N_{AC} \omega_{AC} + N_{BC} \omega_{BC})} \right\} \quad (IV.26)$$

4.1 Regular Solution

In the case of complete randomness:

$$g = \frac{(N_A + N_B + N_C)!}{N_A! N_B! N_C!} \quad (IV.27)$$

Using Sterling's approximation, it is readily seen that g provides the entropy contribution of ideal mixing. Subtracting this contribution, and replacing N_{IJ} by its value $Z N_I N_J / N$ in equation IV.26, the following expression of the excess free energy is obtained:

$$\frac{F^E}{RT} = Z\beta (X_A X_B \omega_{AB} + X_A X_C \omega_{AC} + X_B X_C \omega_{BC}) \quad (IV.28)$$

The generalization of this result is straight forward. In a system of m components:

$$\frac{F^E}{RT} = Z\beta \sum_{i=1}^m \sum_{\substack{j=1 \\ i \neq j}}^m X_i X_j \omega_{ij} \quad (IV.29)$$

Equation IV.28 yields, in particular:

$$\epsilon_{2,3} = Z\beta (\omega_{2,3} - \omega_{1,2} - \omega_{1,3}) \quad (IV.30)$$

4.2 Quasi-chemical Solution

Removing the assumption of a random distribution, a procedure parallel to the one used in the binary is followed. The calculations are, however, much more complicated, as they involve a system of three equations of the second degree with three unknowns. A direct calculation being impossible, a series expansion, coupled with an iteration procedure to determine each term of the series, is adopted. The detailed calculations are given in Appendix (D). The resulting expression for the excess free energy is:

$$\begin{aligned} \frac{F^E}{RT} = & \frac{Z}{2} X_2 \ln(1+\lambda_{1,2}) + \frac{Z}{2} X_3 \ln(1+\lambda_{1,3}) - \frac{Z}{2} \lambda_{1,2} X_2^2 - \frac{Z}{2} \lambda_{1,3} X_3^2 \\ & - Z\mu X_2 X_3 + \frac{Z}{2} \lambda_{1,2}^2 X_2^3 + \frac{Z}{2} \lambda_{1,3}^2 X_3^2 + Z\mu X_2^2 X_3 (\lambda_{1,2} + \mu/2) \\ & + Z\mu X_2 X_3^2 (\lambda_{1,3} + \mu/2) + O(X^4) \end{aligned} \quad (\text{IV.31})$$

where:

$$\lambda_{ij} = e^{2\beta\omega_{ij}} - 1 \quad \text{with} \quad \omega_{ij} = u_{ij} - \frac{u_{ii} + u_{jj}}{2} \quad (\text{IV.32})$$

and:

$$\mu = \exp\{\beta(\omega_{1,2} + \omega_{1,3} - \omega_{2,3})\} - 1 \quad (\text{IV.33})$$

5. First Order Free Energy Interaction Coefficient

Using equation (III.14), the expression of $\epsilon_{2,3}$ in equation IV.31 is easily recognized:

$$\epsilon_{2,3} = -Z\mu = -Z[\exp\{\beta(\omega_{1,2} + \omega_{1,3} - \omega_{2,3})\} - 1] \quad (\text{IV.34})$$

which, if the term of the exponential is small (thus, if $\epsilon_{2,3}$ is small) can be approximated by:

$$\epsilon_{2,3} \approx Z\beta[\omega_{2,3} - \omega_{1,2} - \omega_{1,3}]$$

an expression already given by the regular solution (equation IV.30).

Note, also, that since $\mu = -1$ and $\lambda_{ij} > -1$, the quasi-chemical model yields:

$$\epsilon_{i,j} < Z$$

Each parameter λ_{ij} (or ω_{ij}) may be expressed in terms of thermodynamic coefficients of the binary i-j; for instance,

$$Z\beta\omega_{1,2} = \ln \gamma_2^i \quad \text{or} \quad \lambda_{1,2} = -\frac{\epsilon_{2,2}}{Z}$$

the corresponding binary system being a dilute solution of (2) in (1). However, for $\lambda_{2,3}$ (or $\omega_{2,3}$), we are faced with a difficulty: is $\lambda_{2,3}$ evaluated in a dilute solution of (2) in (3), or (3) in (2)? Theoretically, this should make no difference, since the bonding energies $u_{2,2}$, $u_{2,3}$ and $u_{3,3}$ were assumed to be independent of their surroundings. Practically, it is more realistic to choose for solvent the component j (2 or 3) which is physically closer to the solvent (1). In case of no obvious preference, an arithmetic mean may be adopted.

Equation (IV.34) may, for instance, be rewritten as:

$$\epsilon_{2,3} = Z_1 \left\{ 1 - \frac{(\gamma_2^c \gamma_3^c)^{1/Z_1}}{(\gamma_i^c)_{\text{binary } j-i}^{1/Z_j}} \right\} \quad (\text{IV.35})$$

or:

$$\left(1 - \frac{\epsilon_{2,3}}{Z_1}\right) = \left\{ \frac{\left(1 - \frac{\epsilon_{2,2}}{Z_1}\right) \left(1 - \frac{\epsilon_{3,3}}{Z_1}\right)}{\left(1 - \frac{\epsilon_{ii}}{Z_j}\right) \text{ binary } j-i} \right\}^{1/2} \quad (\text{IV.36})$$

where $j = 2$ or 3 and $i = 3$ or 2 . Equation IV.36 may be preferred, since it eliminates the differences between λ° and λ previously analyzed.

As an application of equation IV.36, the values of $\epsilon_{\text{Cd-Pb}}$ in Bi, Sb and Sn were calculated using the experimental data of Elliott and Chipman.⁽¹⁷⁾ The results are given in Table IV.2

TABLE IV.2

Calculated* and Experimental Values of The
First Order Interaction Coefficient ϵ

<u>Solvent</u>	<u>$\epsilon_{\text{Cd-Pb}}$ (calculated*)</u>	<u>$\epsilon_{\text{Cd-Pb}}$ (experimental)</u>
Bi	1.4	1.6
Sb	2.5	2.8
Sn	0.5	0.0

* Calculated by equation IV.36

The mean value of $\epsilon_{\text{Cd-Pb}}$ taken for the calculation is 0.35; in Cd it is equal to 0.45 and in Pb to 0.25. Noting that Sn and Pb have more similar properties than Cd and Pb, the value of $\epsilon_{\text{Cd-Pb}}$ in Pb may be preferred. Then:

$$\epsilon_{\text{Cd-Pb}}(\text{in Sn}) = 0.1$$

These results show that $\omega_{\text{Cd-Pb}}$ may be considered as nearly constant in the five different solvents: Cd, Pb, Bi, Sb and Sn. However, this constancy of ω is not expected to be the general rule in other systems.

Similar investigations of the predictions of $\epsilon_{2,3}$ by the regular and quasi-chemical solutions have been performed by Alcock and Richardson,⁽⁶⁾ and more recently by Durand.⁽⁷⁾ In general, the agreement between calculated and experimental values is reasonably satisfactory.

Rather than pursue these comparisons here, it seems preferable to turn to the study of the second order interaction coefficients, ρ , which have not yet received any direct attention.

6. Second Order Free Energy Interaction Coefficient

6.1 The Quasi-Chemical Expression

It is convenient to note that equations III.19 and III.7 lead to:

$$\rho_2^{(3)} + 1/2\epsilon_{3,3} = -1/2 K_{1,2}^{(1)} = \phi_{1,2} \quad (\text{IV.37})$$

Using the quasi-chemical result in equation IV.31:

$$\rho_2^{(3)} = -1/2\epsilon_{3,3} + Z\mu(\lambda_{1,3} + \mu/2) \quad (\text{IV.38})$$

which may be rewritten as:

$$\rho_2^{(3)} = -1/2\epsilon_{3,3} + \frac{\epsilon_{2,3}}{Z}(\epsilon_{3,3} + \frac{\epsilon_{2,3}}{2})$$

or:

$$\rho_2^{(3)} = \frac{[\epsilon_{2,3}]^2}{2Z} + \frac{\epsilon_{3,3}}{Z}[\epsilon_{2,3} - \frac{Z}{2}] \quad (\text{IV.39})$$

Recalling that $\rho_2^{(3)}$ is a measure of the curvature at the origin of the curve $\ln\psi_2$ at infinite dilution of X_2 versus X_3 , Fig. IV.3 illustrates the result of equation IV.39. Given the value of the slope $\epsilon_{2,3}$, the sign and the magnitude of the deviation from the straight line depends solely on the coefficient of self-interaction $\epsilon_{3,3}$. To obtain a negative curvature at high value of the slope $\epsilon_{2,3}$, a strongly negative value of $\epsilon_{3,3}$ is needed, while at (algebraic) low value of the slope, a positive value of $\epsilon_{3,3}$ is needed. Reversal of this effect occurs for $\epsilon_{2,3}$ at about half the value of the coordination number Z . In addition to Fig. IV.3, Table IV.3 is given to illustrate the orders of magnitude involved.

The quasi-chemical model also provided an expression for $\rho_2^{(2,3)}$. Equations (III.19, III.7) and (IV.31) yield:

$$\rho_2^{(2,3)} = -\epsilon_{2,3} + 2\phi_{2,1} = -\epsilon_{2,3} + 2Z\mu(\lambda_{1,2} + \mu/2) \quad (\text{IV.40})$$

Therefore:

$$\rho_2^{(2,3)} = -\epsilon_{2,3} + \frac{2\epsilon_{2,3}}{Z}(\epsilon_{2,2} + \frac{\epsilon_{2,3}}{2}) \quad (\text{IV.41})$$

or:

$$\rho_2^{(2,3)} = \frac{\epsilon_{2,3}}{Z}[2\epsilon_{2,2} + \epsilon_{2,3} - Z] \quad (\text{IV.42})$$

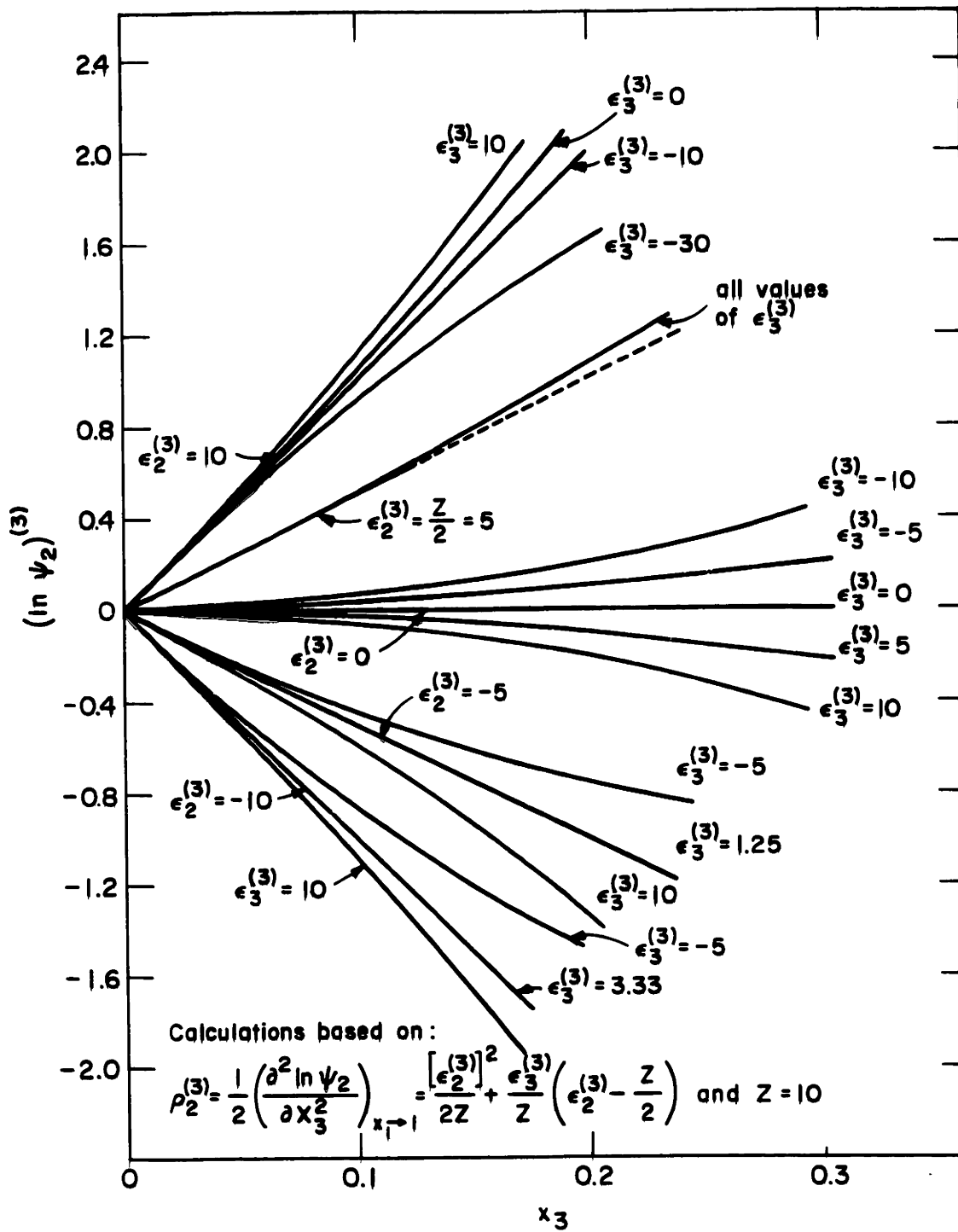


FIG. IV.3 CURVATURES PREDICTED BY THE QUASI-CHEMICAL MODEL

TABLE IV.3

Predicted Values* of $\rho_2^{(3)}$ by the Quasi-Chemical Model

$\epsilon_{2,3} \backslash \epsilon_{3,3}$	-20	-10	-5	0	2	5	10
-20	70	45	32.5	20	15	7.5	- 5
-10	35	20	12.5	5	2	-2.5	-10
- 5	21.25	11.25	6.25	1.25	-0.75	-4.75	- 9.75
0	10	5	2.5	0	-1	-2.5	- 5
2	6.2	3.2	1.7	0.2	-0.4	-1.3	- 2.8
5	1.75	1.25	1.25	1.25	1.25	1.25	1.25
8	-2.8	0.2	1.7	3.2	3.8	4.7	6.2
10	-5	0	2.5	5	6	7.5	10

* Calculations based on equation IV.39 and $Z = 10$

However, it must be recognized that the prediction of the cross effect, represented by $\rho_2^{(2,3)}$, is equivalent to the previously analyzed prediction of a curvature represented by $\rho_2^{(3)}$ or $\rho_3^{(2)}$, since by equation (III.19):

$$\rho_2^{(2,3)} + \varepsilon_{2,3} = 2\rho_3^{(2)} + \varepsilon_{2,2}$$

The choice of estimating $\rho_2^{(2,3)}$ or $\rho_3^{(2)}$ is a matter of convenience.

Before proceeding to test the prediction of these coefficients on a few examples, it is emphasized that, on one hand, the experimental values of ρ are, generally, very unprecise and, on the other hand, not more than a qualitative agreement is to be expected for these high order coefficients. However, as explained in Chapter III, even a qualitative estimate of ρ will yield a better quantitative estimate of the activity coefficient.

6.2 Comparison with Experimental Results

As many of the experimental results are expressed in weight percent, the conversion relationship between $\rho_2^{(3)}$ and $r_2^{(3)}$ (Appendix C) is recalled:

$$r_2^{(3)} = \frac{0.434 \times 10^{-4}}{M_3^2} [M_1^2 \rho_2^{(3)} - M_1(M_1 - M_3)\varepsilon_{2,3} + 1/2(M_1 - M_3)^3] \quad (\text{IV.43})$$

or:

$$\rho_2^{(3)} = \frac{230M_3}{M_1^2} [10^2 \cdot M_3 \cdot r_2^{(3)} + (M_1 - M_3)\varepsilon_{2,3}] + 1/2 \left(\frac{M_1 - M_3}{M_1} \right)^2 \quad (\text{IV.44})$$

It is interesting to note that, in the plot of $\log f_2$ versus weight percent of component 3, a light element 3 will favor a pronounced curvature, merely because its mass enters as a square in the denominator of equation IV.43.

In calculating the second order coefficients by the quasi-chemical result in equation IV.39, some of the experimental corresponding first order coefficients had to be redetermined using the correct conversion relationship between ϵ and e (Appendix C). This study of the comparison between predicted and experimental values is limited to the effects of alloying elements on the behavior of sulfur, oxygen, carbon, nitrogen and hydrogen in liquid iron. A coordination number of 11 is chosen for the calculations. The data are analyzed in detail in the following sections, and the results summarized in Table IV.4.

6.2.1 Sulfur in liquid iron alloys

Sherman and Chipman's experiments⁽¹²⁾ show pronounced curvatures in the plots of $\log f_S$ versus weight percent of carbon, silicon, phosphorus and copper. The effect of manganese is discarded, as the data on the self-interaction coefficient $\epsilon_{Mn}^{(Mn)}$ are not reliable enough to calculate a value of $\rho_S^{(Mn)}$ by equation IV.39. For carbon, the reciprocal coefficient $\epsilon_C^{(S)}$ was measured by Fuwa and Chipman⁽¹⁸⁾ and found larger^(12,3) than $\epsilon_S^{(C)}$ (6,4). It may be noted that an increase in the adopted value of $\epsilon_S^{(C)}$ reduces the experimental value of $\rho_S^{(C)}$ and increases the predicted one. The self-interaction coefficient for phosphorus is positive, but its value is uncertain. Its effect is small, however, on the calculated

TABLE IV.4

Experimental and Calculated* Values of the Second Order
Interaction Coefficient $\rho_2^{(3)}$ in Liquid Iron Alloys

Solute (2)	Solute (3)	$\epsilon_3^{(3)**}$	$e_2^{(3)}$	$\epsilon_2^{(3)}$	$r_2^{(3)} \times 10^2$ (exp)	$\rho_2^{(3)}$ (exp)	$\rho_s^{(3)}$ (calc*)	Ref.
S	C	11.7	0.113	6.4	0.7	12	3	12
	Si	13	0.065	8.1	0.3	21	7.5	12
	P	(+)?	0.043	6.0	0.10	9.5	2	12
	Cu	- 5.6	-0.017	- 4.6	0.05	15	6	12
O	Co	0	0.007	1.6	0.01	2.5	0.2	19
	Cu	- 5.6	-0.0095	- 2.5	0.01	3.3	4.3	19
N	Cr	0	-0.045	- 9.6	0.04	7.3	8.4	20
	Si	13	0.047	5.9	0.12	9.7	3.7	20
	V	3	-0.10	-20.9	0.14	25	13	20
C	Co	0	0.012	2.9	-0.01	- 2.7	0.4	18
	Cu	- 5.6	0.016	4.1	-0.012	- 4.1	1.5	18
H	B	(+8)?	0.050	3.1	0.20	3.8	(-1.2)?	21
	C	11.7	0.060	3.8	0.50	8	-1.1	21
	Cb	(+4)?	-0.0023	- 1.54	-0.01	- 5.7	(-2.5)?	21
	Cr	0	-0.0022	- 0.4	-0.004	- 0.8	0.0	21
	S	- 3.3	0.008	1.5	0.07	5.8	1.3	21

* Calculations based on equation IV.39, with $Z = 11$

** Recalculated values from Appendix C

value of $\rho_S^{(P)}$, as it enters equation IV.39, by multiplying $(\epsilon_S^{(P)} - \frac{Z}{2})/Z$ which is small. The data for copper⁽¹²⁾ indicates a positive curvature, although the authors draw a straight line. The values listed in Table IV.4 are obtained from the curve.

The comparison between experimental and calculated values of $\rho_S^{(3)}$ is satisfactory in all the cases analyzed.

6.2.2 Oxygen in liquid iron alloys

The effects of alloying elements on the activity of oxygen was studied by Floridis and Chipman.⁽¹⁹⁾ The only pronounced curvatures in the line $\log f_0$ versus weight percent of the alloying element occur for cobalt and copper. These curvatures are very small and uncertain for molybdenum and tungsten. For this last element, however, it would be surprising to find an almost straight line ($r_0^{(W)} = 0$), merely because of a mass effect. In equation IV.43, with a value of $\epsilon_0^{(W)}$ equal to 3.8, the sum $M_1(M_3 - M_1)\epsilon_0^{(W)} + 1/2(M_1 - M_3)^2$ is positive and quite large; to balance its effect, $M_1^2 \rho_0^{(W)}$ should be large and negative, so that a value of about -31 is required for $\rho_0^{(W)}$. Given the moderate effect of tungsten on oxygen, as measured by $\epsilon_0^{(W)}$ (+3.8), such a large negative value seems improbable and, consequently, a positive value of $r_0^{(W)}$ quite certain.

The experimental and calculated values for cobalt and copper, listed in Table IV.4, provide satisfactory agreement.

6.2.3 Nitrogen in liquid iron alloys

The effect of alloying elements on the activity of nitrogen in liquid iron was studied by Pehlke and Elliott.⁽²⁰⁾

Positive curvatures seem to be well established, in the case of chromium, silicon and vanadium, and the agreement with the predicted values is fair in all three cases. In the case of carbon, the authors⁽²⁰⁾ have drawn a negative curvature. The data do not seem accurate enough to definitely support it. However, it is interesting to note that the predicted value of $\rho_N^{(C)}$ (+5.3) is small enough to be offset by a mass effect and the result is a predicted negative value for $r_N^{(C)}$ (-0.02×10^{-2}). The values adopted in these calculations for $\epsilon_C^{(C)}$ and $\epsilon_N^{(C)}$ are 11.7 and 7.9, respectively.

6.2.4 Carbon in liquid iron alloys

The data of Fuwa and Chipman⁽¹⁸⁾ on the activity of carbon in liquid iron alloys are not very precise and, consequently, the scatter does not permit a precise evaluation of ρ . It is probable, however, that in the cases of cobalt and copper, the curvatures are negative. The comparison with the calculated values shows a much poorer agreement; however, as the magnitude of the second order effect is small in both cases, the test is not very conclusive.

6.2.5 Hydrogen in liquid iron alloys

The solubility of hydrogen in iron was studied extensively by Weinstein and Elliott.⁽²¹⁾ In their plot of the logarithm of the hydrogen activity coefficient versus weight percent of the alloying element, a curvature seems well established for boron, carbon, columbium, chromium and sulfur. No data are available on the Fe-B and Fe-Cb binary solutions to calculate the self-interaction

coefficients $\epsilon_B^{(B)}$ and $\epsilon_{Cb}^{(Cb)}$; however, values of about +8 and +4 may be assigned, respectively, as rough estimates, from comparison with neighboring elements in the Mendeleev classification. Comparing experimental and calculated values of $\rho_H^{(3)}$, the agreement is poor for boron and carbon. The predicted values of $\rho_H^{(3)}$ would become positive only if the interaction coefficients $\epsilon_H^{(3)}$ are above half the value of the coordination number ($\frac{Z}{2} = 5.5$) and, experimentally, $\epsilon_H^{(B)} = 3.1$, $\epsilon_H^{(C)} = 3.8$. The agreement is more satisfactory for columbium, chromium and sulfur.

6.3 Conclusions

An equation predicting the values of the second order interaction coefficients has been derived from the quasi-chemical model.

$$\rho_2^{(3)} = \frac{[\epsilon_{2,3}]^2}{2Z} + \frac{\epsilon_{3,3}}{2} [\epsilon_{2,3} - \frac{Z}{2}] \quad (\text{IV.39})$$

The values of $\rho_2^{(3)}$ obtained by this equation were compared with experimental ones provided by the study of the activities of sulfur, oxygen, carbon, nitrogen and hydrogen in liquid iron alloys (Table IV.4), and a reasonably good qualitative agreement was obtained. Agreement is poorest for elements of small radii. This result was to be expected, as the lattice model used assumed "substitutional" solutions rather than "interstitial" ones, although these terms lose their strict definition in a liquid.

7. Summary and Conclusions

The values of the first and second order free energy interaction coefficients predicted by the quasi-chemical model

were shown to be in reasonably fair agreement with the experimental values. The advantage of the quasi-chemical model over many other models is the simplicity of its application, because of the restricted number of parameters to be fixed ($\frac{m(m-1)}{2}$ in a system of m components). There are two assumptions in particular, which are subject to criticism. The first is the assumption of pairwise interactions, or of the non-dependence of the bonding energies (as measured by the parameters ω) on the concentrations of the solutes. Its most drastic effect is on the value of the zeroth order interaction coefficient $\ln \gamma^0$, but, by adopting the reference state of infinite dilution of the corresponding solute in the solvent, this difficulty may be eluded. In practical applications, the variations of ω probably are sufficiently slow to permit fair prediction of the first and second order free energy interaction coefficients.

The second assumption is the neglect of the vibrational contribution, with the consequence that the only excess entropies taken into account are configurational - thus, negative. This contradiction with the experimental evidence of frequent positive excess entropies is sufficient to cast a doubt on the validity of the application of the model to the free energy terms. Nevertheless, the model is frequently successful in predicting free energy terms, even though in many cases the contribution of the excess entropy to the excess free energy is by no means negligible. The next chapter studies a way of removing these two assumptions, and partially explains the surprising success of the quasi-chemical model in the free energy terms for systems with large positive excess entropies.

CHAPTER V
THE CELL MODEL

1. Introduction

In Chapter IV, the usefulness of the quasi-chemical model was found to be limited mainly by the inadequacy of two assumptions. First, the bonding energy between two atoms is treated as independent of its surroundings. Second, all vibrational contributions to the excess thermodynamic properties are neglected. The removal of these assumptions will introduce many complications, but the more accurate a model is to be, the more intricate it becomes (certainly a consequence of the empirical "law of diminishing returns"!) At a certain stage of the development which follows in the next sections, the assumption of pairwise interaction will be reintroduced, but, then, its application will constitute only a particular case of a more general model, and the significance of this assumption will be appreciated better.

The treatment given in this chapter draws heavily on the cell model of the liquid state, first introduced by Eyring⁽²²⁾ in 1936 and Eyring and Hirschfelder⁽²³⁾ in 1937. For densities as high as those in the liquid state, far below the critical temperature, a certain order may be expected in the distribution of the atoms. Inter-atomic distances between first neighbors, smaller than the atomic diameter, are prohibited by large repulsive forces, and distances much larger are statistically unlikely. This introduces a regularity in the spacing of neighboring atoms, with a mean interatomic distance of the

order of the atomic diameter. Consequently, it is assumed that each atom is confined to its own cell. The field acting on each atom in its cell is rapidly fluctuating, and then may be replaced by an average field of spherical symmetry.

In the application of this model, we chose to describe the partition function in terms of probabilities associated with different configurations in the nearest neighbor shell (the configurations mostly depending upon the number of atoms present of any one kind) and in terms of the influence of those configurations on the field of spherical symmetry acting on the central atom.

2. Partition Function of a Binary Solution

The partition function of a binary solution of N_A atoms A and N_B atoms B is approximated by the following formula:

$$Q = q_A^{N_A} q_B^{N_B} \sum g e^{-E/kT} \quad (V.1a)$$

q_A and q_B are the average partition functions of the atoms A and B. The summation is extended over all the possible levels of the configurational potential energy E , and g is the degeneracy of a level, or the number of possible arrangements of atoms A and B, corresponding to the same value of the energy E . The maximum term method⁽⁹⁾ (classical approximation in statistical mechanics, and already used in the quasi-chemical model - Appendix D) allows the replacement of the sum by its maximum term:

$$Q = q_A^{N_A} q_B^{N_B} \bar{g} e^{-\bar{E}/kT} \quad (\text{V.1b})$$

In the cell theory, ⁽¹⁰⁾ q_A and q_B may be expressed as:

$$q_A = \frac{v_f^A e h^3}{(2 \pi m_A kT)^{3/2}} ; \quad q_B = \frac{v_f^B e h^3}{(2 \pi m_B kT)^{3/2}} \quad (\text{V.2})$$

where m_A and m_B are the masses of atoms A and B, h is Planck's constant, and v_f the "free volume". The main feature of q is that it is proportional to v_f , which depends on the composition of the solution. The constant of proportionality disappears in the expression of the excess properties. An analysis of the term v_f is given in the next section.

3. "Free Volume"

The interaction potential ψ , between a given atom and all other atoms, is assumed to be spherical and a function of the position r in the cell; the origin $r = 0$ is located at the minimum of ψ , i.e., at the equilibrium position. The probability of observing the central atom in a given element of volume is not uniform throughout the cell, but must be obtained from a Boltzman factor. If $\psi(r) = \psi(0)$, the "effective" volume occupied by the atom would simply be:

$$v = \int_{\text{cell}} dr = \frac{V}{N}$$

However, with $\psi(r) - \psi(0) \neq 0$, v is replaced by:

$$v_f = \int_{\text{cell}} e^{-[\psi(r) - \psi(0)]/kT} dr \quad (\text{V.3})$$

Under the simplifying assumption that the potential ψ of an atom is parabolic with respect to the distance r , it is shown in Appendix (F) that v_f may be approximated by:

$$v_f = \left[\frac{1}{2\pi kT} \left(\frac{\partial^2 \psi}{\partial r^2} \right) \right]^{-3/2} \quad (V.4)$$

Note that the compressibility χ is equal to $-\frac{1}{v} \frac{\partial v}{\partial p}$, or by expressing p as $-\frac{\partial E}{\partial v}$:

$$\frac{1}{\chi} = -v \frac{\partial p}{\partial v} = -v \frac{\partial^2 E}{\partial v^2} \quad (V.5)$$

In the calculations used to establish the bonding energy, the energy per atom is obtained as a function of r_s , defined in such a way that:

$$v = \frac{4}{3} \pi r_s^3 \quad (V.6)$$

Therefore:

$$\frac{1}{\chi} = \frac{1}{12\pi r_s} \left(\frac{\partial^2 E}{\partial r^2} \right) = \frac{1}{12\pi r_s} \times \frac{\partial^2 \psi}{\partial r^2} \quad (V.7)$$

and v_f is thus proportional to $\chi^{3/2}$.

v_f may also be related to an Einstein's characteristic temperature since:

$$\theta = \frac{h\nu}{k} = \frac{2\pi h}{k} \frac{f}{m} = \frac{2\pi h}{km^{1/2}} \times \left(\frac{\partial^2 \psi}{\partial r^2} \right)^{1/2} \quad (V.8)$$

where ν is the vibrational frequency of the corresponding harmonic oscillator and f the force acting on this oscillator.

These results may be summarized by expressing the proportionality of the following terms: q , v_f , $(\frac{\partial^2 \psi}{\partial r^2})^{-3/2}$, $\chi^{3/2}$, θ^{-3} :

$$d \ln q = d \ln v_f = -\frac{3}{2} d \ln \left(\frac{\partial^2 \psi}{\partial r^2} \right) = \frac{3}{2} d \ln \chi = -3 d \ln \theta \quad (\text{V.9})$$

4. Probabilities Associated with Different Configurations

Different configurations of atoms A and B are possible around a central atom A or B. The probabilities assigned to each of these configurations has to be examined. It is reasonable to assume that g and E , determined by the maximum term method, will correspond to these probabilities.

In a random solution, where the configurational entropy is ideal, the probability for an atom A to be surrounded in the nearest shell by i atoms B and $(Z-i)$ atoms A is $C_Z^i X_A^{Z-i} X_B^i$, where C_Z^i is the combinatorial factor $\frac{Z!}{(Z-i)!i!}$. In a non-random solution, a correction factor $f(A, iB)$ must be introduced. The following notation is adopted. The first letter in the parenthesis identifies the central atom. The second term identifies the number of B atoms among the Z nearest neighbors. As the value of f is relative, it is possible to choose:

$$f(A \text{ or } B, 0B) = 1 \quad (\text{V.10})$$

f may be, for instance, a Boltzman factor:

$$f(A, iB) = \exp(-U_{iB}^A/kT) \quad (\text{V.11a})$$

$$f(B, iB) = \exp(-U_{iB}^B/kT) \quad (\text{V.11b})$$

where U_{1B}^A (or U_{1B}^B) is the energy of the central atom A (or B) when surrounded by i atoms B (and $(Z-i)$ atoms A), relative to the state where it is surrounded by $0B$ or all atoms A. It is not necessary, however, to specify at this stage the value of $f(A, iB)$. Its main feature is that it is independent of the concentrations of A and B in the solution.

The probability associated with the configuration (A, iB) becomes:

$$P_{iB}^A = \frac{C_Z^i X_A^{Z-i} X_B^i f(A, iB)}{P} \quad (V.12)$$

where P is a normalizing factor:

$$P = \sum_{i=0}^Z C_Z^i X_A^{Z-i} X_B^i f(A, iB) \quad (V.13)$$

since all the probabilities p_{iB}^A must add to 1.

A series expansion of p_{iB}^A , with respect to X_B , yields:

$$P_{0B}^A = 1 - ZX_B f(A, 1B) + ZX_B^2 \left\{ f^2(A, 1B) - \frac{Z-1}{2} f(A, 2B) - f(A, 1B) \right\} + O(X_B^3) \quad (V.14a)$$

$$P_{1B}^A = ZX_B f(A, 1B) - ZX_B^2 f(A, 1B) [Zf(A, 1B) - 1] + O(X_B^3) \quad (V.14b)$$

$$P_{2B}^A = \frac{Z(Z-1)}{2} X_B^2 f(A, 2B) + O(X_B^3) \quad (V.14c)$$

p_{iB}^B is obtained in a parallel way. Its expression is identical to that of p_{iB}^A , after replacing $f(A, iB)$ by $f(B, iB)$.

5. Excess Enthalpy and Vibrational Entropy

A simplifying assumption is now introduced, which will be reconsidered in section 8. The correcting factors f are assumed to be practically independent of the temperature. As:

$$F = - kT \ln Q \quad (V.15)$$

or:

$$F = \bar{E} - T(k \ln \bar{g} + k \ln q_A^{N_A} q_B^{N_B}) \quad (V.16)$$

therefore:

$$H = \bar{E} \quad (V.17)$$

$$S = k(\ln \bar{g} + \ln q_A^{N_A} q_B^{N_B}) \quad (V.18)$$

5.1 Excess Enthalpy

H may be expressed as:

$$H = \bar{E} = \frac{1}{2} X_A \sum_{i=0}^Z p_{iB}^A U_{iB}^A + \frac{1}{2} X_B \sum_{i=0}^Z p_{iB}^B U_{iB}^B \quad (V.19)$$

U_{iB}^A (or U_{iB}^B) is the energy term defined in the previous section. It is equal to the change of the potential energy of the central atom A (or B), when i atoms B are substituted for i atoms A in a first shell of all A atoms. The factor of $1/2$ is introduced to avoid counting twice the bonding energies.

The excess enthalpy is obtained by subtracting the contributions of the pure components A and B.

$$H^E = \bar{E} - X_A E_A - X_B E_B = \bar{E} - \frac{1}{2} X_A U_{0B}^A - \frac{1}{2} X_B U_{ZB}^B \quad (V.20)$$

and, by equations (V.19) and (V.20), H^E may be expressed as:

$$H^E = -\frac{1}{2}X_B \left\{ U_{ZB}^B - Zf(A, 1B)U_{1B}^A \right\} + \frac{Z}{2}X_B^2 \left\{ f(B, 1B)U_{1B}^B - Zf^2(A, 1B)U_{1B}^A + \frac{Z-1}{2}f(A, 2B)U_{2B}^A \right\} + O(X_B^3) \quad (V.21)$$

5.2 The Excess Vibrational Entropy

The entropy of the solution has been identified as

$$S = k[\ln \bar{g} + \ln(q_A^{N_A} q_B^{N_B})] \quad (V.18)$$

It may be seen that the configurational entropy arises solely from the term $k \ln \bar{g}$. In an ideal solution, it equals:

$$k \ln \bar{g} = k \ln \frac{(N_A + N_B)!}{N_A! N_B!} = -k(N_A \ln \frac{N_A}{N_A + N_B} + N_B \ln \frac{N_B}{N_A + N_B})$$

and another expression was obtained by the quasi-chemical model (Appendix D). Therefore it is possible to distinguish between the configurational and vibrational entropy:

$$S_{\text{conf}} = k \ln \bar{g} \quad (V.22)$$

$$S_{\text{vib}} = k \left\{ \ln q_{(A)}^{N_A} + \ln q_{(B)}^{N_B} \right\} \quad (V.23)$$

Among the N_A atoms A, $p_{iB}^A N_A$ are in the configuration (A, iB) associated with a value of q_A equal to q_{iB}^A . Thus:

$$S_{\text{vib}} = k \left[N_A \sum_{i=0}^Z p_{iB}^A \ln q_{iB}^A + N_B \sum_{i=0}^Z p_{iB}^B \ln q_{iB}^B \right] \quad (\text{V.24})$$

Note the similarity with equation V.19 for the enthalpy; the parallelism is pursued in obtaining the excess vibrational entropy, by subtraction of the contributions of the pure components. For a solution of 1 mole:

$$S_{\text{vib}}^E = R X_A \left\{ \left(\sum_{i=0}^Z p_{iB}^A \ln q_{iB}^A \right) - \ln q_{0B}^A \right\} + R X_B \left\{ \left(\sum_{i=0}^Z p_{iB}^B \ln q_{iB}^B \right) - \ln q_{0B}^B \right\}$$

or:

$$\frac{S_{\text{vib}}^E}{R} = X_A \sum_{i=0}^Z p_{iB}^A \delta \ln q_{iB}^A + X_B \sum_{i=0}^Z p_{iB}^B \delta \ln q_{iB}^B - X_B \delta \ln q_{0B}^B \quad (\text{V.25})$$

where:

$$\delta \ln q_{iB}^A = \ln \frac{q_{iB}^A}{q_{0B}^A} \quad \text{and} \quad \delta \ln q_{iB}^B = \ln \frac{q_{iB}^B}{q_{0B}^B} \quad (\text{V.26})$$

and, replacing the probabilities p_{iB}^A and p_{iB}^B by their series expansion with respect to X_B ,

$$\begin{aligned} \frac{S_{\text{vib}}^E}{R} = & - X_B \left\{ \delta \ln q_{0B}^B - Z f(A, 1B) \delta \ln q_{1B}^A \right\} + Z X_B^2 \left\{ f(B, 1B) \delta \ln q_{1B}^B \right. \\ & \left. - Z f^2(A, 1B) \delta \ln q_{1B}^A + \frac{Z-1}{2} f(A, 2B) \delta \ln q_{2B}^A \right\} + O(X_B^3) \quad (\text{V.27}) \end{aligned}$$

The striking similarities of the expression of H^E and S_{vib}^E (equations V.21 and V.27) will be exploited now.

6. "Quasi-Regular Solutions"

In a random solution, the factors f are equal to 1. The regular solution theory assumes, in addition, pairwise interactions to compute the energy terms. Applying these assumptions here immediately yields:

$$U_{iB}^A = i(u_{AB} - u_{AA})$$

$$U_{iB}^B = i(u_{BB} - u_{BA}) = i(u_{BB} - u_{AB})$$

Thus, H^E becomes:

$$H^E = -\frac{1}{2} X_B \left\{ Z(u_{BB} - u_{AB}) - (u_{AB} - u_{AA}) \right\} \\ + \frac{Z}{2} \left\{ (u_{BB} - u_{AB}) - Z(u_{AB} - u_{AA}) + (Z-1)(u_{AB} - u_{AA}) \right\}$$

or, after simplification:

$$H^E = ZX_B \omega_{AB} - ZX_B^2 \omega_{AB} = ZX_A X_B \omega_{AB} \quad (V.28)$$

where:

$$\omega_{AB} = u_{AB} - \frac{u_{AA} + u_{BB}}{2} \quad (V.29)$$

which as expected is the result of the regular solution theory.

It is now proposed to adopt an assumption of pairwise interactions for the entropy, as well as for the energy. $\ln q_{iB}^A$ is

the relative change occurring in the characteristic vibrational partition function of atom A, when surrounded by i atoms B and $(Z-i)$ atoms A. Under the pairwise interaction assumption, it is then possible to write:

$$\delta \ln q_{iB}^A = i \delta \ln q_{1B}^A \quad (\text{V.30a})$$

and

$$\delta \ln q_{iB}^B = i \delta \ln q_{1B}^B \quad (\text{V.30b})$$

Therefore, equation V.27 becomes:

$$S_{\text{vib}}^E = -X_B (Z \delta \ln q_{1B}^B - Z \delta \ln q_{1B}^A) + ZX_B^2 (\delta \ln q_{1B}^B - Z \delta \ln q_{1B}^A + \frac{Z-1}{2} \cdot 2 \delta \ln q_{1B}^A)$$

or, after arrangement:

$$S_{\text{vib}}^E = ZX_A X_B (\delta \ln q_{1B}^A - \delta \ln q_{1B}^B) \quad (\text{V.31})$$

Let:

$$\varpi_{AB} = R (\delta \ln q_{1B}^A - \delta \ln q_{1B}^B) \quad (\text{V.32})$$

Then, equation V.31 is rewritten:

$$S_{\text{vib}}^E = ZX_A X_B \varpi_{AB} \quad (\text{V.33})$$

The quasi-chemical theory shows, in particular, that the configurational excess entropy is of higher order:

$$S_{\text{conf}}^E = -X_A^2 X_B^2 \frac{\varpi_{AB}^2}{RT^2}$$

Therefore, in sufficiently dilute solutions, the configurational contribution may be neglected and S_{vib}^E assumed to represent the total excess entropy S^E :

$$S^E = S_{\text{vib}}^E = Z X_A X_B \omega_{AB} \quad (\text{V.34})$$

and, consequently:

$$F^E = Z X_A X_B (\omega_{AB} - T \tau_{AB}) \quad (\text{V.35})$$

The same result may be expressed in a slightly different way. Let:

$$\omega_{AB} = \tau_{AB} \varpi_{AB} \quad (\text{V.36})$$

Then, equation V.35 becomes:

$$F^E = Z X_A X_B \varpi_{AB} \left(1 - \frac{T}{\tau_{AB}}\right) \quad (\text{V.37})$$

Section 7 examines whether τ_{AB} is a physical constant or a parameter. If it can be predicted with sufficient accuracy, then this model becomes a one-parameter model which has the simplicity of the regular solution, but with the additional important advantage of predicting correctly excess entropies.

This single parameter model ($\tau_{AB} = \tau$) may be designated by the name of "First Quasi-Regular" model, and the two-parameter model (which identifies τ_{AB} as an adjustable parameter) by the name of "Second Quasi Regular" model. Actually, in practical applications, the distinction between these two models is a matter of convenience.

These results may be generalized, readily, to a system of m components:

$$F^E = \sum_{\substack{i=1 \\ i \neq j}}^m \sum_{j=1}^m Z X_i X_j \omega_{ij} \left(1 - \frac{T}{r_{ij}}\right) \quad (V.38)$$

$$H^E = \sum_{\substack{i=1 \\ i \neq j}}^m \sum_{j=1}^m Z X_i X_j \omega_{ij} \quad (V.39)$$

and

$$S^E = \sum_{\substack{i=1 \\ i \neq j}}^m \sum_{j=1}^m Z X_i X_j \left(\frac{\omega_{ij}}{r_{ij}}\right) \quad (V.40)$$

where:

$$\omega_{ij} = u_{ij} - \frac{u_{ii} + u_{jj}}{2} = (\delta U_{1B}^A - \delta U_{1B}^B) \quad (V.41)$$

and:

$$r_{ij} = \frac{\omega_{ij}}{\varpi_{ij}} \quad \text{with} \quad \varpi_{ij} = R(\delta \ln q_{1B}^A - \delta \ln q_{1B}^B) \quad (V.42)$$

For a "First Quasi-Regular Solution", all the r_{ij} are equal to r , while for a "Second Quasi-Regular Solution" all the r_{ij} may be different.

The simplicity of these two models is attractive. They introduce some critical assumptions which, however, are not unreasonable. An analysis of the consequences of these models and a comparison with experimental data are made in the context of a more general study in the following section.

7. Correlation Between Excess Enthalpy and Excess Entropy

Comparing equation V.21 and V.27, one sees immediately that it is possible to pass from the expression of H^E to that of $\frac{S_{vib}^E}{R}$ by the mere change of $\frac{1}{2}U_{iB}^A$ to $\delta \ln q_{iB}^A$ and $\frac{1}{2}U_{iB}^B$ to $\delta \ln q_{iB}^B$. It is always possible to write:

$$\frac{1}{2}U_{iB}^A = R \tau_{iB}^A \delta \ln q_{iB}^A \quad (V.43)$$

and, since the changes $\delta \ln q$ are expected to be small, equation V.9 yields:

$$\frac{1}{2}U_{iB}^A = R \tau_{iB}^A \delta \ln q_{iB}^A = - \frac{3R}{2} \tau_{iB}^A = \frac{\delta \left(\frac{\partial^2 \psi}{\partial r^2} \right)_{iB}^A}{\left(\frac{\partial^2 \psi}{\partial r^2} \right)_{OB}^A} = \frac{3R}{2} \frac{\delta X_{iB}^A}{X_{OB}^A} \quad (V.44)$$

If the constant τ_{iB}^A is independent of i , this means that a change in the configuration around the central atom A is reflected by a proportional change in the compressibility or, in other words, the "depth of the potential well" is proportional to its curvature. In a dilute system (thus, for i small) τ_{iB}^A and τ_{iB}^B may be reasonably assumed to be independent of i and consequently:

$$\frac{1}{2}U_{iB}^A = R \tau_A \delta \ln q_{iB}^A ; \quad \frac{1}{2}U_{iB}^B = R \tau_B \delta \ln q_{iB}^B \quad (V.45)$$

In the expressions of H^E and S_{vib}^E (equations V.21 and V.25), the terms involving a central atom A may be separated from the terms involving a central atom B:

$$H^E = H_{(A)}^E + H_{(B)}^E \quad (V.46)$$

and

$$S_{\text{vib}}^E = S_{\text{vib}(A)}^E + S_{\text{vib}(B)}^E \quad (V.47)$$

Therefore, from equations V.19 and V.24, it may be seen that:

$$H_{(A)}^E = r_A S_{\text{vib}(A)}^E ; H_{(B)}^E = r_B S_{\text{vib}(B)}^E \quad (V.48)$$

and

$$H^E = r_A S_{\text{vib}(A)}^E + r_B S_{\text{vib}(B)}^E \quad (V.49)$$

The ordering factors f were assumed to be practically independent of the temperature in the two previous sections (6 and 7), and also in this derivation. With the following notation:

$$q = q_A^{N_A} q_B^{N_B} - (\text{contributions of the pure components A and B}) \quad (V.50)$$

$$\ln g = \ln \bar{g} - \ln g_{\text{ideal}} = \ln \bar{g} - N_A \ln X_A - N_B \ln X_B \quad (V.51)$$

the vibrational and configurational entropies were identified readily as:

$$S_{\text{vib}}^E = k \ln q \quad (V.52)$$

$$S_{\text{conf}}^E = k \ln g \quad (V.53)$$

and the excess entropy of the solution was:

$$S^E = S_{\text{vib}}^E + S_{\text{conf}}^E \quad (\text{V.54})$$

With the removal of the assumption that f is independent of T , another term is now introduced in equation V.54:

$$S^E = S_{\text{vib}}^E + S_{\text{conf}}^E + \left\{ kT \left[\frac{\partial \ln q}{\partial T} + \frac{\partial \ln g}{\partial T} \right] - \frac{\partial E}{\partial T} \right\} \quad (\text{V.55})$$

or:

$$S^E = S_{\text{vib}}^E + S_{\text{conf}}^E + S_{\text{corr}}^E \quad (\text{V.56})$$

Equation V.55 was obtained through relations V.16, V.15 and the following thermodynamic formula:

$$S^E = - \frac{\partial F^E}{\partial T} \quad (\text{V.57})$$

It is obvious that the term TS_{corr}^E is now to be added to the previous definition of H^E (equation V.49), so that:

$$H^E = \tau_A S_{\text{vib}}^E(A) + \tau_B S_{\text{vib}}^E(B) + TS_{\text{corr}}^E \quad (\text{V.58})$$

The two proportionality constants τ_A and τ_B are not expected to be equal. However, the variation of τ with the nature of the central atom (A or B) may be of less importance than the variations of U and $\delta \ln q$, with changes in the configurations of the atomic shells, and, consequently, it is reasonable to assume:

$$\tau_A = \tau_B = \tau \quad (\text{V.59})$$

The term S_{conf}^E is expected to be much smaller than S_{vib}^E and, as the order of magnitude of τ will be seen in section 8 to be comparable to the temperatures T usually considered in liquid metallic solutions (1000 to 2000°K), it follows that:

$$H^E \approx \tau(S_{\text{vib}(A)}^E + S_{\text{vib}(B)}^E + S_{\text{corr}}^E) \quad (\text{V.60})$$

and

$$H^E \approx \tau(S_{\text{vib}}^E + S_{\text{corr}}^E) \quad (\text{V.61})$$

or:

$$H^E \approx \tau(S^E - S_{\text{conf}}^E) \quad (\text{V.62})$$

It may be noted that this last result was also obtained in a different way, by the assumption of pairwise interactions (section 7). Important consequences may be deduced from the proportionality expressed in equation V.62, but a preliminary result must be established first.

An expression for the excess configurational entropy is not developed in this study. Instead, it is reasonable to adopt the quasi-chemical result derived from equations IV.13 and V.57 .

$$S_{\text{conf}}^E = - Z \left(\frac{\omega_{AB}}{RT} \right) X_B^2 + O(X_B^3) \quad (\text{V.63})$$

With this expression of S_{conf}^E , it is noted that the contribution of S_{conf}^E to the zeroth order interaction coefficients $S_B^{E^0}$ and $\ln \gamma_B^0$ is

null, since there is no linear term with respect to X_B in equation V.63. Its contribution to the first order interaction coefficient is small, since it involves the square of ω :

$$\frac{\sigma_{2,2(\text{conf})}}{R} = - 2Z \left(\frac{\omega}{RT}\right)^2 \quad (\text{V.64})$$

$\sigma_{2,2(\text{conf})}$ is to be compared to $\varepsilon_{2,2}$, since:

$$\varepsilon_{2,2} = \frac{n_{2,2}}{RT} - \frac{\sigma_{2,2}}{R} \quad (\text{V.65})$$

But, by the quasi-chemical:

$$\varepsilon_{2,2} \approx - \frac{2Z\omega}{RT} \quad (\text{V.66})$$

Thus:

$$\frac{\sigma_{2,2(\text{conf})}}{R} = - \varepsilon_{2,2} \cdot \frac{\varepsilon_{2,2}}{2Z} \quad (\text{V.67})$$

and, therefore, $\sigma_{2,2(\text{conf})}$ may be neglected, since it is very often much smaller ($Z \approx 10$) than the terms to which it must be compared. It makes little difference if it is the quasi-chemical expression of $\varepsilon_{2,2}$, which is retained in equation V.66, instead of the quasi-regular expression, as this does not change the orders of magnitude involved. Consequently, it may be concluded that the proportionality of H^E and S^E (instead of $S^E - S_{\text{conf}}^E$) is valid up to and including the second order term in X_B .

$$H^E \approx \tau S^E \quad (\text{V.68})$$

or

$$F^E \approx H^E(1 - T/T_1) \quad (\text{V.69})$$

Extension of these equations to multi-component systems is straight forward.

If a relationship is found between the zeroth and first order enthalpy interaction coefficients:

$$f(H_1^{E^c}, \dots, H_j^{E^c}, n_{ii}, \dots, n_{ij}, \dots) = 0 \quad (\text{V.70a})$$

Then, because of equations V. 68 and V.69, the same functional relationship must hold for the entropy interaction coefficients:

$$f(S_1^{E^c}, \dots, S_j^{E^c}, \sigma_{ii}, \dots, \sigma_{ij}, \dots) = 0 \quad (\text{V.70b})$$

and the free energy interaction coefficients:

$$f(\ln\gamma_1^c, \dots, \ln\gamma_j^c, \epsilon_{ii}, \dots, \epsilon_{ij}, \dots) = 0 \quad (\text{V.70c})$$

In fact, any one of the three equations (V.70) yields the two others.

From equation V.37, it may be shown that the "quasi-regular" model yields:

$$n_{2,2} = -2H_2^{E^c} \quad (\text{V.71a})$$

$$\sigma_{2,2} = - 2S_2^{E^{\circ}} \quad (\text{V.71b})$$

and

$$\epsilon_{2,2} = - 2\ln\gamma_2^{\circ} \quad (\text{V.71c})$$

Also, from equation V.38:

$$h_{2,3} = (H_2^{E^{\circ}})_{\text{in (3)}} - (H_2^{E^{\circ}} + H_3^{E^{\circ}})_{\text{in (1)}} \quad (\text{V.72a})$$

$$\sigma_{2,3} = (S_2^{E^{\circ}})_{\text{in (3)}} - (S_2^{E^{\circ}} + S_3^{E^{\circ}})_{\text{in (1)}} \quad (\text{V.72b})$$

$$\epsilon_{2,3} = (\ln\gamma_2^{\circ})_{\text{in (3)}} - (\ln\gamma_2^{\circ} + \ln\gamma_3^{\circ})_{\text{in (1)}} \quad (\text{V.72c})$$

where all the terms on the right are binary terms. Chapter IV showed that the approximations of the regular solution theory and the quasi-chemical model, as expressed in equations V.71a, V.71c, V.72a and V.72c, were reasonably successful. However, it was not understood why these approximations were still successful, when applied to systems exhibiting large positive excess entropies. The reason is now clear. The parameter involved, ω , was improperly identified in terms of the physical properties to which it is related and, in view of the findings of this chapter, should be replaced by $\omega(1 - T/\tau)$, this change leading to a better evaluation of the entropy.

8. The Proportionality Constant τ

The importance of an a priori estimation of τ has been noted already. In dilute solutions, it would permit the evaluation of the enthalpy and entropy contributions from the free energy data or, inversely, would permit the evaluation of the free energy function from enthalpy data. In particular, it would allow the use of the simple first quasi-regular model instead of the more complicated second quasi-regular solution.

As shown in the previous section, τ measures the correlation between two effects: a change in the energy and the corresponding change in the compressibility. Is this correlation strongly dependent on the nature of the atoms involved? A partial answer to this question may be obtained from Fig. V.1, where $H_2^{E^\circ}$ is plotted versus $S_2^{E^\circ}$ for a wide variety of liquid solutions and disordered solid alloys. The zeroth order interaction coefficients were chosen, to eliminate the contribution of the configurational excess entropy. In spite of a considerable scatter (due, certainly, to questionable theoretical assumptions, but probably also to large experimental errors), the correlation is well established, indicating for τ a restricted range of permissible values.

Quite generally, an increase in the temperature tends to bring a system closer to ideality. Intuitively, τ then may be considered as the hypothetical state at which the system would become ideal ($F^E = 0$). A value of $3000 \pm 1000^\circ\text{K}$ is then suggested, which is within the permissible range of Figure V.1. The consideration of this hypothetical state, however, is only an appeal to intuition, and is not supported by any theoretical ground. Of more interest is

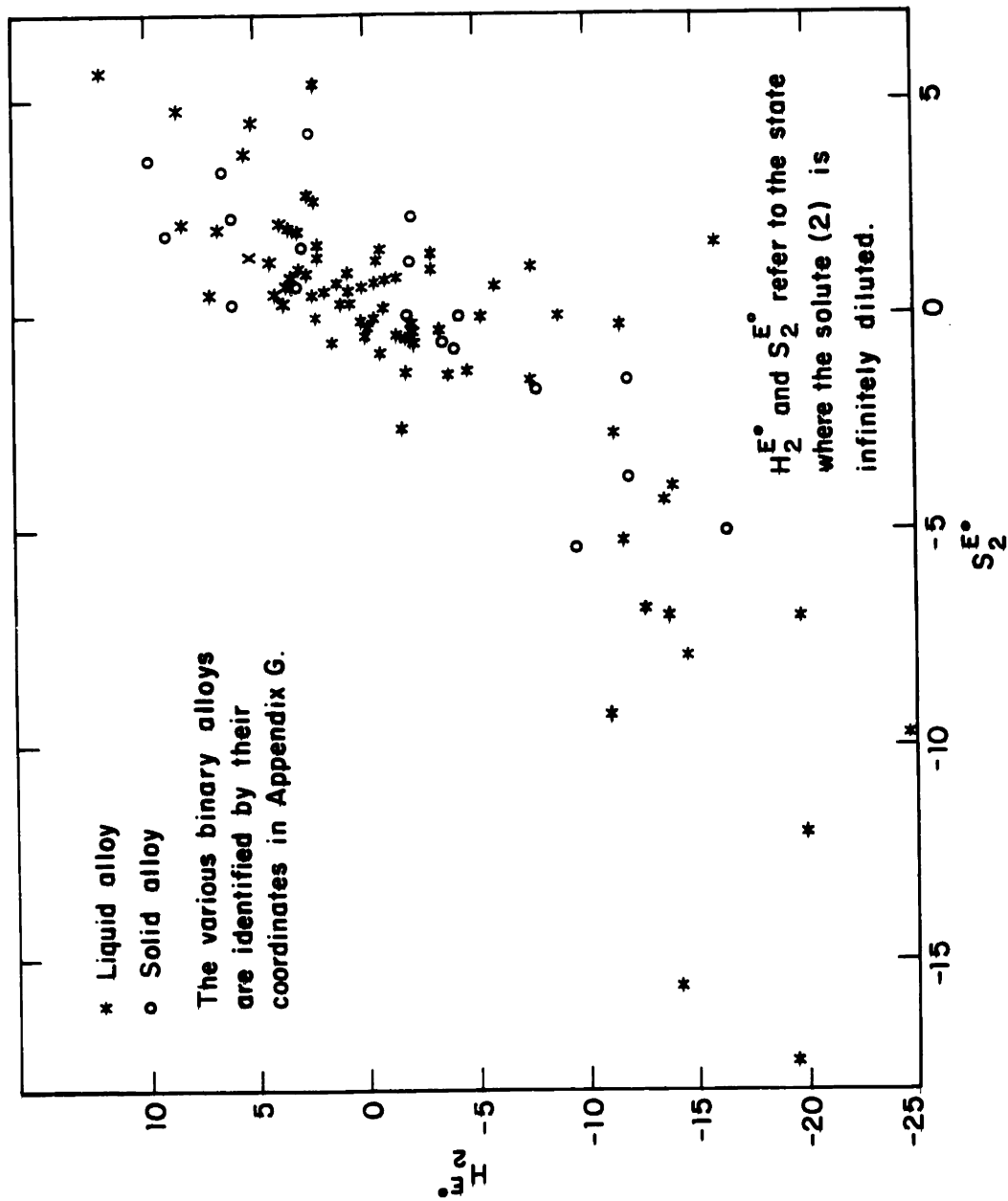


FIG. 1. CORRELATION BETWEEN EXCESS ENTHALPY AND ENTROPY.

the possible application of the electron theory of metals. As shown by the calculations of Blandin and Déplanté,⁽²⁴⁾ it should be possible to limit the variation of τ and to distinguish certain patterns by considering, for example, the effects of differences in valence between solvent and solute, or in considering the effects of different solutes on the same solvent.

This last idea is strongly supported by the empirical correlation of Chipman and Corrigan⁽²⁵⁾ between first order free energy and enthalpy interaction coefficients in ternary solutions. Plotting $\epsilon_2^{(i)}$ versus $n_2^{(i)}$ for different alloying elements (i), the authors accommodate, with little scatter, a straight line passing by the origin. Note that the smaller the scatter, the more constant is τ . According to the analysis of this chapter, the slope of this straight line is equal to:

$$\frac{\epsilon_{2,i}}{n_{2,i}} = \frac{n_{2,i}(1 - T/\tau)}{RT} \times \frac{1}{n_{2,i}} = \frac{1}{R} \left(\frac{1}{T} - \frac{1}{\tau} \right) \quad (\text{V.73})$$

It is simpler, however, to use the reported values of $T\sigma_{2,i}/n_{2,i}$, since

$$T\sigma_{2,i}/n_{2,i} = \frac{T}{\tau} \quad (\text{V.74})$$

The calculated values of τ are shown in Table V.1.

Except for the case of the solubility of hydrogen in liquid aluminum alloys, where the values are uncertain, all the values of τ are within the range of $3000 \pm 1000^\circ\text{K}$.

From all these experimental results, it seems possible,

TABLE V.1Calculated* Values of τ in Some Ternary Alloys

<u>Group</u>	<u>T, °K</u>	<u>$T\sigma_{2,i}/\eta_{2,i}$ **</u>	<u>τ</u>
Fe-N-i liquid	1873	.47	3900
Fe-N-i solid	1473	.66	2210
ln-S-i liquid	1673	.69	2390
Fe-H-i liquid	1865	.66	2800
Al-H-i liquid	1175	.76?	1550?

* Calculated by equation V.74

** Values reported by Chipman and Corrigan⁽²⁵⁾

therefore, to consider τ as a constant which value has to be selected, not for a particular solution but for a class of solutions. Interesting perspectives should then be opened, one of which would be the use of the "first quasi-regular" model for dilute solutions.

9. Conclusions

The Regular Solution model may be considered of a special case (for $\tau = \infty$) of the quasi-regular model. The superiority of the latter lies in the correct prediction of the excess entropy. In particular, the model explains the inconsistency of the quasi-chemical predictions which are fair for the free energy terms, but very unsatisfactory for the excess entropy terms. Its simplicity evidently has the advantages, as well as the drawbacks, of the Regular

Solution model. Both models apply best to dilute solutions.

For concentrated solutions, and more accurate results, many refinements are needed. Reference must be made to the general form of the model which expressed the thermodynamic properties of the solution as the weighted sum of relative changes in some related physical property, these changes being caused by variations in the configuration of the nearest neighbor's shell. The assumption of pairwise interaction gave a very simple form to the otherwise cumbersome expression of these changes, but it also over-simplified the description of the phenomena involved. It is probable that the use of even a simple functional dependence of these changes on electron concentrations will result in much better agreement. In that respect, Engel's correlations⁽²⁶⁾ seem particularly indicative. Also, it may be noted that the number of possible configurations is finite, so that the series expressions of the excess thermodynamic properties are also finite. Different coordination numbers for the solvent and the solute may be assumed, without complications in the expression of the probabilities associated with these different configurations (equation V.12). All these possible refinements indicate that the approach described in this chapter to the study of liquid metallic solutions may, very well, bring further useful results for the prediction and interpretation of thermodynamic properties.

CHAPTER VI
CONCLUSIONS ON THE THEORETICAL WORK

The introduction of generalized interaction coefficients permits a systematic and convenient analysis of the effects of alloying elements on a particular solute. The mathematical definition of these coefficients is particularly suitable to their study, by means of statistical models, since in many of the models the closed form of a function is analytically impossible, whereas the series expansion of this function is readily available.

An investigation of the chemical theory shows that the first order free energy interaction coefficient is satisfactorily predicted by the "Regular Solution" and "Quasi-Chemical" models, and that even the second order free energy interaction coefficient is qualitatively accounted for by the quasi-chemical theory. However, these models are very inadequate in their prediction of the excess entropy. This discrepancy may be explained by another theory, the outline of which is derived in Chapter V, essentially from the cell model. This proposed theory improves on the quasi-chemical one, by a better prediction of the excess entropy, and also may offer a better description of a liquid metallic alloy. There is growing evidence in the literature^(27, 23, 29, 24) of the dependence of the thermodynamic properties of a metallic solution on electron concentrations. If known, these electron concentrations could be taken into account easily in the proposed model, or, inverseley, experimentally observed thermodynamic

properties may bring some valuable information on electronic structures. In Chapter II, it was mentioned that, as the electron theory becomes more refined, it will resemble the chemical theory more and more. It is not surprising to observe that, as the chemical theory becomes more refined, it will also resemble the electron theory more and more. Evidently, an accurate description of a metallic solution should include both aspects.

A great deal of experimental data is needed to systematically explore these theories and, in particular, to study the partition of the free energy into enthalpy and entropy terms, which is so crucial to the test of a model. The next chapters present a modest contribution to our capital of experimental observations.

CHAPTER VII
OUTLINE OF EXPERIMENTAL WORK

Solubility measurements are usually fairly sensitive to temperature changes, and it was felt that an investigation of the solubility of oxygen in liquid silver alloys could yield data on the enthalpy and entropy interaction coefficients, as well as on the free energy interaction coefficients.

One of the drawbacks of the silver-oxygen system is the restricted possibilities in the choice of the alloying elements. Only those few elements which have an appreciable solubility in liquid silver and, in addition, have a sufficiently low affinity for oxygen (in order to avoid the formation of an oxide) could be used. Consequently, this investigation is restricted to the interactions of oxygen, gold, platinum, palladium and copper with oxygen in liquid silver.

CHAPTER VIII
LITERATURE SURVEY

In gas solubility studies, the fact that unusual amounts of oxygen are dissolved in molten silver, and that there is a spattering evolution of oxygen upon solidification of the silver, was well known since the beginning of the 19th Century. More recently, however, little work has been done on the solubility of oxygen in liquid silver, although a sizable amount of work was performed on the solubility of oxygen in solid silver.

1. Solubility of Oxygen in Solid Silver

The first thorough investigation was conducted by Steacie and Johnson.⁽³⁰⁾ They indicated a pronounced minimum at 400°C in the curve of the solubility of oxygen versus temperature. No satisfactory explanation was found. Recently, Eichenauer and Müller⁽³¹⁾ redetermined the solubility of oxygen and observed lower values with minimum at 400°C. They represent their data by the equation:

$$\log S = - 0.597 - \frac{2593}{T} + \frac{1}{2} \log P \quad (\text{VIII.1})$$

where S, the lattice solubility of oxygen, is given in cubic centimeters of oxygen per gram, the temperature, T, in °K, and the pressure, P, in Torr. They proposed that the anomaly asserted by Steacie and Johnson was caused by surface adsorption, as the silver used was in the shape of thin foils.

A subsequent investigation by Podgurski and Davis⁽³²⁾ is in close agreement above 500°C with the results of Eichenauer and

and Müller.⁽³¹⁾ The equation proposed to describe the oxygen solubility is:

$$\log S = - 0.840 - \frac{2250}{T} + \frac{1}{2} \log P \quad (\text{VIII.2})$$

where the units are the same as in equation VIII.1. The authors studied the oxidation of copper in silver and deduced that Steacie and Johnson's results are more likely accounted for by the oxidation of trace impurities.

2. Solubility of Oxygen in Liquid Silver

Data on the oxygen in liquid silver, was collected as early as 1819 by Lucas⁽³³⁾ and 1820 by Chevillot.⁽³⁴⁾ The century that followed saw many other investigators, but their work remained very qualitative in nature, so we shall just mention Graham⁽³⁵⁾ in 1866, Dumas⁽³⁶⁾ in 1878, Brauner⁽³⁷⁾ in 1889, Neuman⁽³⁸⁾ in 1892, Heycock and Neville⁽³⁹⁾ in 1895, Holborn and Day⁽⁴⁰⁾ in 1900, Berthelot⁽⁴¹⁾ in 1901, Richards and Wells⁽⁴²⁾ in 1906, and Sieverts⁽⁴³⁾ in 1908. The first thorough quantitative investigation is due to Sieverts and Hagenacker⁽⁴⁴⁾ in 1909. During approximately the same period, Donnan and Shaw⁽⁴⁵⁾ performed a similar investigation, but deferred the publication of their preliminary and confirming data, due to the simultaneous completion of Sieverts and Hagenacker's results. These results, which form the basis of the presently accepted high temperature portion of the silver oxygen phase diagram compiled by Hansen,⁽⁴⁶⁾ are summarized in Table VIII.1.

TABLE VIII.1
SIEVERTS AND HAGENACKER'S DATA FOR THE SOLUBILITY
OF OXYGEN IN LIQUID SILVER

$10^3/T \text{ } ^\circ\text{K}^{-1}$	p_{O_2} (mm Hg)	% O	$1 + \log K'^*$
0.8025	752	0.3039(?)	0.4850(?)
0.7709	760	0.2927	0.4668
0.7418	760	0.2769	0.4427
0.7418	760	0.2752	0.4400
0.7152	755	0.2634	0.4208
0.7152	359	0.1848	0.4301
0.7152	37	0.0629	0.4551
0.7418	1203	0.3522	0.4474
0.7418	488	0.2230	0.4450
0.7418	346	0.1905	0.4511
0.7418	209	0.1541	0.4685
0.7418	150	0.1323	0.4744
0.7418	128	0.1164	0.4530
0.7418	39	0.0623	0.4401

* $K' = \%O/\sqrt{p_{O_2}}$ and p_{O_2} is in atmosphere

At 1075°C ($10^3/T = 0.7418$), the mean of $\log K'$ is 0.4514
and the standard deviation 0.0116

Recently, Johnstone⁽⁴⁷⁾ determined the depression of the freezing point of silver under oxygen pressure up to 147 atmospheres. Previous work on this subject by Allen⁽⁴⁸⁾ ranged up to 13.9 atmospheres.

Mizikar, Grace and Parlee⁽⁴⁹⁾ studied the diffusion of oxygen in liquid silver. Their diffusion coefficient is calculated using the oxygen solubility results of Sieverts and Hagenacker and Donnan and Shaw, whose results for the oxygen concentration at one atmosphere are represented by:

$$\log \%O = \frac{723.7}{T} - 1.095 \quad (\text{VIII.3})$$

In the calculations of the diffusion coefficient D , it may be noted that D appears as a function of the square of the oxygen concentration, and that an overestimate of the oxygen solubility leads to an underestimate of D .

CHAPTER IX
APPARATUS, MATERIALS AND EXPERIMENTAL PROCEDURE

1. SIEVERTS' APPARATUS

The Sieverts' apparatus used in this investigation is shown in Figure IX 1. Its construction is described by Carlin⁽⁵⁰⁾ Many modifications of the apparatus were made during the program reported in this thesis, the most important one being the development of a new reaction chamber.

The most pertinent details of the apparatus are described under the following headings:

- 1.1 Gas Purification Trains
- 1.2 Vacuum System
- 1.3 Measuring Instruments
- 1.4 Heating Unit
- 1.5 Reaction Chamber
- 1.6 Refractories
- 1.7 Device for Dropping the Alloying Additions

1.1 Gas Purification Trains

The argon used to measure the "hot volume" was purified by first passing it through a copper gauze furnace, then over anhydrous. The oxygen was passed through successive towers of drierite, anhydrous, palladinized asbestos pellets at 100°C, ascarite, anhydrous again and finally through a butyl phthalate bubbler.

1.2 Vacuum System

Vacuum of a few microns of mercury was obtained with a mechanical pump. No diffusion pump was added because the rate limiting step in the evacuation of the system was the rate at which the charge degassed, rather than the evacuation rate provided by the pump. Moreover, at high temperatures, pro-

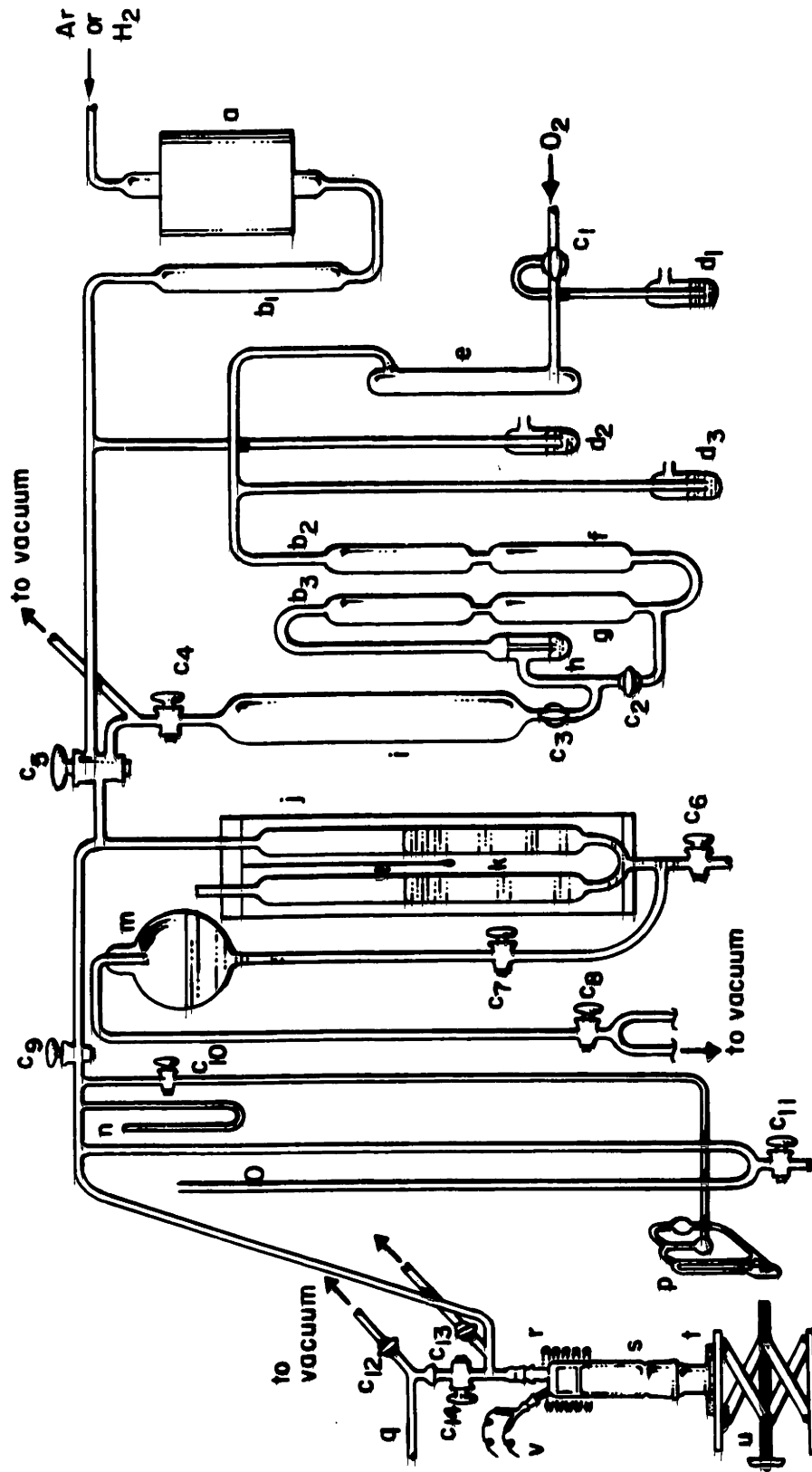


FIG. IX 1. THE SIEVERTS' APPARATUS

NOMENCLATURE

- | | | | |
|----------------|-------------------------------|----|-----------------------------|
| a. | Copper Gauze Furnace | l. | Thermometer |
| b ₁ | Anhydrous Drying Tower | m. | Mercury Reservoir |
| c ₁ | Stopcock | n. | Closed End Manometer |
| d ₁ | Safety Mercury Bubbler | o. | Open End Manometer |
| e. | Drierite Drying Tower | p. | McLeod Gauge |
| f. | Palladinized Asbestos Pellets | q. | Additions Storage Reservoir |
| g. | Ascarite | r. | Induction Coils |
| h. | Butyl fthalate Bubbler | s. | Reaction Chamber |
| i. | Oxygen Storage Reservoir | t. | Foam Cushion |
| j. | Constant Temperature Bath | u. | Jack |
| k. | Legs of the Burette | v. | Thermocouple Wires |

FIGURE IX.1. THE SIEVERTS' APPARATUS.

longed exposures to low pressures were undesirable because of the evaporation of the silver. It may also be noted that the absence of leaks was the most important consideration, as the system would be isolated from the pump after evacuation.

1.3 Measuring Instruments

a. **Manometers** - Three different mercury manometers were used. The first had an open end to the atmosphere and was used throughout each run. The second had a closed end; absolute values of the pressure ranging from 0 to 150 mm could be read directly. Both were made of capillary tubing. The third, a McLeod gauge not included in the "hot volume", was only used to determine that a good vacuum was obtained before each run, and occasionally during the run.

b. **The Gas Burette** - The gas burette had a capacity of 100 cubic centimeters and could be read to the nearest 0.1 cubic centimeter. It was enclosed in an isothermal water-jacket constructed from a pyrex tube. A thermometer completely immersed in the water was hanging next to the burette and measured the water temperature with an accuracy of 0.1°C.

c. **The Thermocouple** - The temperature was read by a platinum-platinum 10 percent rhodium thermocouple. Both insulating and protection tubes were of high purity alumina and the latter had an outside diameter of 1/16 inch. The wires of the thermocouple were taken out of the system through a glass seal.

Each thermocouple was checked against the melting point of silver; agreement was obtained within half a degree.

1.4 Heating Unit

Heating of the silver charge was effected by an induction coil with the power supplied by a Tocco motor-generator of 10,000 cycles per second. It proved extremely difficult to entirely melt a charge of silver pellets as the upper part of the charge tended to "bridge over". This difficulty was overcome by premelting the charge (in the same apparatus) and only using the solid block of silver for an actual run.

1.5 Reaction Chamber

The reaction chamber used in this investigation is shown in Figure IX.2. Made of vycor glass, it was connected to the rest of the apparatus by a conical ground joint. The inner edge of the joint was beveled to avoid risks of hanging additions. This arrangement was more satisfactory than a ball joint which was used instead at the beginning of this investigation.

A water-jacket surrounded the reaction chamber to protect the "hot volume" from changes in the air temperature. It was, however, abandoned and replaced by an air-fan after adoption of the conical joint, because of the increased difficulties in the assembly of the apparatus. The disadvantage was offset by the consequent reduction in the "hot volume".

1.6 Refractories

A flat bottom alumina crucible contained the melt, as shown in Figure IX 2, and was placed in a larger crucible to protect the reaction chamber in case of breakage. To premelt the charge, however, a clear quartz crucible was used, because, after cooling, the melt was more easily separated from the walls. Its diameter was slightly smaller, to avoid breakage of the alumina crucible caused otherwise by the expansion on heating of the silver ingot.

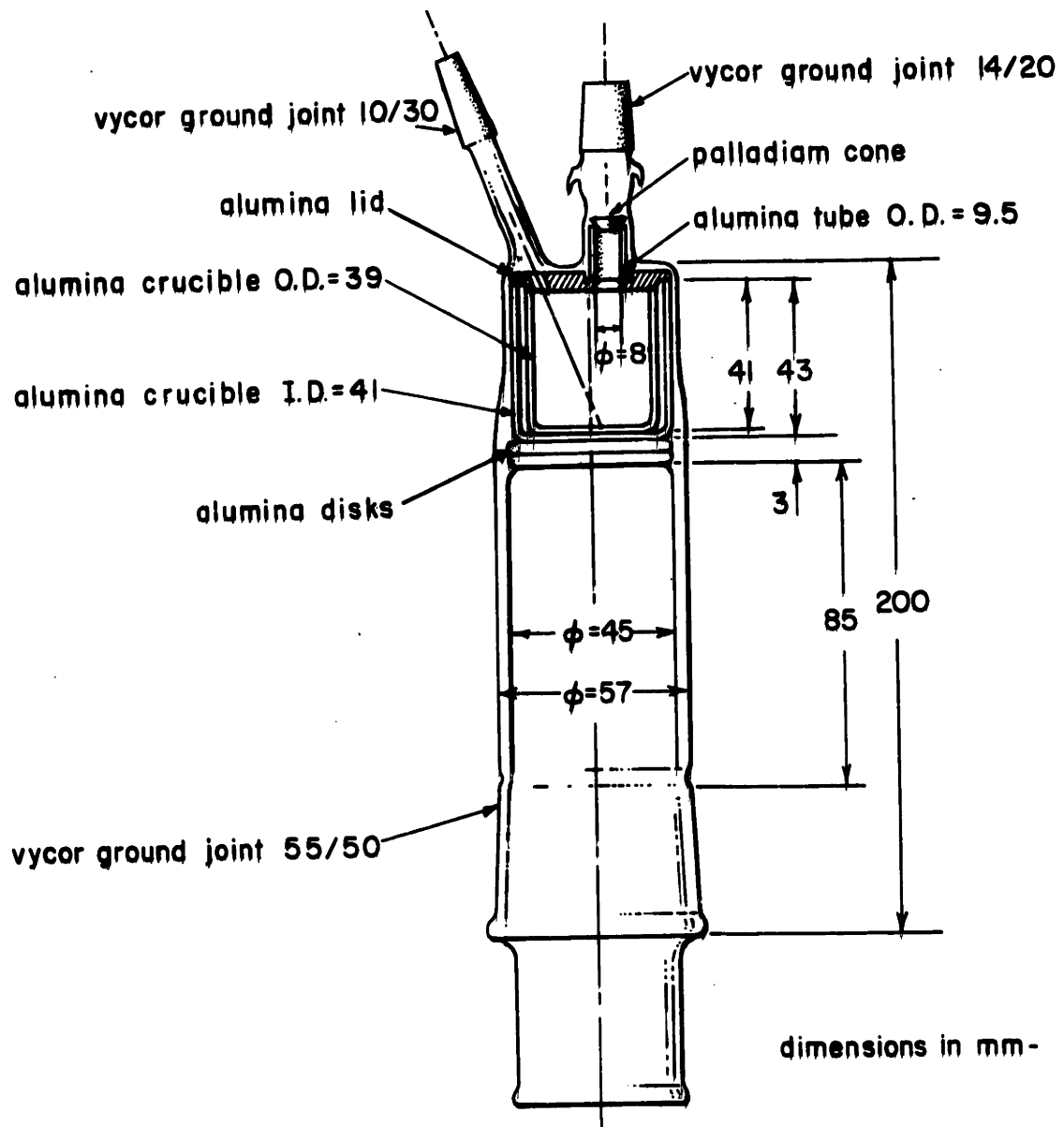


FIG. IX.2. THE REACTION CHAMBER

1.7 Device for Dropping the Alloying Additions

It was possible, with the device shown in Figure IX 3, to alter the composition of the bath during a run. The additions could be stored at any time in the side arm when it was disconnected from the reaction chamber by the stopcock C₁₄. A small rod-shaped magnet was added last. By moving another magnet outside the system, it was possible to push the additions into the melt.

The problem of possible contamination by the grease of stopcock C₁₄ (Figure IX 3) was satisfactorily resolved, mainly by two precautions. First, the bore of C₁₄ was thoroughly cleaned by acetone before each run. Second, the stopcock C₁₄ was opened to the maximum extent before dropping an addition from the side arm. It is also possible that the conical shape of the bore (Figure IX 3) also helped to avoid the minute amounts of grease which still might have been collected by turning this stopcock.

The additions were guided into the melt by an alumina tube and a palladium cone as shown in Figure IX 2.

2. MATERIALS

The characteristics of the gases and metals used in this investigation are summarized in Table IX 1. The effect of the impurities in the oxygen and on the silver will be discussed in Chapter XI.

The alumina refractory materials, crucibles, lids and disks were made of high purity alundum cement (RA 1135) from Norton Company. They were manufactured by the Ceramics Division of the Massachusetts Institute of Technology.

The high purity alumina thermocouple tubes were made by the McDanel Refractory Porcelain Company. The single bore protection tubes were closed

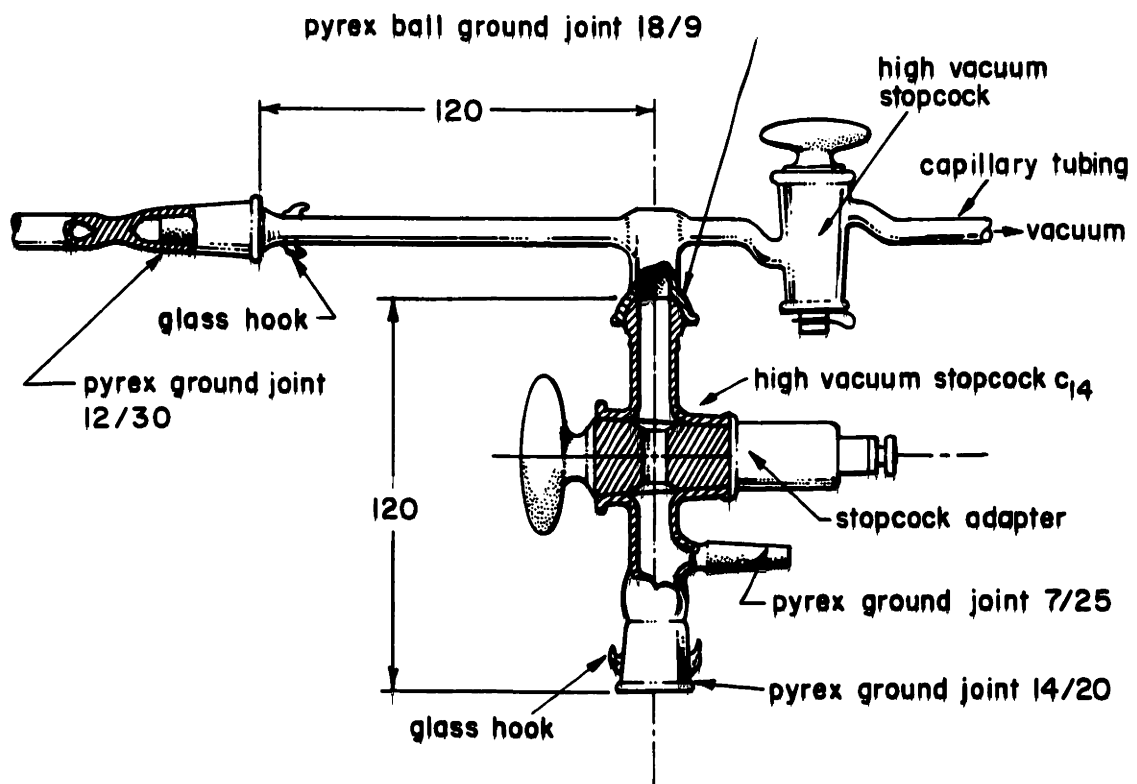


FIG. IX 3. ADDITIONS RESERVOIR

TABLE IX 1

MATERIALS CHARACTERISTICS

<u>Material</u>	<u>Source</u>	<u>Shape</u>	<u>Assay</u>	<u>Main Impurities</u>
Argon	AIRCO	gas	99.996%	O ₂ : 0.0005%; N ₂ : 0.003%
Oxygen	AIRCO	gas	99.5%	Ar: 0.15 to 0.3%; N ₂ : 0.1 to 0.25%; CO ₂ : 0.0005%
Silver	American Smelting and Refining Company	shot	99.99 ⁺ %	Cu: 0.005%
Copper	Allied Chemical	shot	99.90%	Sb + Sn: 0.01%; Fe: 0.005%; Pb: 0.005% Insoluble in dilute HNO ₃ : 0.02%
Gold	Handy and Harman	foil 7 mm thick	99.99 ⁺ %	Balance of Cu and Ag
Platinum	Engelhardt Ind.	rod 0.100 inch diameter	99.8%	Max. usual impurity level of all but precious metals: 15-20 ppm.
Palladium	United Mineral & Chemical Corp.	foil 0.002 inch diameter	99.9 ⁺ %	Metals of the platinum group

at one end by the Ceramics Division of the Massachusetts Institute of Technology with high purity alundum cement (38X) from Norton Company.

Finally, the clear quartz crucibles were made by Syncor Products Company.

3. EXPERIMENTAL PROCEDURE

Before each run, the silver was premelted in a silica crucible first under hydrogen, then under vacuum. In the solid block thus obtained, a hole was drilled at an angle of approximately 22° corresponding to the angle of the thermocouple arm of the reaction chamber. All the tools used were carefully cleaned with acetone and the cutting rate was slow to prevent excessive heating of the material.

Then the silver, the refractory materials and the palladium cone were placed in the reaction bulb, which in turn was connected to the rest of the apparatus. The system was then evacuated, isolated from the pump, and checked for leaks over several hours.

The high frequency motor-generator was started and the metal charge heated to approximately 500 or 600°C. The sequence of operations at this temperature was:

- a. Degas the system for 30 to 60 minutes.
- b. Place it under a hydrogen atmosphere.
- c. Degas the system again (60 minutes).
- d. Place it under an argon atmosphere.

In some instances, between steps a and b, a few cubic centimeters of oxygen were introduced to remove possible impurities at the surface of the charge (such as carbon). The vacuum was then reestablished after 3 to 5 minutes.

The power output of the generator was then slowly increased and the thermocouple checked at the melting point of silver.

With argon in the measuring burette, the mercury legs of the burette were levelled and a reference value recorded, together with the temperature of the water and the atmospheric pressure.

The system was then evacuated for approximately one minute and a certain quantity of argon admitted. The difference between the initial level of the burette and the new one was yielding the number of cubic centimeters introduced. The "hot volumes" of the system, both with and without the addition reservoir included, were measured and their dependence on the pressure and the temperature determined.

After these measurements, the burette was evacuated and refilled with oxygen. Then, the reaction chamber was also evacuated for 30 to 50 seconds and the oxygen introduced. The temperature was adjusted to the desired level and the gas-metal system allowed to come to equilibrium, which was usually attained in approximately 15 minutes. As a precaution, it was allowed at least 30 minutes. The effect of temperature was studied at fixed amounts of oxygen in the system (not in the metal) but varying pressures.

In many runs, an extra step was added to this experimental procedure. After measuring the "hot volume" and evacuating the system, a few cubic centimeters of oxygen were added to the reaction chamber to oxidize the impurities in the bulk of the metal which possibly had not yet been removed. Then the system was again evacuated. The necessity of this measure is discussed in Chapter XI.

After investigation of the solubility of oxygen in pure silver,

pieces of alloying elements were dropped into the melt. Each time new additions were stored, the reservoir was first placed under vacuum, then isolated from the vacuum line and finally brought to equilibrium with the remainder of the system. Only then would any addition be dropped into the melt.

CHAPTER X
THERMODYNAMICS OF GAS SOLUBILITIES AND CALCULATIONS

The theoretical considerations of Chapter III are now applied to the thermodynamics of gas solubilities in alloys. The example of oxygen in liquid silver alloys is naturally adopted, but the generality of the study is retained.

1. Thermodynamics of Gas Solubilities

The dissolution reaction of oxygen in pure liquid silver is:



The reference state for the oxygen in the gas phase will be the perfect gas, and the corresponding standard state is the pure gas at one atmosphere. For the oxygen in solution, the reference state will be the state of infinite dilution in pure silver. Therefore:

$$\lim_{\%O \rightarrow 0} \frac{a_O}{\%O} = \lim_{\%O \rightarrow 0} f_O = 1 \quad (X.2)$$

The standard free energy of the reaction (X.1) is:

$$\Delta F_s^\circ = -RT \ln K_s = -RT \ln \frac{\%O}{(p_{O_2})^{1/2}} \cdot f_O \text{ (in silver)} \quad (X.3)$$

If oxygen follows Sieverts' law when we choose weight percent as our composition coordinate, f_O is constant and consequently equals its value at infinite dilution, i.e. equals 1.

For an alloy, the dissolution reaction is:



The same reference state is kept for the oxygen in the gas phase. The reference state for the oxygen in solution is also kept as the state of infinite dilution in pure silver. Consequently:

$$\lim_{\substack{\%O \rightarrow 0 \\ \%M \neq 0}} \frac{a_O}{\%O} = \lim_{\substack{\%O \rightarrow 0 \\ \%M \neq 0}} f_O \neq 1 \quad (\text{X.5})$$

The standard free energy of the reaction (X.4) is:

$$\Delta F_a^\circ = -RT \ln K_a = -RT \ln \frac{\%O}{(p_{O_2})^{1/2}} f_O(\text{in alloy}) \quad (\text{X.6})$$

Because of the identity of our reference states in reactions (X.1) and (X.4), the standard free energies of the two reactions are equal.

$$\Delta F_s^\circ = \Delta F_a^\circ = \Delta F^\circ$$

and

$$\ln K_s = \ln K_a = \ln K \quad (\text{X.7})$$

It is convenient to adopt the notation K' for the value of the ratio

$$\frac{\%O}{(p_{O_2})^{1/2}} .$$

Equation (X.3) and (X.6) may then be rewritten:

$$\log f_O(\text{silver}) = \log K - \log K'_s \quad (\text{X.8})$$

and

$$\log f_O(\text{in alloy}) = \log K - \log K'_a \quad (\text{X.9})$$

a - If Sieverts' law is followed in the pure silver,

$$\text{Then } \log K = \log K'_s \quad (\text{X.10})$$

and

$$\log f_0(\text{in alloy}) = \log \frac{K'_s}{K'_a} \quad (\text{X.11})$$

so that we may rewrite:

$$\log f_0(\text{in alloy}) = \log \left(\frac{\%O(\text{in silver})}{\%O(\text{in alloy})} \right)_{P_{O_2}, T} \quad (\text{X.12})$$

The two concentrations have to be taken at the same temperature and same pressure of oxygen.

Equation (X.11) may also be written as:

$$\log f_0(\text{in alloy}) = \frac{1}{2} \log \left(\frac{(P_{O_2} \text{ in equilibrium with } \%O \text{ in alloy})}{(P_{O_2} \text{ in equilibrium with the same } \%O \text{ in silver})} \right)_{\%O, T} \quad (\text{X.13})$$

In the "dropping technique", this expression may be preferred, especially if the "hot volume" is small.

If Sieverts' law is not followed in the alloy. $\log f_0$ depends on $\%O$ as well as $\%M$, so that the ratios in Equations (X.12) and (X.13) depend on the oxygen potential.

b - If Sieverts' law is not followed in the pure silver,

$$\text{Then } \log K \neq \log K'_s$$

or

$$\log f_0(\text{in silver}) \neq 0$$

As gas concentrations are generally very small, to a very good approximation $\log f_0$ may be assumed to be proportional to the gas concen-

tration.

$$\log f_0(\text{in silver}) = \log K - \log K'_s = e_0^{(0)} \%0 \quad (\text{X.14})$$

With the notation of Chapter III, it is possible to write:

$$\log f_0(\text{in alloy}) = (\log f_0)^{(0)} + (\log f_0)^{(M)} + r_0^{(M,0)} \%0 \%M \quad (\text{X.15})$$

so that

$$\log f_0(\text{in alloy}) = e_0^{(0)} \%0 + e_0^{(M)} \%M + r_0^{(M)} (\%M)^2 + r_0^{(M,0)} \%0 \%M \quad (\text{X.16})$$

or

$$-\log K'_a = -\log K + e_0^{(0)} \%0 + e_0^{(M)} \%M + r_0^{(M)} (\%M)^2 + r_0^{(M,0)} \%0 \%M \quad (\text{X.17})$$

Neglect of higher order interaction coefficients implies that deviations from Sieverts' law in the alloy, as measured by $\frac{\partial \log K'_a}{\partial \%0}$, are linear with respect to the concentration of the alloying element.

$$\left(\frac{\partial \log f_0(\text{in alloy})}{\partial \%0} \right) \%0 \rightarrow 0 = - \left(\frac{\partial \log K'_a}{\partial \%0} \right) \%0 \rightarrow 0 = e_0^{(0)} + r_0^{(M,0)} \%M \quad (\text{X.18})$$

The effect of the temperature may be easily analyzed by expressing the temperature dependence of each free energy term of Equations (X.16) or (X.17), i.e. by expressing each of these terms as the sum of an enthalpy and an entropy term. However, most often the accuracy of the data does not permit us to determine the temperature dependence of such coefficients as $e_0^{(0)}$, $r_0^{(M)}$, and $r_0^{(M,0)}$. If this is the case for those coefficients, Equation (X.17) is rewritten as:

$$\begin{aligned} -\log K'_a = & -\frac{\Delta e^f}{2.3R} + \frac{\Delta H}{2.3R} = \frac{1}{T} + e_0^{(0)} \%0 - \frac{s_0^{(M)}}{2.3R} \%M + \frac{h_0^{(M)}}{2.3R} \cdot \frac{1}{T} \cdot \%M \\ & + r_0^{(M)} (\%M)^2 + r_0^{(M,0)} \%0 \%0 \end{aligned} \quad (\text{X.19})$$

Differentiation of Equation (X.19) with respect to $\frac{1}{T}$ immediately yields:

$$- 2.3R \left(\frac{\partial \log K'_a}{\partial \frac{1}{T}} \right)_{\%O, \%M} = \Delta H_a = \Delta H + h_O^{(M)} \%M \quad (X.20)$$

and

$$2.3R \left\{ \log K'_a - \frac{1}{T} \left(\frac{\partial \log K'_a}{\partial \frac{1}{T}} \right)_{\%O, \%M} \right\} = \Delta \phi_a = \Delta \phi + s_O^{(M)} \%M \quad (X.21)$$

which are obtained directly from our definitions in Chapter III (Equations III.64 and 65) of the enthalpy and entropy interaction coefficients.

2. Practical Method of Calculation

The most useful experimental variable for analysis of the data is $\log K' = \log \frac{\%O}{(p_{O_2})^{1/2}}$. For instance, if at a given temperature, it is a constant regardless of the oxygen concentration, then Sieverts' law is followed. If it is not, its linear dependence on the oxygen percent in the pure silver will yield $e_O^{(0)}$ (Equation (X.14)), then $r_O^{(M)}$ in the alloy (Equation (X.18)).

In general, each interaction coefficient can be calculated separately by isolating its effect, or all of them can be obtained at once by using Equation (X.19) and a computer program of multidimensional least-square analysis (the regression variable are: $\%O$, $\%M$, $\frac{1}{T}$, $\frac{\%O}{T}$, $\frac{\%M}{T}$, etc.). The first method gives a better insight as to the significance of each parameter and to the errors. But the second one is very powerful and in many cases quite easy to apply. Both methods were combined in this investigation by utilizing a computer program of stepwise regression analysis.⁽⁵¹⁾ Operations on the input variables could be performed and consequently, different effects could be separated. For instance, in studying the effect of an alloying element, deviations from

Sieverts' law in the pure silver could be discarded if $\log K' + e_0^{(0)} Z_0$ was used as the dependent variable instead of $\log K'$. Moreover, the statistical level of significance ("F level") of each variable was also given, and if judged too low, the corresponding variable was eliminated. Specific examples are discussed further in the analysis of the experimental results.

CHAPTER XI
PRESENTATION AND ANALYSIS OF RESULTS

The experimental data on the solubility of oxygen in liquid silver, which were obtained in this study, are tabulated in Appendix (H). Attention must be brought to the fact that it was not possible to remove all the oxygen from the melt after its preparation. The origin of the oxygen concentration had, therefore, to be adjusted. This adjustment was done in two steps. A first origin was determined by extrapolation of the data in the plot of $\sqrt{p_{O_2}}$ versus %O. Then, with this origin, the values of $\log K'$ were recalculated and a second origin was determined on the basis of the shape of the curve $\log K'$ versus %O. It should be noted that these successive adjustments correspond to only one correction. The following section justifies and describes in detail this procedure.

1. Determination of the Origin for the Oxygen Concentration in the Melt

1.1 Experimental Difficulties

In the experimental procedure, after the determination of the "hot volume", the melt must be free of impurities and free of oxygen. These two requirements could not be simultaneously satisfied. The most critical impurities are those, such as carbon and sulfur, which react with oxygen to form volatile species. Very minute amounts may be the source of large errors. For instance, one or two parts per million of carbon in a melt of 200g of silver would build a partial pressure of approximately 3 to 7 mm of Hg in the reaction system, and, on a scale of the square root of the

pressure, will cause an error near the origin of about 10% of the total range (approximately 760 mm Hg). It is possible to oxidize these impurities first and then remove them by evacuating the system. However, in this procedure only a part of the oxygen introduced would combine to form an oxide, while the remainder would go into solution in the melt. This amount of oxygen in the silver could not be significantly reduced by evacuation, without a prolonged exposure to the vacuum and, as a consequence, a large evaporation of silver. Removal of the oxygen by hydrogen was not a better solution, because of a similar problem: the removal of water vapor.

To minimize the error resulting from residual oxygen in the reaction bulb, the following procedure was adopted. Before determination of the hot volume, and at low temperature (approximately 500°C), the solid block of silver was exposed first to oxygen and then to vacuum, in order to remove, as far as possible, surface impurities. The silver was melted then and, after measurement of the "hot volume" with argon, removal of the argon by evacuation over a short time (thirty to sixty seconds), a few cubic centimeters (STP) of oxygen were introduced; this is equivalent to a concentration Δ of approximately 0.0015 to 0.0070 percent. Almost invariably, the observed corresponding pressure was much higher than the equilibrium one: 3 to 8 mm of mercury, for example, instead of 0.1 to 0.5 mm. In some instances, a light blackish deposit also was observed on the walls of the reaction chamber, which, upon analysis, revealed traces of carbon. The system was re-evacuated for a short time. After this evacuation, and before admitting more oxygen to the melt, there

was still a residual amount of oxygen; on a weight percent basis, it will be designated by Y_0 . An estimate of the value of Y_0 is based on the theoretical considerations in section 1.2 which follows.

1.2 Theoretical Determination of Y_0

For convenience, the weight percent of oxygen in the melt will be designated by y . Because of the experimental difficulties discussed in section 1.1, the true value of y in an experiment is unknown. By extrapolating the data in a plot of $\sqrt{p_{O_2}}$ versus %O, a first estimate of the location of the origin may be obtained. Consequently, the unknown values of y and Y_0 are estimated at, respectively, $y - y_0$ and $Y_0 - y_0$, where y_0 is a constant fixed by our choice of the origin. Then, it is not K' which is measured but K'' where:

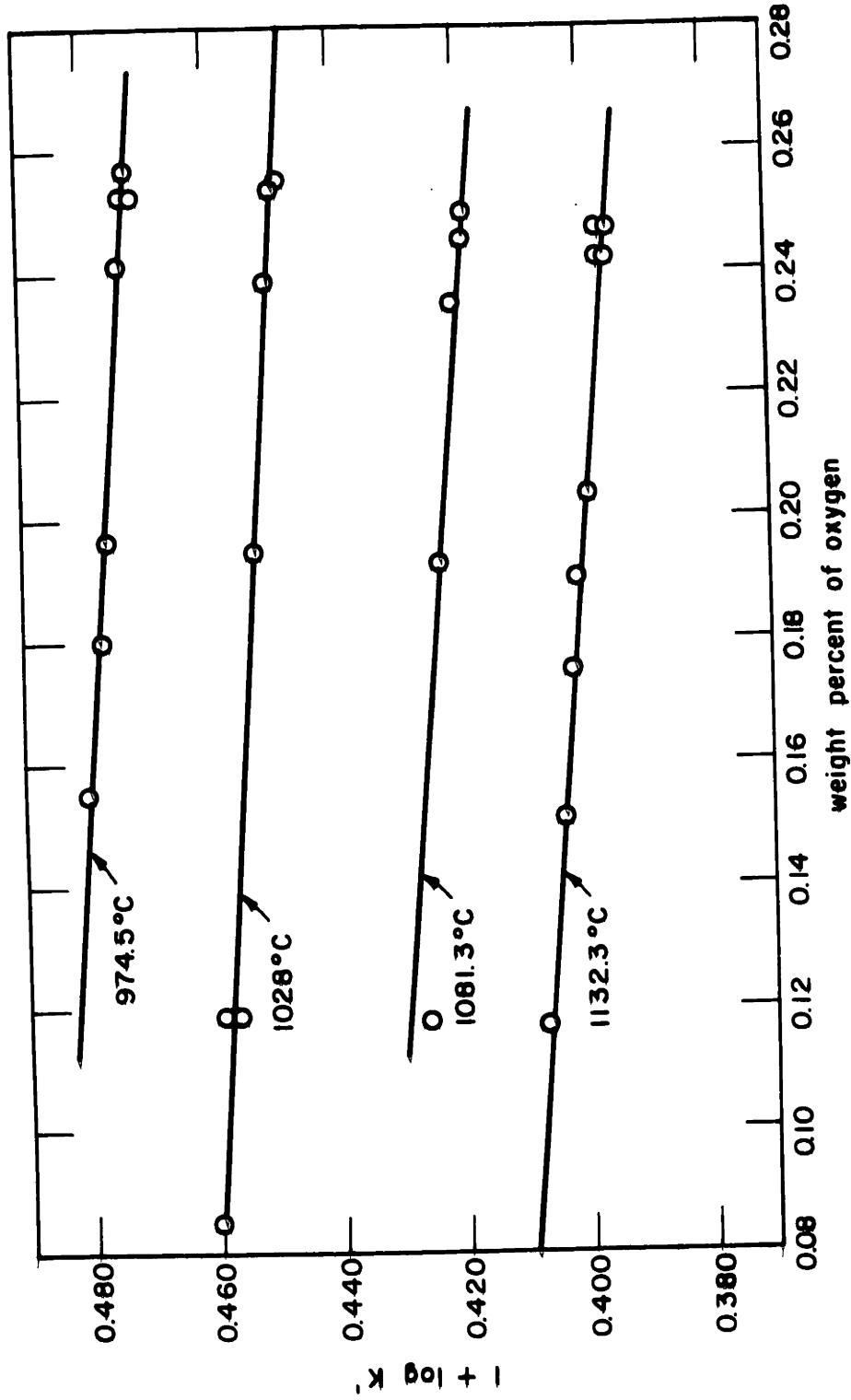
$$K'' = \frac{y - y_0}{\sqrt{p_{O_2}}} = K' \left(1 - \frac{y_0}{y}\right) \quad (\text{XI.1})$$

or

$$\log K' = \log K'' - \log \left(1 - \frac{y_0}{y}\right) \quad (\text{XI.2})$$

In this investigation, the method used to determine y_0 is based on the following considerations. On one hand, the deviations from Sieverts' law appear to be small (Fig. XI.1) and, on the other hand, the range of possible concentrations of oxygen in the melt is quite limited (0 to 0.3 weight percent). Therefore, it is permissible to write:

$$\log K' = \log K - e_0^{(0)} \%O = \log K - e_0^{(0)} y \quad (\text{XI.3})$$



Experimental results from run 4828. Origin of the oxygen concentration adjusted for best linear correlation between $\log K'$ and $\%O$

FIG. XI 1. SELF-INTERACTION OF OXYGEN IN SILVER

and neglect the second order term $r_0^{(0)} (\% 0)^2$. The shape of the curve $\log K'$ versus $\% 0$, as deduced from equation XI.2, is extremely sensitive to the value of y_0 , i.e., to the location of the origin. Therefore, the value of y_0 , ultimately adopted, will be the value which best converts this curve into the theoretical straight line of equation XI.3.

The effect of the choice of y_0 may be analytically clarified through equations XI.2 and XI.3:

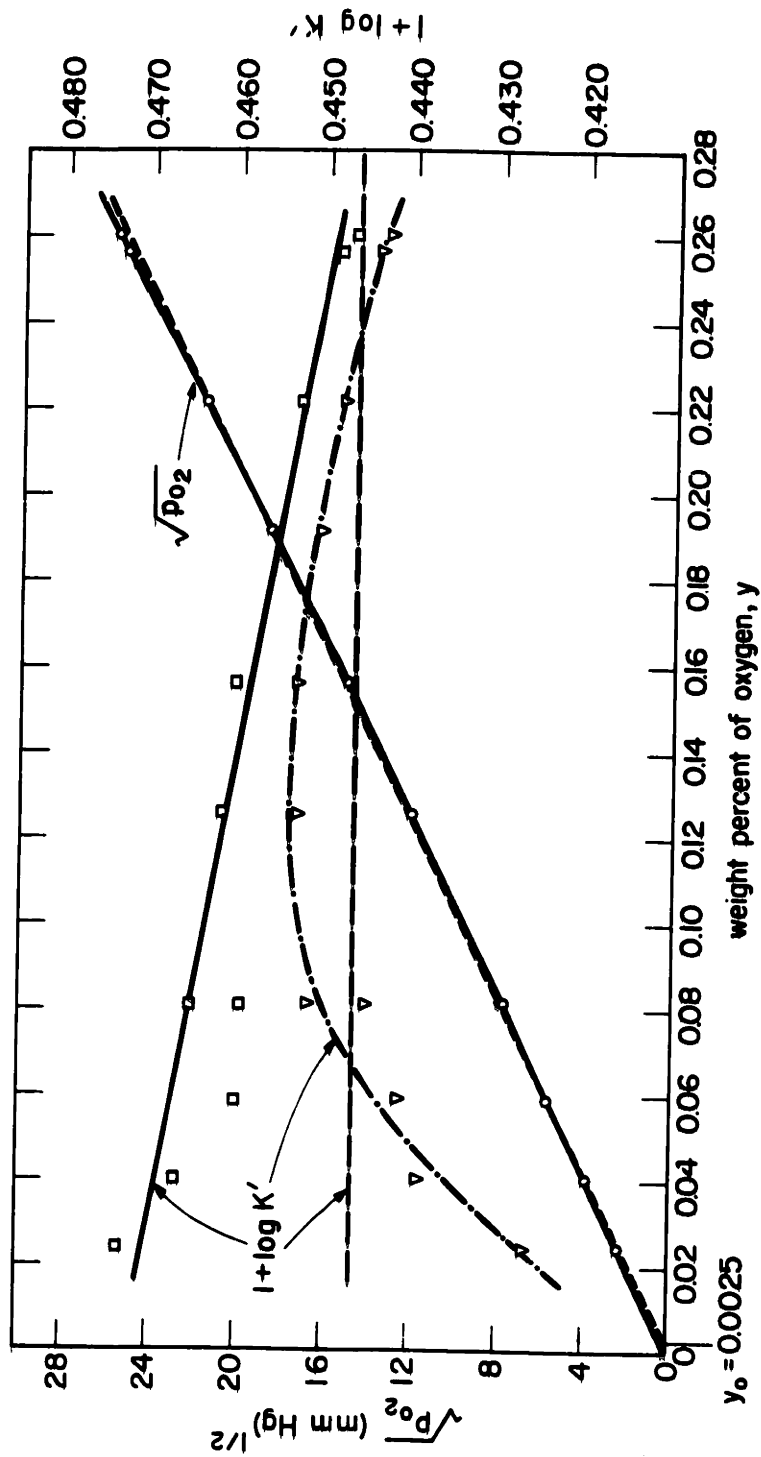
$$\log K'' = \log K - e_0^{(0)} y + \log\left(1 - \frac{y_0}{y}\right) \quad (\text{XI.4})$$

and differentiating this equation twice, with respect to y , yields:

$$\frac{\partial^2 \log K''}{\partial y^2} = - \frac{y_0 (2y - y_0)}{y^2 (y - y_0)^2} \quad (\text{XI.5})$$

If y_0 is negative, i.e., if the value of the oxygen concentration has been overestimated ($y'' > y$), the curve representing our estimates of $\log K'$ (i.e., $\log K''$) versus $\% 0$ shows a positive curvature. If y_0 is positive, then a negative curvature is obtained. This latter case is illustrated in Fig. XI.2. It may be noted that the best straight line obtained for $\log K'$ versus $\% 0$ is not horizontal ($e_0^{(0)} \neq 0$).

The scatter of the data, especially at low concentrations of oxygen, introduces a difficulty in the determination of y_0 . A statistical way of judging the results is needed; the following procedure was adopted. Given a value of y_0 , the corresponding values of $\log K'$ were expressed as:



Data at 1017°C (or $10^3/T = 0.7751^\circ\text{K}^{-1}$) from Run 4917

- experimental values of $\sqrt{p_{\text{O}_2}}$ for %O = y
- straight line fitting the points ○ if Sieverts' law is followed. Fixes an origin at $y_0 = 0.0025$
- value of $\log k'$ corresponding to the previous Sieverts' line, (i.e. line -----)
- ▽ and ——— Experimental points and fitted curve for $1 + \log k'$ based on %O = $y - y_0 = y - 0.0025$
- experimental values of $1 + \log k'$ based on %O = y
- curve and straight line of best fit through the points ○ and □

FIG. XI.2. DETERMINATION OF THE ORIGIN FOR THE OXYGEN CONCENTRATION IN THE MELT

$$\log K' = \log K - e_0^{(0)}\% - \frac{\Delta H}{2.3R} \cdot \frac{1}{T} \quad (\text{XI.6})$$

The computer program, mentioned in Chapter X, section 2, was used to determine the variance σ and the coefficient of multiple correlation ρ (or simple correlation coefficient, if the data are taken at the same temperature). Then, the value of y_0 was changed and new values of ρ and σ obtained. The maximum of ρ , or the minimum of σ , fixed the value of y_0 and, by the same token, the values of $e_0^{(0)}$ and ΔH . This optimum value of y_0 was obtained by trial and error within 0.0005%. The data in Tables XI.1 and XI.2 refer to this choice of y_0 . The corresponding values of Y_0 and Δ (both defined in section 1.1) also are given for each run. They illustrate the orders of magnitude involved.

2. Solubility of Oxygen in Liquid Silver

2.1 The Self-Interaction Coefficient of Oxygen

A summary of the results permitting the evaluation of the self-interaction coefficient of oxygen $e_0^{(0)}$ is given in Table XI.1. The values of Y_0 are fixed by the procedure outlined in the previous section. Exceptions occur for runs 4531 and 4624 where these values correspond to direct estimates. For run 4711, the values of Y_0 and Δ are unknown, because of difficulties encountered in the course of the run at low concentrations of oxygen. However, the origin is extrapolated from higher concentration data, according to the same optimum-ization technique. The last three runs include large numbers of data and are considered to be the most reliable.

TABLE XI.1
 SELF-INTERACTION COEFFICIENT OF OXYGEN $e_0^{(O)}$ IN LIQUID SILVER

Run	Y_0	Δ	$K' (1060^\circ\text{C},$ $\%O=0.27)$	$\rho(\log K')$	$\sigma(\log K')$	$e_0^{(O)} \times 10^2$ $\pm 1 \text{ std. dev.}$	$\frac{\partial e_0^{(O)}}{\partial Y_0} \times 10^3$
3923	0.0065	0.0031	0.2635	0.9941	0.0024	11.9 ± 0.8	-2.2
4531	0.0071	0.0071	0.2709	0.9982	0.0013	5.4 ± 0.7	-1.1
4624	0.0030	-	0.2658	-	-	9	-
4711	-	-	0.2659	0.9988	0.0016	7.0 ± 0.6	-1.6
4729	0.0032	0.0016	0.2691	0.9621	0.0027	9.5 ± 1.2	-6.2
4809	0.0026	0.0069	0.2649	0.9724	0.0055	8.7 ± 1.1	-3.0
4828	0.0129	0.0181	0.2673	0.9938	0.0032	7.5 ± 1.0	-3.7
4917	0.0023	0.0013	0.2667	0.9971	0.0021	9.0 ± 0.5	-3.3

Y_0 is the assumed residual amount of oxygen, after a short evacuation of the reaction chamber. This evacuation followed an exposure to a quantity Δ of oxygen. Units are in weight percent.

$K' = \frac{\%O}{\sqrt{PO_2}}$, with PO_2 in atmospheres, is calculated at 1060°C (or $10^3/T = 0.750^\circ\text{K}^{-1}$) and $\%O = 0.27$, using the corresponding value of $e_0^{(O)}$.

ρ and σ are, respectively, the multiple correlation coefficient and the standard deviation of the data ($\log K'$).

$\frac{\partial e_0^{(O)}}{\partial Y_0} \times 10^3$ measures the change in the calculated value of $e_0^{(O)} \times 10^2$ consecutive to a change of 0.001% in the value of Y_0 (or y_0).

TABLE XI.2

DISSOLUTION OF OXYGEN IN LIQUID SILVER: THE REACTION CONSTANT K' AND THE ENTHALPY ΔH

Run	Y_0	Δ	$K' \ast$	(1 + log K') ± 1 std. dev.	$\frac{\Delta H}{2.3R}$ ± 1 std. dev.	N
3923	0.0065	0.0031	0.2635	0.4207 \pm 0.0016	-824 \pm 29	7
3114	0.0028	-	0.2682	0.4284 \pm 0.0011	-831 \pm 22	6
4510	0.0071	0.0057	0.2640	0.4215 \pm 0.0008	-824 \pm 16	5
4531	0.0071	0.0071	0.2709	0.4328 \pm 0.0013	-830 \pm 12	8
4624	0.0030	-	0.2658	0.4245 \pm 0.0011	-858 \pm 15	7
4711	-	-	0.2659	0.4248 \pm 0.0010	-824 \pm 12	7
4729	0.0032	0.0016	0.2691	0.4299 \pm 0.0015	-851 \pm 20	5
4809	0.0026	0.0069	0.2649	0.4230 \pm 0.0003	-845 \pm 3	7
4828	0.0129	0.0181	0.2673	0.4278 \pm 0.0008	-848 \pm 6	16
4917	0.0023	0.0013	0.2667	0.4261 \pm 0.0006	-838 \pm 8	7

For an explanation of the symbols Y_0 and Δ , see section 1.1 or Table XI.1.

$K' \ast$ is the value of K' at 1060°C and %O = 0.27.

N is the number of experimental points on which the value of ΔH is calculated.

The data yield a mean value of 0.085 for $e_0^{(0)}$, with a standard error of approximately 0.014.

It is important to note a systematic error introduced by inert impurities (nitrogen and argon) in the oxygen gas, although the maximum percent of impurities was guaranteed by the manufacturer to be less than 0.5%. If p_i designates the partial pressure in the system, due to these inert impurities, the experimental results of this study do not measure K' but K''' , where

$$K''' = \frac{y}{(p_{O_2} + p_i)^{1/2}} = \frac{y}{(1 + p_i/p_{O_2})^{1/2}} \quad (XI.7)$$

or

$$\log K''' = \log K' - \frac{1}{2} \log (1 + p_i/p_{O_2}) \quad (XI.8)$$

At approximately one atmosphere of oxygen, 350 to 400 cubic centimeters of oxygen have been introduced, which, for a 0.5 percent concentration of impurities, have also introduced 1.8 to 2 cubic centimeters of impurities. With the data on the hot volume listed in Appendix H, one calculates that these impurities account for a partial pressure of approximately 20/760 atmosphere. Thus, equation XI.8 yields:

$$\log K''' - \log K' = -0.0055 \quad (XI.9)$$

The effect of these impurities leads to an underestimate of K' and an artificial deviation from Sieverts' law, resulting in an overestimate of the interaction coefficient $e_0^{(0)}$. At one atmospheric pressure, an oxygen concentration of nearly 0.27 is

attained, so that the extent of this overestimate for $e_0^{(0)}$ may be $0.0055/0.27$ or 0.02 . Consequently, the following evaluation of $e_0^{(0)}$ is proposed:

$$e_0^{(0)} = 0.07 \pm 0.03 \quad (\text{XI.10})$$

2.2 Free Energy, Enthalpy and Entropy

The data permitting the evaluation of the free energy, enthalpy and entropy of the dissolution reaction of oxygen in liquid silver are summarized in Table XI.2 and Fig. XI.3. Because of the self-interaction coefficient $e_0^{(0)}$, the data on $\log K'$ are normalized to a fixed oxygen concentration of 0.27 percent and, in each run, only the data referring to a concentration near this value are selected to evaluate the enthalpy.

The following results are obtained:

$$1 + \log K'_{(1060^\circ\text{C})} = 0.4252 \pm 0.0028 \quad (\text{XI.11})$$

and

$$\frac{\Delta H}{2.3R} = 840 \pm 17 \text{ } ^\circ\text{K} \quad (\text{XI.12})$$

In the calculations, a heavier weight (3 to 1) was attributed to runs 4809, 4828 and 4917, and, for the standard deviations (0.0028 and 17), the individual standard deviations listed in Table XI.2 were taken into account. The systematic error of equation XI.8 does not affect, in any marked way, the previous results for the enthalpy, and the proposed values of the thermodynamic functions characterizing the reaction:

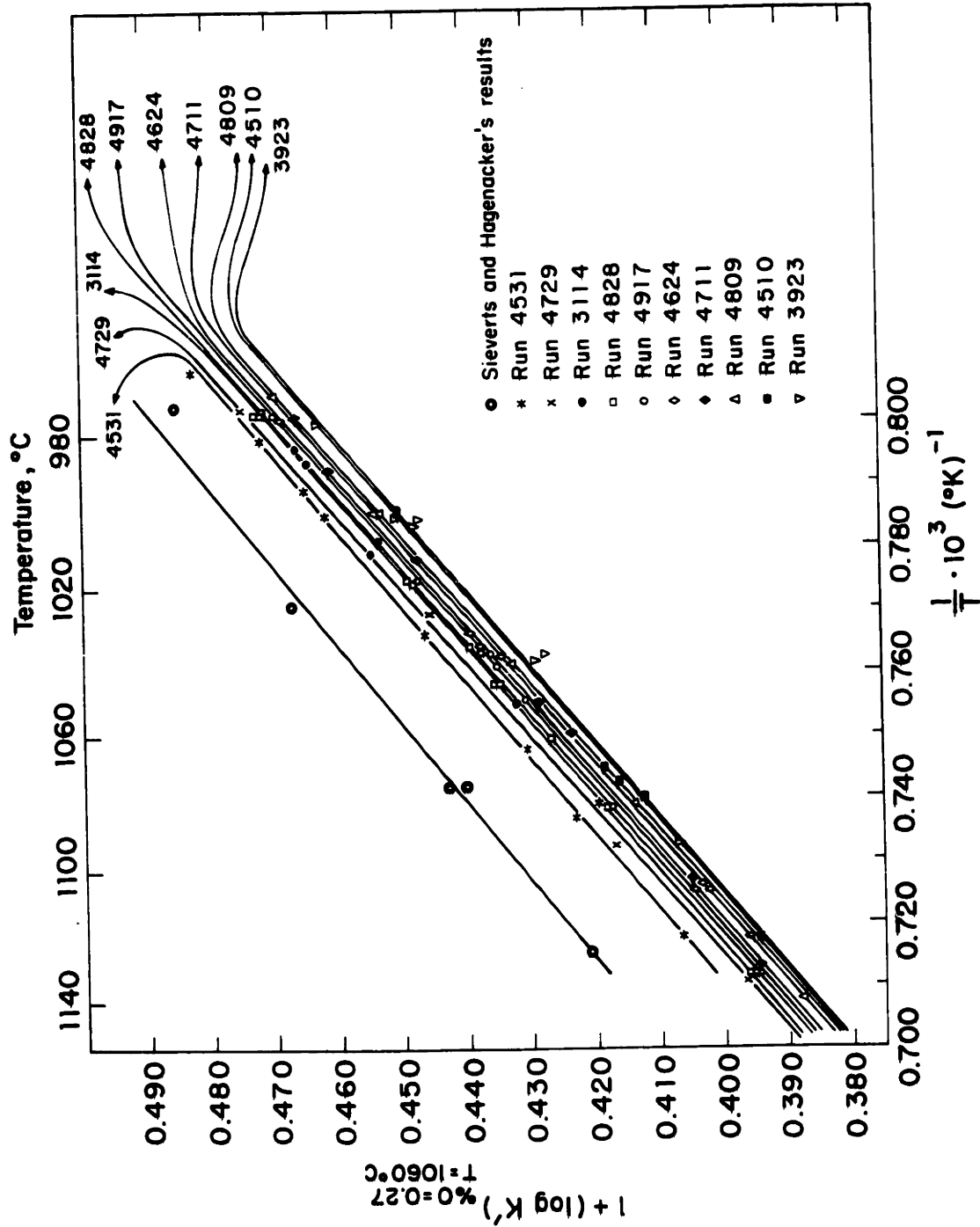
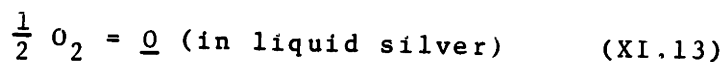


FIG. XI 3. THE SILVER - OXYGEN SYSTEM



are:

$$1 + \log K' \text{ (at \%O} = 0.27) = 0.4290 \pm 0.0043 \quad (\text{XI.14})$$

$$\Delta H(\text{calc. at \%O} = 0.27) = -3843 \pm 78 \text{ cal} \quad (\text{XI.15})$$

$$\Delta S(\text{calc. at \%O} = 0.27) = -5.495 \pm 0.065 \text{ cal}^\circ\text{K}^{-1} \quad (\text{XI.16})$$

and

$$\Delta F_{1060^\circ\text{C}}^\circ = 3600 \pm 75 \text{ cal} \quad (\text{XI.17})$$

2.3 Self-interaction Enthalpy and Entropy Coefficients of Oxygen

In Table XI.2 it was noted that, in the determination of ΔH and $\log K'$ at 1060°C and 0.27 percent of oxygen, only the data near this concentration of oxygen were taken into account. Taking all the data into account (at any concentration of oxygen) for the determination of ΔH , increased the scatter, but also showed, in many runs, a slight trend downwards of the absolute value of ΔH with decreasing oxygen concentrations. A negative value of the first order enthalpy interaction coefficient would account for this effect, since:

$$h_0^{(0)} = \left(\frac{\partial \Delta H}{\partial \%O} \right)_{\%O \rightarrow 0}$$

At low concentrations of oxygen, however, the scatter of the data (because of the relatively larger errors introduced by the pressure readings) is much too pronounced to enable one to calculate a precise value of $h_0^{(0)}$.

The problem of the determination of $h_0^{(0)}$ also can be approached by studying the temperature dependence of $e_0^{(0)}$, since:

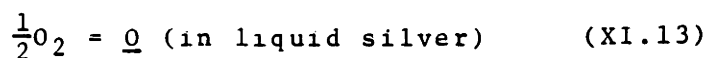
$$e_0^{(0)} = \frac{h_0^{(0)}}{2.3RT} - \frac{s_0^{(0)}}{2.3R}$$

A very slight increase of $e_0^{(0)}$, with increasing temperature, was found, thus constituting a further check on the previous observation on the enthalpy function.

A rough estimate of $h_0^{(0)}$ is -1000 ± 600 cal, and the corresponding value of $s_0^{(0)}$ is -1.1 ± 0.5 cal. $^{\circ}\text{K}^{-1}$. It may be noted that a change in the temperature from 980 to 1140 $^{\circ}\text{C}$ results in a change of approximately 0.02 in the value of $e_0^{(0)}$ (0.07 ± 0.03).

2.4 Summary of the Thermodynamic Properties of the Solubility of Oxygen in Liquid Silver

All the information gathered in this study of the solubility of oxygen in liquid silver, according to the reaction:



may be summarized by the following equations:

$$\Delta F^{\circ}(\%)_{1060^{\circ}\text{C}} = 3600 \pm 75 \text{ cal} \quad (\text{XI.18})$$

$$\Delta H(\%) = \Delta H^{\circ}(\%) + h_0^{(0)}\% \text{O} = (-3843 \pm 78) - (1000 \pm 600)(\% \text{O} - 0.27) \quad (\text{XI.19})$$

$$\Delta S(\%) = \Delta S^{\circ}(\%) + s_0^{(0)}\% \text{O} = (-5.495 \pm 0.055) - (1.1 \pm 0.5)(\% \text{O} - 0.27) \quad (\text{XI.20})$$

$$\log K'_{1060^{\circ}\text{C}} = (-0.5710 \pm 0.0043) - (0.07 \pm 0.03)(\% \text{O} - 0.27) \quad (\text{XI.21})$$

3. Solubility of Oxygen in Liquid Silver-Gold Alloys

Gold additions to the silver decrease the solubility of oxygen and, consequently, increase the activity coefficient of oxygen, as illustrated by the data at 1030.5°C (or $10^3/T=0.7670^\circ\text{K}^{-1}$) in Fig. XI.4. The values of $\log f_0$ are corrected by the coefficient $e_0^{(0)}$, to apply to the state of infinite dilution of oxygen. At a concentration of 2.2 percent of gold, five data points are very nearly superimposed. They do not correspond to the same concentration of oxygen. First, this is an indication that the deviation from Sieverts' law, in pure silver, is not drastically affected by the presence of gold, and second, it constitutes a check on the accuracy of those data.

A multi-dimensional least square analysis of the data yields the results summarized in Table XI.3.

TABLE XI.3

INTERACTION COEFFICIENTS OF GOLD ON OXYGEN IN LIQUID SILVER

<u>Composition Coordinate</u>	<u>First Order Interaction Coefficient</u>		
	<u>Free Energy at 1030.6°C</u>	<u>Enthalpy (cal.)</u>	<u>Entropy (cal. °K⁻¹)</u>
weight percent	$e_0^{(\text{Au})} = 0.019 \pm 0.001$	$h_0^{(\text{Au})} = 62 \pm 16$	$s_0^{(\text{Au})} = -0.040 \pm 0.012$
mole fraction	$\epsilon_{\text{Au},0} = 7.2 \pm 0.4$	$\eta_{\text{Au},0} = 11,300 \pm 2900$	$\sigma_{\text{Au},0} = -5.7 \pm 2.2$

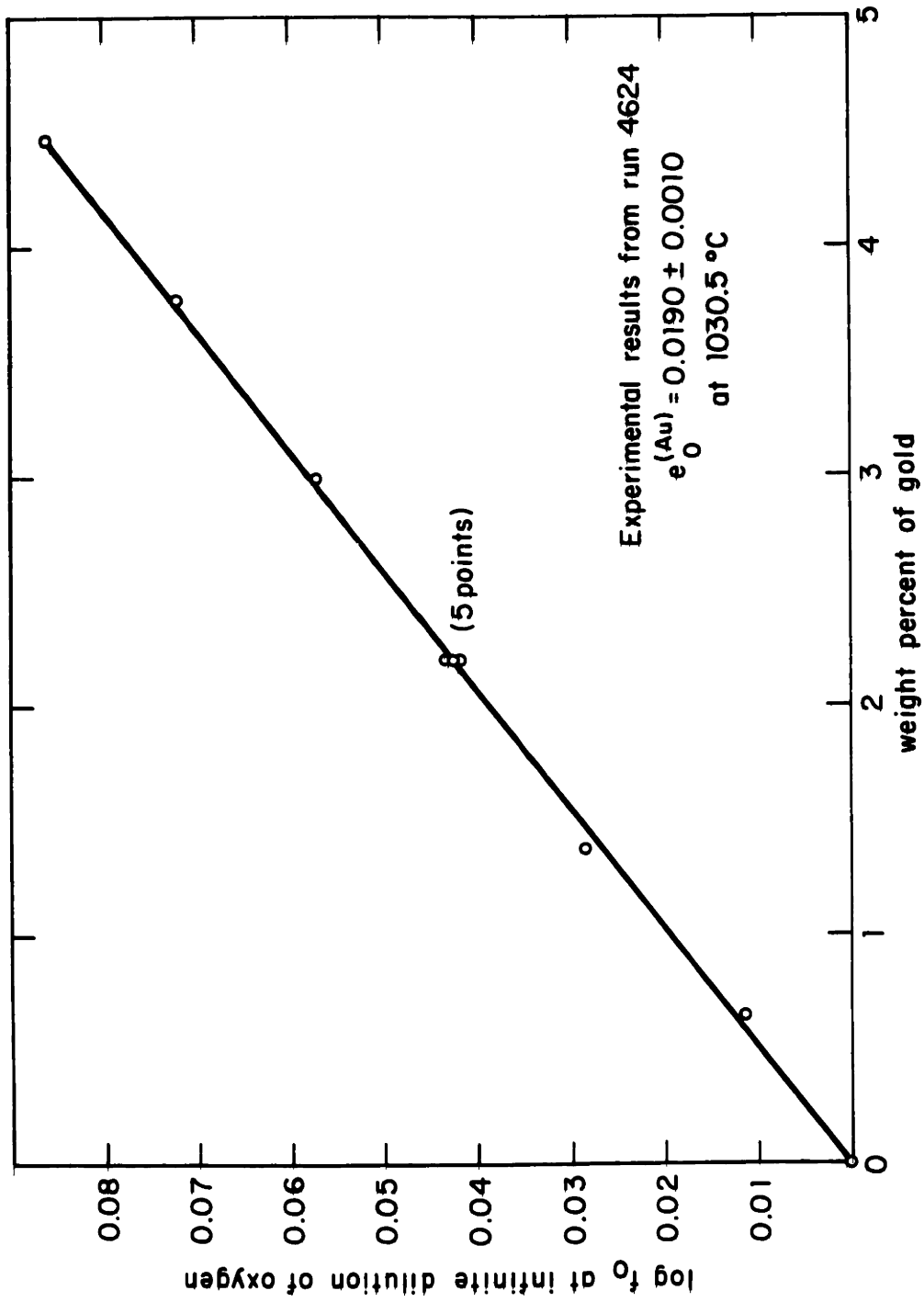


FIG. XI 4. EFFECT OF GOLD ON THE ACTIVITY COEFFICIENT OF OXYGEN IN SILVER

4. Solubility of Oxygen in liquid Silver-Platinum Alloys

Platinum additions to the silver decrease the solubility of oxygen and increase its activity coefficient. This effect is illustrated in Fig. XI.5 at four different temperatures. The interaction is smaller at higher temperatures. The best precision is obtained at 1018°C or $-0.7745 \cdot 10^{-3} (\text{°K})^{-1}$. An investigation of the value of $e_0^{(0)}$ was made at a platinum concentration of 5.43 percent. The value observed lies in the range of those recorded in the silver-oxygen system. A difference, however, of approximately 0.012 was observed in the absolute values of $1 + \log K'$ (order of magnitude: 0.320) and is, most probably, due to an extensive vaporization of the silver when evacuating the system to obtain low concentrations of oxygen (operation which took place between the results number 78 and 79 in run 4828, Appendix H).

The results are summarized by the values of the interaction coefficients in Table XI.4.

TABLE XI.4

INTERACTION COEFFICIENTS OF PLATINUM ON OXYGEN IN LIQUID SILVER

Composition Coordinate	Firts Order Interaction Coefficients		
	Free Energy at 1018°C	Enthalpy (cal.)	Entropy (cal. °K ⁻¹)
weight percent	$e_0^{(\text{Pt})} = 0.0210 \pm 0.0003$	$h_0^{(\text{Pt})} = 86 \pm 15$	$s_0^{(\text{Pt})} = -0.030 \pm 0.010$
mole fraction	$\epsilon_{\text{Pt},0} = 7.95 \pm 0.12$	$\eta_{\text{Pt},0} = 15,560 \pm 2750$	$\sigma_{\text{Pt},0} = -3.8 \pm 2.0$

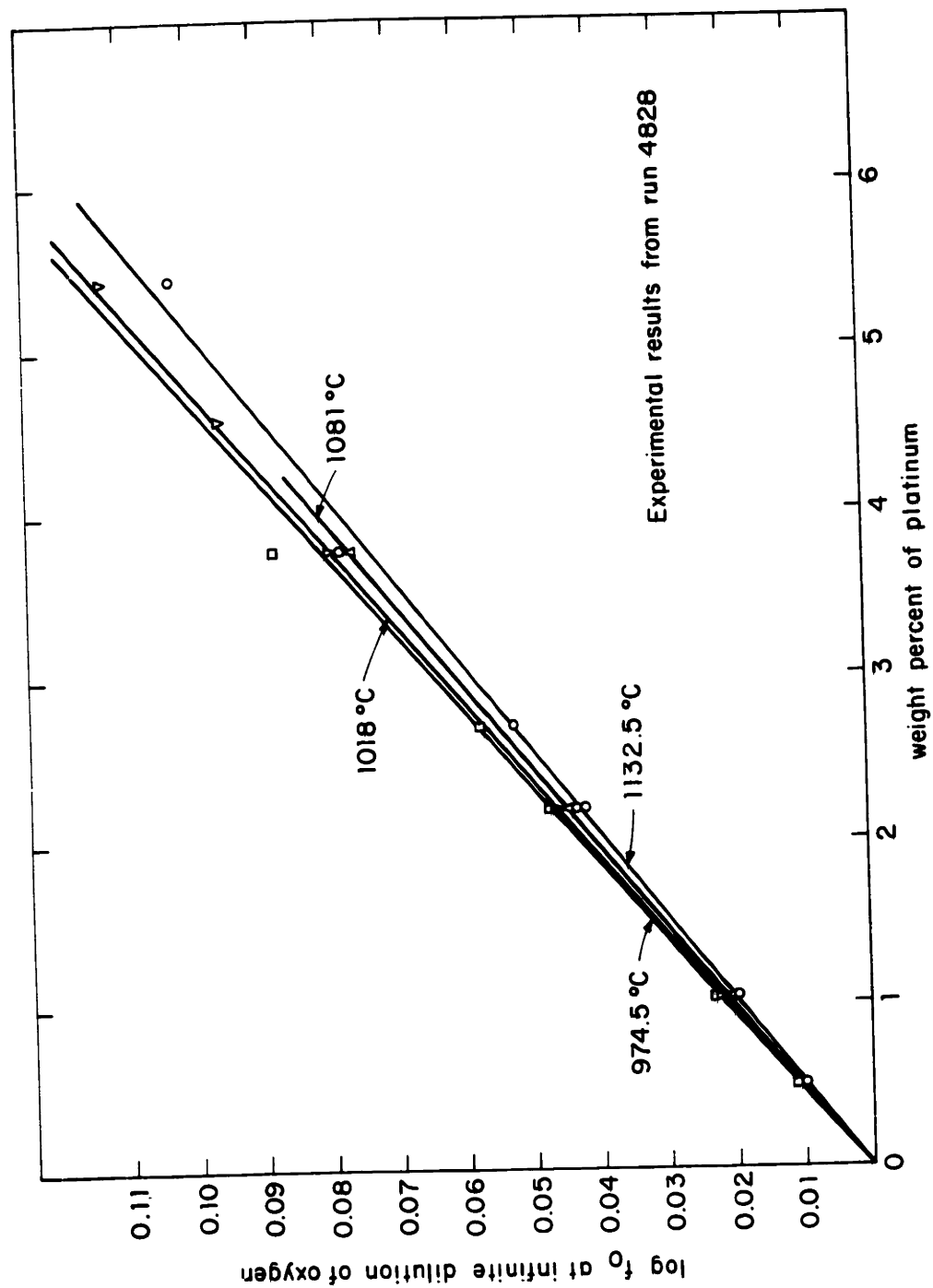


FIG. XI.5. EFFECT OF PLATINUM ON THE ACTIVITY COEFFICIENT OF OXYGEN IN LIQUID SILVER

5. Solubility of Oxygen in Liquid Silver-Palladium Alloys

Palladium additions to the silver decrease the solubility of oxygen and increase its activity coefficient. Fig. XI.6 illustrates this effect at 1050°C (or $10^3/T=0.7558^\circ\text{K}^{-1}$). The data are taken from run 4917. Two extensive investigations of the values of $e_0^{(O)}$ indicate no significant change from the results observed in pure silver. Absolute values of $\log K'$ are satisfactorily consistent. The data points in Fig. XI.6 belong to the three phases of the run defined by these two investigations of $e_0^{(O)}$.

The results are summarized by the values of the interaction coefficients in Table XI.5.

TABLE XI.5

INTERACTION COEFFICIENTS OF PALLADIUM ON OXYGEN IN LIQUID SILVER

<u>Composition Coordinate</u>	<u>First Order Interaction Coefficients</u>		
	<u>Free Energy at 1050°C</u>	<u>Enthalpy (cal.)</u>	<u>Entropy (cal. °K⁻¹)</u>
weight percent	$e_0^{(Pd)} = 0.0350 \pm 0.0012$	$h_0^{(Pd)} = 138 \pm 29$	$s_0^{(Pd)} = -0.055 \pm 0.020$
mole fraction	$\epsilon_{Pd,0} = 7.96 \pm 0.27$	$\eta_{Pd,0} = 13.650 \pm 2900$	$\sigma_{Pd,0} = -5.4 \pm 2.0$

6. Solubility of Oxygen in Liquid Silver-Copper Alloys

The solubility of oxygen in liquid silver is increased, considerably, by small additions of copper. The corresponding decrease of the oxygen activity coefficient is shown in Fig. XI.7.

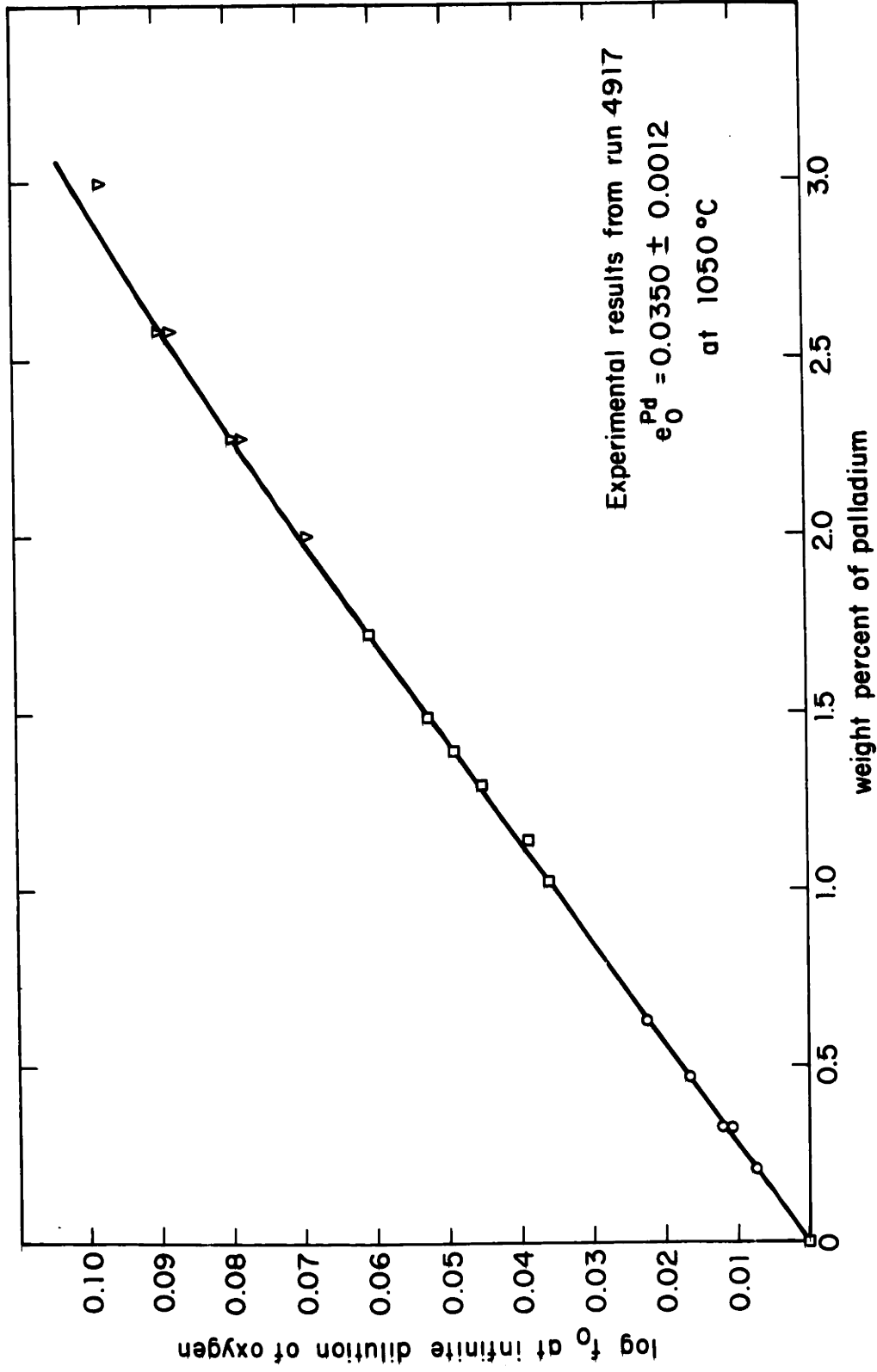


FIG. XI 6. EFFECT OF PALLADIUM ON THE ACTIVITY COEFFICIENT OF OXYGEN IN SILVER

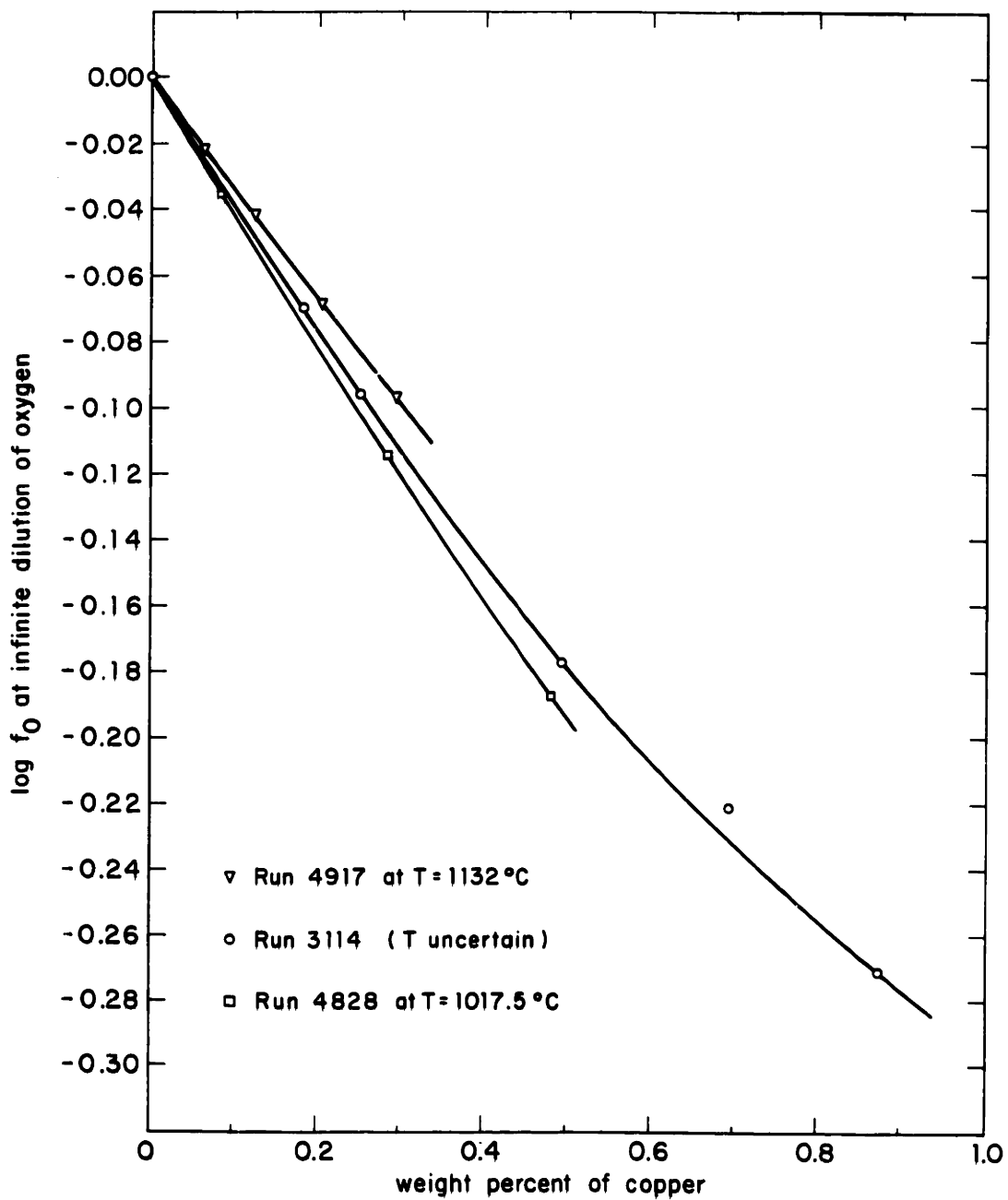


FIG. XI 7. EFFECT OF COPPER ON THE ACTIVITY COEFFICIENT OF OXYGEN IN LIQUID SILVER

Values of the interaction coefficients are based on the data of five runs - 3114, 4019, 4120, 4828 and 4917 - and are summarized in Table XI.7. In run 3114, experimental troubles were encountered in the temperature measurements. It is considered, however, that the temperature at which most of the data were taken was stable throughout the run. The main result of this run is the marked curvature of $\log f_0$ versus %Cu. In run 4019, the results are less precise than those obtained in most runs; the cause may be a small leak in the system. In run 4120, the data were taken at low concentrations of oxygen. On one hand, the relative error, resulting from readings of low pressures, is larger than the one which occurred at pressures near one atmosphere, but, on the other hand, these data show that the concentration of copper has no marked effect on the dependence of $\log f_0$ versus %Cu (or, in other words, the term $r_0^{(Cu,O)}\%Cu\%O$ may be neglected). Runs 4828 and 4917 studied the effect of copper on oxygen in silver-palladium alloys and silver-platinum alloys, respectively. Figures XI.8 and XI.9 show the marked increase in the value of $\log K'$ and the slope $\frac{d \log K'}{d(1/T)}$ with copper additions. It must be noted that in the experimental investigation of the heat effect, the data were taken at constant amount of oxygen in the system, rather than at constant concentration of oxygen in the melt. The correction is small but may be calculated through the following equation:

$$\left(\frac{\partial \log K'}{\partial 1/T}\right)_{\%O} d\frac{1}{T} = d \log K' - \left(\frac{\partial \log K'}{\partial \%O}\right)_T d\%O \quad (\text{XI.22})$$

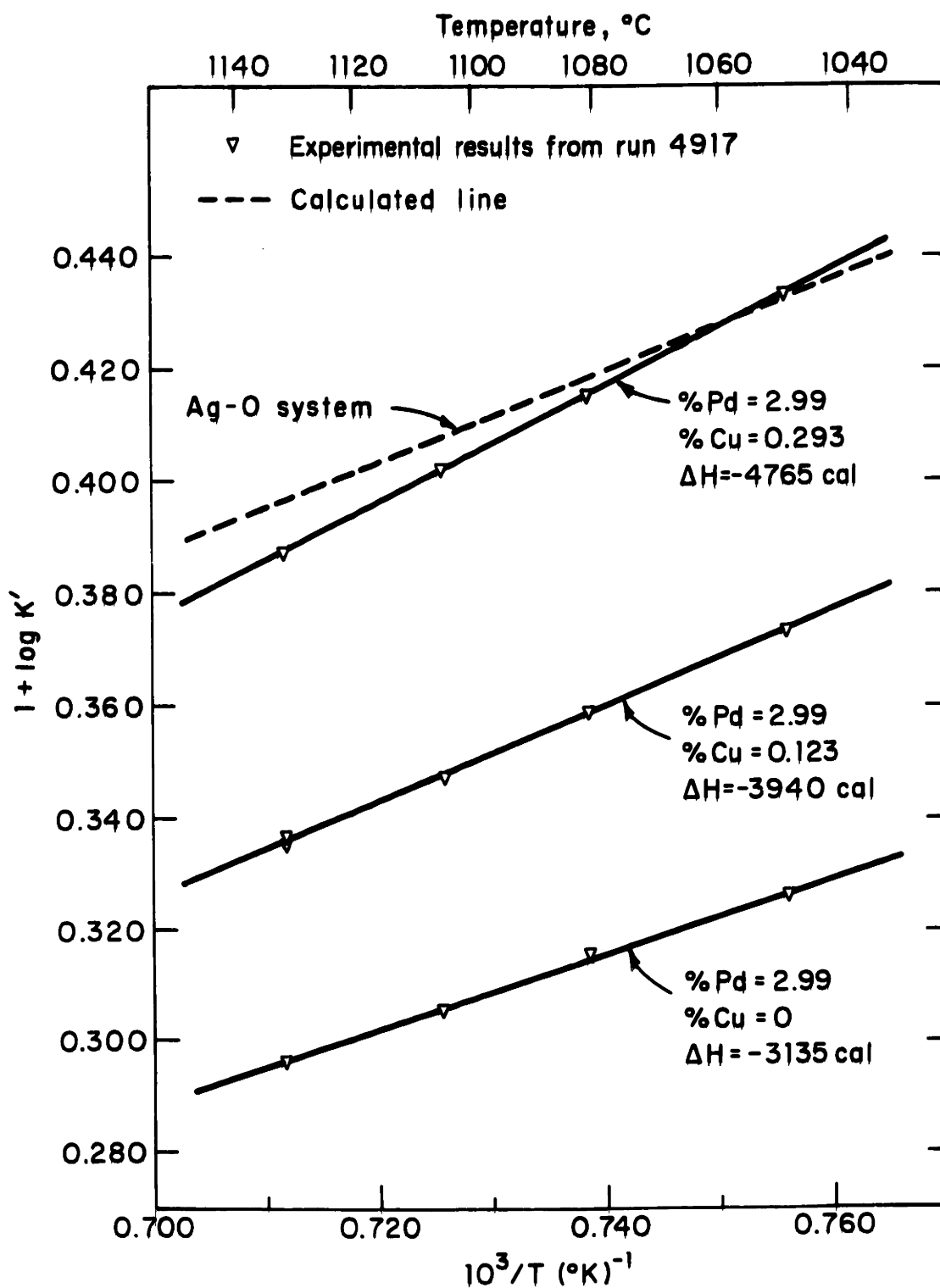


FIG. XI 8. EFFECT OF COPPER ON OXYGEN IN LIQUID SILVER-PALLADIUM ALLOYS

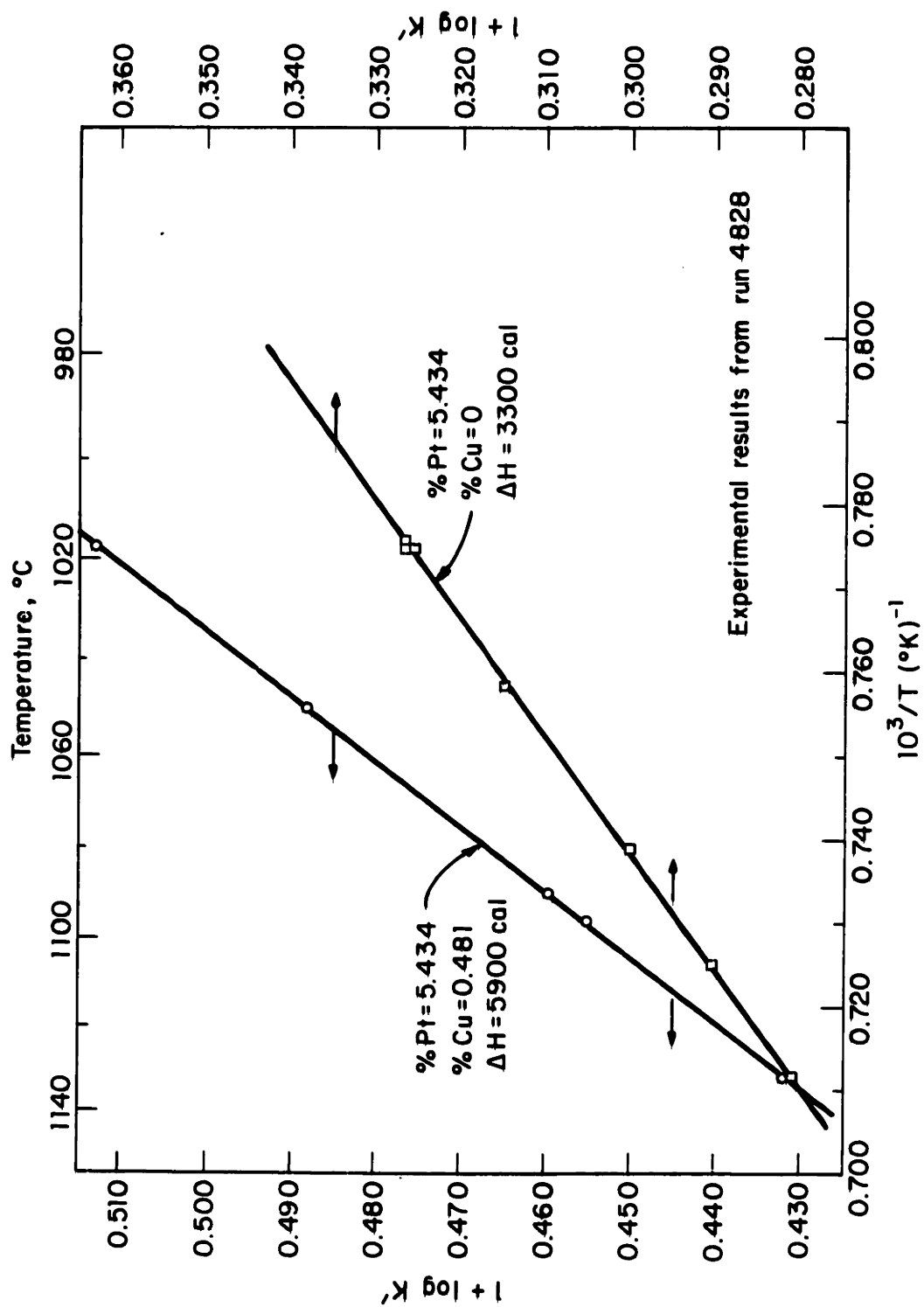


FIG. XI 9. EFFECT OF COPPER ON OXYGEN IN LIQUID SILVER-PLATINUM ALLOYS

or

$$\left(\frac{\partial \log K'}{\partial 1/T}\right)_{\%O} = \frac{d \log K'}{d 1/T} + e_0^{(O)} \frac{d \%O}{d 1/T} \quad (\text{XI.23})$$

Values of $e_0^{(\text{Cu})}$ also may be deduced, assuming that terms involving $r_0^{(\text{Cu,Pt})}$ or $r_0^{(\text{Cu,Pd})}$ are negligible. It may be noted in Fig. XI.7 that the data on a plot of $\log f_0$ versus %Cu show pronounced positive curvatures ($r_0^{(\text{Cu})} > 0$) for the three runs (3114, 4828 and 4917), although they were calculated from quite different alloys. Results of all five runs are summarized in Table IX.6.

TABLE XI.6

EXPERIMENTAL DATA ON THE FIRST ORDER FREE ENERGY AND ENTHALPY INTERACTION COEFFICIENTS

<u>Run</u>	<u>$e_0^{(\text{Cu})}$ (1060°C)</u>	<u>$h_0^{(\text{Cu})}$ calculated at %Cu</u>	
4120	-0.38 ± 0.02	~ -6040 cal.	0.140 to 0.199
4190	-0.38 ± 0.03	~ -5720 cal.	0 to 0.3
3114	-0.38 ± 0.04		
4917	-0.39 ± 0.007	-6500 cal.	0.123
4917		-5580 cal.	0.293
4828	-0.385 ± 0.007	-5410 cal.	0.481

$h_0^{(\text{Cu})}$ seems to decrease, with increasing copper concentrations. This would indicate a positive curvature for the dependence of ΔH on %Cu, thus a positive second order enthalpy interaction coefficient, an observation in agreement with the positive second order free energy interaction coefficient, $r_0^{(\text{Cu})}$, noted above.

The data, however, are not sufficiently conclusive to permit an estimation of this second order enthalpy coefficient.

Estimated values of the various interaction coefficients are given in Table XI.7.

TABLE XI.7

INTERACTION COEFFICIENTS OF COPPER ON OXYGEN IN LIQUID SILVER

<u>Composition Coordinate</u>	<u>First Order Interaction Coefficients</u>			<u>Second Order Free Energy</u>
	<u>Free Energy at 1060°C</u>	<u>Enthalpy (Kcal.)</u>	<u>Entropy (cal. °K⁻¹)</u>	
weight percent	$e_0^{(Cu)} =$ -0.385±0.010	$h_0^{(Cu)} =$ -6.4±1.0	$s_0^{(Cu)} =$ -3.10±0.75	$r_0^{(Cu)} = 6.5 \times 10^{-2}$
mole fraction	$\epsilon_0^{(Cu)} = -52 \pm 1$	$\eta_0^{(Cu)} =$ -380±60	$\sigma_0^{(Cu)} =$ - 182±45	$\rho_0^{(Cu)} = 500$

CHAPTER XII
DISCUSSION OF ERRORS AND CONCLUSIONS ON
EXPERIMENTAL WORK

The solubility of oxygen in liquid silver and silver alloys was measured and several interaction coefficients calculated. The precision and accuracy of these results must be discussed now.

1. Systematic Errors

The systematic errors, connected with the determination of the origin for the oxygen concentration in the melt or arising from impurities in the gas phase, have been discussed already. The other possible systematic errors stem, mainly, from the measurement of the hot volume, the vaporization of the silver and the impurities in the melt.

1.1 Hot Volume

It has been assumed, in the previous calculations, that the hot volume, as measured by argon, is a true measure of the volume of oxygen necessary to fill the dead space of the reaction chamber at a specific temperature and pressure. To investigate this assumption, an experiment was done in which nitrogen and hydrogen (reported insoluble in silver⁽⁴⁶⁾) were used to determine the hot volume. The results are shown in Fig. XII.1. For argon and nitrogen, the agreement is excellent; the results show a slightly smaller hot volume for hydrogen, most likely due to its high thermal conductivity. The chronological order of the points must be noted; three short evacuations of the system which,

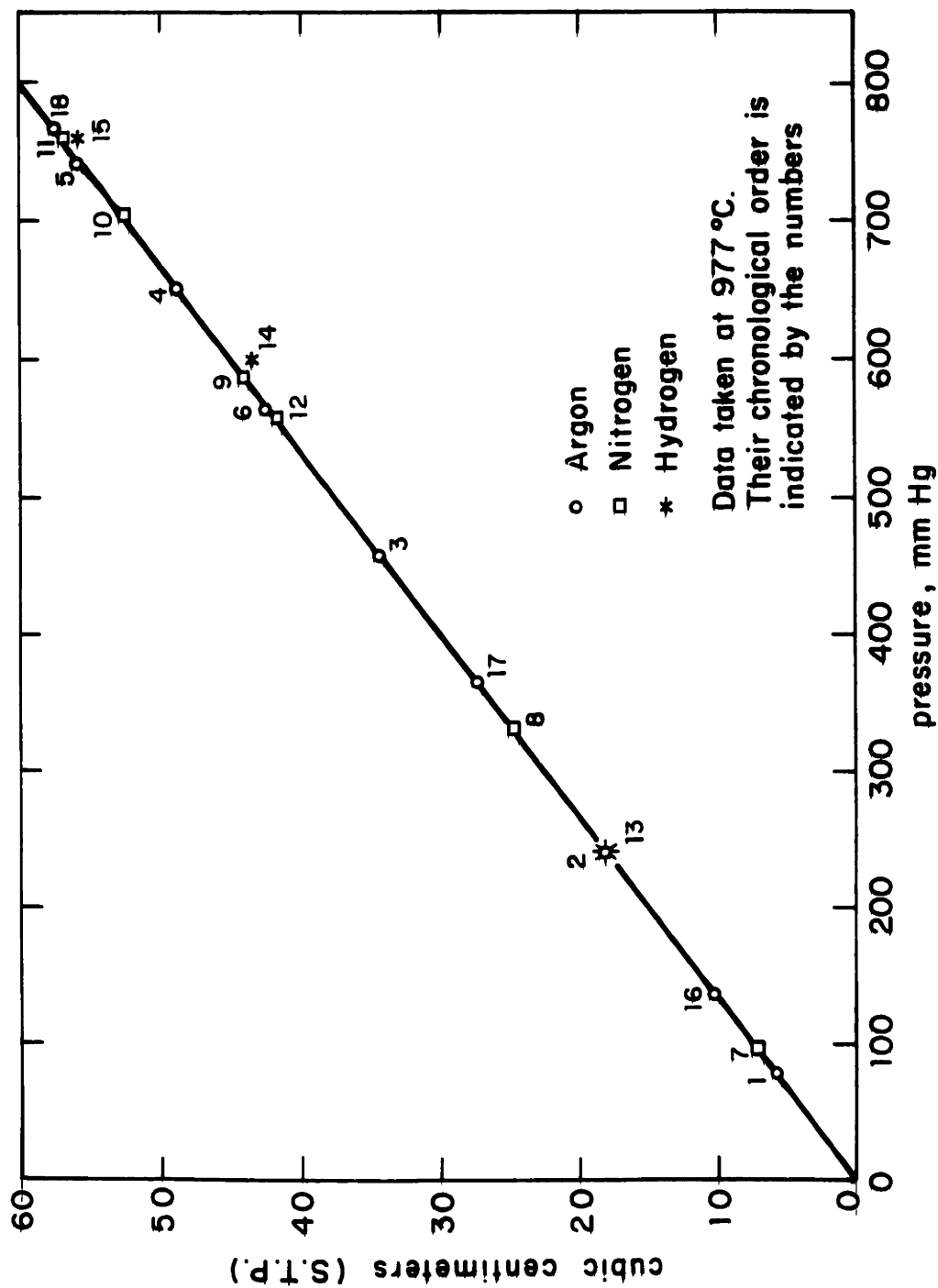


FIG. XII 1. "HOT VOLUME" STUDY

because of the possibility of consequent vaporization of the silver, could have resulted in a change of the hot volume, did not seem to affect the results. The temperature coefficient of the hot volume, for argon and nitrogen, also fell within the experimental error.

1.2 Vaporization of the Silver

Deposits of silver on the lid of the crucible and walls of the reaction chamber were kept to a minimum, by keeping the molten melt under vacuum for the shortest time allowed by the method. Podgurski and Davis,⁽³²⁾ in their experiments on oxygen solubility in solid silver, reported a continuous drift of the pressure of oxygen. Such a drift was never observed in this investigation, even after a considerable time (15 hours).

1.3 Impurities in the Melt

Analysis of the silver used revealed a copper content of 0.005 percent. Although very small, it accounts for an apparent increased solubility of oxygen or an error, in the value of $\log K'$, of $-e_0^{(0)} \cdot 0.005 = 0.40 \cdot 0.005 = 0.0020$. This error, however, is in the range of the scatter of the data and will be neglected.

The results of Sieverts and Hagenacker show higher solubilities of oxygen than those reported in this study. It must be noted that the authors do not give an analysis of their silver, and that a copper content of 0.04 percent would account for these differences in solubility. These differences also may be accounted for by a temperature error of 4°C. The contribu-

tion of both factors is likely.

2. Random Errors

The following approximate random errors may be calculated.

If N is the total number of cm^3 (STP) of oxygen in the system, n and n' the numbers of cm^3 dissolved in the melt and present in the gas phase, respectively, then:

$$N = n + n'$$

and

$$\delta \log \%O \quad \delta \log n = \frac{\delta n}{n} = \frac{\delta N + \delta n'}{n}$$

and, with a random error of 0.05 cm^3 in the readings of the burette,

$$\delta \log \%O = \frac{0.5 + 0.2}{400} = 0.0017 \quad (\text{XII.1})$$

For readings of the pressure near one atmosphere:

$$\delta \log p = \frac{1}{760} = 0.0013 \quad (\text{XII.2})$$

Assuming an error of $\pm 1^\circ\text{C}$ in the temperature:

$$\delta (10^3/T) = 0.0006 \quad (\text{XII.3})$$

The resulting error in $\log K'$ is:

$$\delta \log K' = \delta \log \%O + \frac{1}{2} \delta \log p + \frac{\partial \log K'}{\partial \frac{1}{T}} \delta \frac{1}{T}$$

$$= 0.0017 + 0.0007 + 0.840 \cdot 0.0006$$

$$= 0.0029$$

(XII.4)

For $e_0^{(0)}$, the random error may be calculated as follows:

$$e_0^{(0)} = - \frac{\Delta \log K'}{\Delta \%O}$$

$$\delta e_0^{(0)} = \frac{\Delta \%O \cdot \delta \Delta \log K' + \delta \Delta \%O \cdot \Delta \log K'}{(\Delta \%O)^2}$$

$$= \frac{0.2 \cdot 0.004 + 0.001(0.2 \cdot 0.07)}{(0.2)^2} = \frac{0.004}{0.2}$$

$$= 0.02$$

(XII.5)

Similarly, for $\frac{\Delta H}{2.3R}$:

$$\frac{\Delta H}{2.3R} = \left(\frac{\partial \log K'}{\partial \frac{1}{T}} \right)_{\%O} \cdot \frac{\Delta \log K'}{\Delta \frac{1}{T}}$$

$$\delta \frac{\Delta H}{2.3R} = \frac{\Delta \left(\frac{1}{T} \right) \delta \Delta \log K' + \delta \Delta \left(\frac{1}{T} \right) \cdot \Delta \log K'}{[\Delta \left(\frac{1}{T} \right)]^2} = \frac{\delta \Delta \log K'}{\Delta \left(\frac{1}{T} \right)} \quad (\text{XII.6})$$

At a fixed amount of oxygen in the system, the error on $\Delta \log K'$

is reduced considerably and may be estimated as 0.0020, which yields:

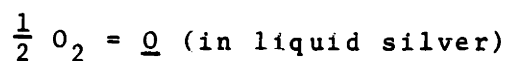
$$\frac{\Delta H}{2.3R} = \frac{0.002}{0.1 \cdot 10^3} = 20 \quad (\text{XII.7})$$

These errors of 0.0029, 0.02 and 20 on $\log K'$, $e_0^{(0)}$ and $\frac{\Delta H}{2.3R}$ may be compared, respectively, with the standard deviations of 0.0028, 0.014 and 17 yielded by the statistical analysis of Tables XI.1 and XI.2. Similar calculations are possible for the ternary interaction coefficients. They, also, agree satisfactorily with the standard deviations previously reported. Errors in the concentrations of the alloying elements are assumed negligible, as the masses of the additions were weighed twice to ± 0.0002 g and, after the runs were completed, qualitative analyses were performed on the alloys.

3. Conclusions on Experimental Work

The solubility of oxygen in liquid silver and silver alloys has been determined as a function of temperature and pressure. Estimates of the corresponding thermodynamic functions, taking into account random and systematic errors, are given below.

a. The free energy, enthalpy and entropy of the reaction:



are, respectively:

$$\Delta F(\%)_{1060^\circ\text{C}} = (3483 \pm 26) + (43 \pm 18)(\% \text{O} - 0.27) \text{ cal.}$$

$$\Delta H(\%) = (-3843 \pm 78) - (1000 \pm 600)(\%O - 0.27) \text{ cal.}$$

$$\Delta S(\%) = (-5.495 \pm 0.055) - (1.1 \pm 0.5)(\%O - 0.27) \text{ cal. } ^\circ\text{K}^{-1}$$

b. The effects of gold, platinum, palladium and copper on the activity coefficient of oxygen are summarized in Fig. XII.2, and the values of the interaction coefficients are reported in Table XII.1.

TABLE XII.1
INTERACTION COEFFICIENTS OF VARIOUS ELEMENTS ON OXYGEN
IN LIQUID SILVER

<u>Alloying element (i)</u>	<u>$\epsilon_0^{(i)}$ (at 1060°C)</u>	<u>$\eta_0^{(i)}$ (kcal.)</u>	<u>$\sigma_0^{(i)}$ (cal. °K⁻¹)</u>
O	3.2 ± 1	- 1.5 ± 0.9	- 7.5 ± 2.1
Au	7.1 ± 0.4	11.3 ± 2.9	- 5.7 ± 2.2
Pt	7.8 ± 0.1	15.6 ± 2.8	- 3.8 ± 2.0
Pd	7.9 ± 0.3	13.7 ± 2.8	- 5.4 ± 2.0
Cu	- 52 ± 1	-380 ± 60	-182 ± 45

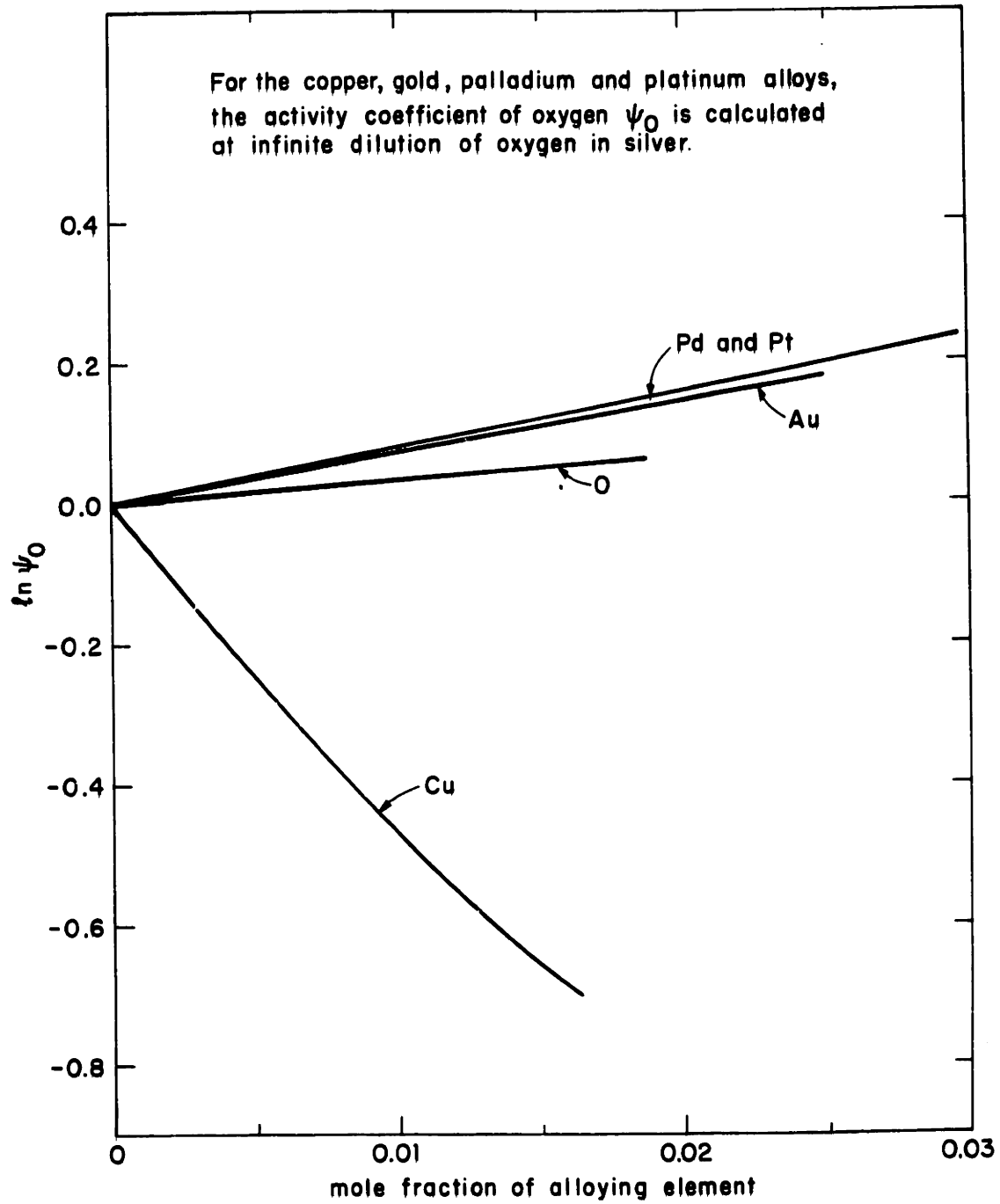


FIG. XII 1. EFFECT OF ALLOYING ELEMENTS ON THE ACTIVITY COEFFICIENT OF OXYGEN IN LIQUID SILVER AT 1060°C

CHAPTER XIII
CORRELATION BETWEEN THE EXPERIMENTAL RESULTS
AND THE THEORETICAL MODELS

The study of the effect of an alloying element on the solubility of oxygen in liquid silver is experimentally limited to only a few elements, and, consequently, this also restricts the possibilities of an extensive comparison between experimental and theoretical results. However, the interactions of various elements on sulfur in liquid copper, which were determined by Alcock and Richardson,⁽⁶⁾ offer many valuable complementary observations, since the electronic structures and chemical properties of the copper-sulfur system are very similar to those of the silver-oxygen system. In terms of either the modified cell model or the quasi-chemical theory, the effects of a third element on these two binaries is predicted to be also very similar. Indeed, this is what is observed for the cases of gold and platinum, as shown by Table XIII.1.

TABLE XIII.1
COMPARISON OF THE EFFECTS OF GOLD AND PLATINUM ON SULFUR
IN COPPER AND OXYGEN IN SILVER

<u>Solute M</u>	<u>ϵ_S^M (in copper)</u>	<u>ϵ_O^M (in silver)</u>
Au	6.9 ± 1.0 at 1115°C	6.9 ± 0.5 at 1115°C
Pt	9.2 ± 0.2 at 1200°C	7.95 ± 0.12 at 1018°C extrapolated to: 7.2 ± 0.3 at 1200°C

It is interesting to note that, for gold, the curve $\ln \psi_S$ versus mole fraction of gold in copper, shows a positive deviation from linearity ($\rho_S^{(Au)} > 0$), whereas such a curvature is not found in the silver system, although the interaction coefficients $\epsilon_S^{(Au)}$ and $\epsilon_0^{(Au)}$ are equal. A possible explanation may be given by the quasi-chemical model which predicts the relation (equation IV.39):

$$\rho_2^{(Au)} = \frac{[\epsilon_2^{(Au)}]^2}{2Z} + \frac{\epsilon_{Au}^{(Au)}}{Z} \left[\epsilon_2^{(Au)} - \frac{Z}{2} \right]$$

All three terms, $\frac{(\epsilon_2^{(Au)})^2}{2Z}$, $\frac{\epsilon_{Au}^{(Au)}}{Z}$ and $(\epsilon_2^{Au} - \frac{Z}{2})$, are positive.

But, $\epsilon_{Au}^{(Au)}$ in copper⁽⁵²⁾ equals 8.5, while in silver⁽⁵²⁾ it only equals 2.3. Thus:

$$\rho_S^{(Au)} (\text{in Cu}) > \rho_0^{Au} (\text{in Ag})$$

a result which agrees with the experimental observations.

The strongly negative interaction of copper on oxygen ($\epsilon_0^{(Cu)} = -52$ at 1060°C), and the similar positive interaction coefficients of gold, platinum and palladium on oxygen ($\epsilon_0^{(Au)} = 7.1$, $\epsilon_0^{(Pt)} = 7.8$ and $\epsilon_0^{(Pd)} = 7.9$ at 1060°C) are qualitatively well accounted for by either the quasi-chemical or the modified cell model, on the basis of the affinities of these alloying elements for oxygen (as measured, for example, by the stability of the corresponding oxides). In addition, for copper, a value of approximately 500 was observed for $\rho_0^{(Cu)}$. The value calculated

by the quasi-chemical model is:

$$\begin{aligned} \rho_0^{(\text{Cu})} &= \frac{(\epsilon_0^{\text{Cu}})^2}{2Z} + \frac{\epsilon_{\text{Cu}}^{(\text{Cu})}}{Z} \left[\epsilon_0^{(\text{Cu})} - \frac{Z}{2} \right] \\ &= \frac{(52)^2}{20} + \left(\frac{-4.7}{10} \right) (-52 - 5) = + 162 \end{aligned}$$

a result in satisfactory agreement with the experimental value.

$(\epsilon_{\text{Cu}}^{(\text{Cu})})$ is estimated from values of the activity coefficients γ_{Cu} reported by Hultgren, et. al. (52)

Experimentally determined values of enthalpy and entropy interaction coefficients may be compared with the theoretical models. The modified cell model (Chapter V) proposed a proportionality between a change in the energy and the corresponding change in the vibrational entropy. It may be noted that, in the assumption of pairwise interactions:

$$n_{2,3} \approx Z\beta(\omega_{2,3} - \omega_{1,2} - \omega_{1,3})$$

which, with

$$\omega_{i,j} = u_{i,j} - \frac{u_{ii} + u_{jj}}{2}$$

may be rewritten as:

$$n_{2,3} = Z\beta[(u_{2,3} - u_{1,2}) + (u_{1,1} - u_{1,3})]$$

or:

$$\eta_{M,O} = Z\beta[(u_{M,O} - u_{Ag,M}) - (u_{Ag,Ag} - u_{Ag,O})]$$

and, thus:

$$\sigma_{M,O} = Z\beta[\tau'(u_{M,O} - u_{Ag,M}) - \tau''(u_{Ag,Ag} - u_{Ag,O})]$$

If τ' is approximately equal to τ'' , and is independent of the nature of the element M, then a proportionality between $\eta_{M,O}$ and $\sigma_{M,O}$ should be observed. As shown by the experimental values in Table XII.2, this is not the case. However, if the effect of τ'' is subtracted, a better agreement should be obtained. This is supported by the fact that, although the values of $\eta_0^{(M)}$ and $\sigma_0^{(M)}$ are not proportional, increasing values of $\eta_0^{(M)}$ correspond to increasing values of $\sigma_0^{(M)}$ (for Pt and Pd, the reversal in the order is within experimental error).

The constancy of the proportionality parameter, τ , irrespective of the nature of the atoms involved, is not very well supported, in the case of the oxygen solubility in silver alloys, although the test is not conclusive. As already mentioned, the agreement should be much superior if τ is taken as approximately constant for elements which are not too dissimilar in their physical properties.

CHAPTER XIV
SUMMARY AND CONCLUSIONS

The concept of generalized interaction coefficient was shown to permit a convenient and systematic approach to the problem of evaluating activities in a multicomponent system. Sherman and Chipman's⁽¹²⁾ semi-empirical method of calculating activities was analyzed and an alternative method proposed. The role of the composition coordinate in the calculations was underlined, and the importance of a free energy second order interaction coefficient ρ particularly stressed. The use of ρ eliminates some discrepancies in the literature and provides a simple solution to a problem of data reduction.

The quasi-chemical model was reviewed critically, and its predictions for free energy terms found to be satisfactory. The expression yielded by the model for the second order interaction ρ was calculated and compared, with fair success, to experimental data.

A modified version of the cell model was presented, which explains some of the discrepancies found in the applications of the quasi-chemical theory, while improving on it by introduction of the vibrational contribution. Under its simplest form, this cell model introduces the first quasi-regular solution - a model which has the simplicity of expression of the regular solution model, but which would permit a better evaluation of the enthalpy and entropy terms by a prior evaluation of a constant, τ . The prediction of the constant τ was seen to be possible by analysis of the data on various alloys. A systematic study of enthalpy

and entropy interaction coefficients seemed rich in possibilities.

Data on free energy, enthalpy and entropy interaction coefficients were experimentally obtained by an investigation of the solubility of oxygen in molten silver alloys. These coefficients express the effects of oxygen, gold, platinum, palladium and copper on oxygen in liquid silver. The comparison of the enthalpy and entropy coefficients with the results of the modified cell model was not conclusive. More satisfactory was this comparison for the free energy terms, and, in particular, quite fair agreement was found with the results of Alcock and Richardson⁽⁶⁾ on the solubility of sulfur in copper alloys.

CHAPTER XVSUGGESTIONS FOR FURTHER WORK

A compilation of the values of the second order free energy interaction coefficients would certainly prove useful for the three following reasons. First, the use of tabulated values is often more convenient than the use of graphs for which reading errors may be quite large. Second, such a compilation would permit a better estimation of coefficients presently unknown. Third, it would provide a test for expressions predicted by theoretical models (the quasi-chemical in particular).

A similar compilation of the values of the enthalpy and entropy first order interaction coefficients would permit a better evaluation of the configurational and vibrational contributions, and thus, a better description of a liquid solution. The introduction of electron concentrations in the approach of the modified cell model (Chapter V) seems rich in possibilities.

An experimental investigation of those systems for which very marked effects can be predicted is of special interest.

REFERENCES

1. Wagner, C., Thermodynamics of Alloys, Addison-Wesley Publishing Co., Inc., Reading, Mass., p. 51-53, 1962.
2. Wagner, C., Z. Phys. Chem., 193, 407 (1944).
3. Wagner, C., J. Chem. Phys., 19, 626 (1951).
4. Himmler, W., Z. Phys. Chem., 195, 244-253 (1950).
5. Alcock, C.B., The Physical Chemistry of Metallic Solutions and Intermetallic Compounds, Paper 2E, H.M. Stationery Office, London, 1959.
6. Alcock, C.B. and F.D. Richardson, Acta Met., 6, 385-395 (1958).
7. Durand, F., "Contribution à l'étude des interactions dans les alliages ternaires liquides," Sc.D. Thesis, Université de Grenoble, 1962.
8. Oriani, R.A., The Physical Chemistry of Metallic Solutions and Intermetallic Compounds, Paper 2A, H.M. Stationery Office, London, 1959.
9. Hill, T.L., An Introduction to Statistical Thermodynamics, Addison-Wesley Publishing Co., Inc., Reading, Mass., 1960.
10. Prigogine, I., The Molecular Theory of Solutions, North Holland, Amsterdam, 1957.
11. Ramachandran, S., R.A. Walsh and J.C. Fulton, J. of Metals, 13, No. 12, 915 (December, 1961).
12. Sherman, C.W. and J. Chipman, J. of Metals, 597-602 (June, 1952).
13. Lupis, C. and J.F. Elliott, "The Relationship between the Interaction Coefficients ϵ and e ," Trans., Met. Soc. AIME (in press).
14. Lupis, C. and J.F. Elliott, "Free Energy, Entropy and Enthalpy Interaction Coefficients," Trans., Met. Soc. AIME (in press).
15. Guggenheim, E.A., Mixtures, Oxford Clarendon Press, 1952.
16. Brewer, L., "Prediction of High Temperature, Metallic Phase Diagram," Office of Technical Services, U.S. Dept. of Commerce, Washington, D.C. (July, 1963).

17. Elliott, J.F. and J. Chipman, Trans. Farad. Soc., 47, 138-148 (1951).
18. Fuwa, T. and J. Chipman, Trans., Met. Soc. AIME, 215, 708-716 (1959).
19. Floridis, T.P. and J. Chipman, Trans., Met. Soc. AIME, 221, 549-553 (1958).
20. Pehlke, R. and J.F. Elliott, Trans., Met. Soc. AIME, 218, 1088 (1960).
21. Weinstein, M. and J.F. Elliott, Trans., Met. Soc. AIME, 227, 382 (1963).
22. Eyring, H., J. Chem. Phys., 4, 283 (1936).
23. Eyring, H. and J. Hirschfelder, J. Chem. Phys., 41, 249 (1937).
24. Blandin, A. and J.L. Deplante, Metallic Solid Solutions, Paper IV, J. Friedel and A. Guinier, Eds., W.A. Benjamin, Inc., New York, 1963.
25. Chipman, J. and D. Corrigan, "Effect of Temperature on Thermodynamic Interactions in Dilute Alloys," presented at Conference on Applications of Fundamental Thermodynamics to Metallurgical Processes, University of Pittsburgh (November 30, 1964).
26. Engel, N., ASM Trans. Quarterly, 57, 610-619 (1964).
27. Hume-Rothery, W., Atomic Theory for Students of Metallurgy, Institute of Metals, 1960.
28. Kleppa, O.J., Acta Met., 6, 225-232 (1958).
29. Kleppa, O.J., Acta Met., 6, 233-242 (1958).
30. Steacie, E.W.R. and F.M.G. Johnson, Proc. Roy. Soc. (London), Ser. A, 112, 542 (1926).
31. Eichenauer, W. and G. Müller, Z. Metallk., 53, 321 (1962).
32. Podgurski, H.H. and F.N. Davis, Trans., Met. Soc. AIME, 230, 731 (1964).
33. Lucas, Ann. Chim. Phys., 12, 402 (1819).
34. Chevillot, Ann. Chim. Phys., 13, 299 (1820).
35. Graham, Proc. Roy. Soc. (London), 15, 502 (1866).

36. Dumas, Comptes Rendus, 86, 68 (1878).
37. Brauner, Bull. Acad. Belg., 18, 81 (1889).
38. Neumann, Monats. f. Chemie, 13, 40 (1892).
39. Heycock and Neville, J. Chem. Soc. (London), 67, 1024 (1895).
40. Holborn and Day, Drud. Ann., 2, 528 (1900).
41. Berthelot, Ann. Chim. Phys., 22, 289 (1901).
42. Richards and Wells, Z. Anorg. Chem., 47, 79 (1906).
43. Sieverts, Z. Phys. Chem., 60, 129 (1908).
44. Sieverts and Hagenacker, Z. Phys. Chem., 68, 115-128 (1909).
45. Donnan and Shaw, J. Soc. Chem. Ind., 29, 9870989 (1910).
46. Hansen, Constitution of Binary Alloys, McGraw-Hill Book Company, Inc., New York, 37-39, 1958.
47. Johnstone, J.K., private communication (1964).
48. Allen, N.P., J. Inst. Metals, 49, 317-340 (1932).
49. Mizikar, E.A., R.E. Grace and N.A.D. Parlee, ASM Trans. Quarterly, 101 (March, 1963).
50. Carlin, J.F., M.S. Thesis, Department of Metallurgy, M.I.T., 1962.
51. Efroymsen, M.A., Stepwise Multiple Regression with Variable Transformations, ERMPR3, IBM Share Distribution, September, 1961.
52. Hultgren, R., L.R. Orr, P.D. Anderson and K.K. Kelley, Selected Values of Thermodynamic Properties of Metals and Alloys, John Wiley & Sons, Inc., New York, 1963.
53. Elliott, J.F., M. Gleiser and V. Ramakrishna, Thermochemistry for Steelmaking, Vol. II, Addison-Wesley Publishing Co., Reading, Mass., 1963.
54. Dealy, J.M. and R.D. Pehlke, Trans., Met. Soc. AIME, 227, 88-93 (1963).
55. Dealy, J.M. and R.D. Pehlke, Trans., Met. Soc. AIME, 227, 1030 (1963).
56. Schroeder, D. and J. Chipman, Trans., Met. Soc. AIME, 230, 1492-1494 (1964).

APPENDIX AGENERALIZED INTERACTION COEFFICIENTS - SUMMARY1. Definitions

Free energy interaction coefficients K:

$$\ln \gamma_i = \sum_{n_2} \dots \sum_{n_j} \dots \sum_{n_m} K_{n_2 \dots n_j \dots n_m}^{(i)} X_2^{n_2} \dots X_j^{n_j} \dots X_m^{n_m}$$

Enthalpy interaction coefficients I:

$$H_i^E = \sum_{n_2} \dots \sum_{n_j} \dots \sum_{n_m} I_{n_2 \dots n_j \dots n_m}^{(i)} X_2^{n_2} \dots X_j^{n_j} \dots X_m^{n_m}$$

Entropy interaction coefficients J:

$$S_i^E = \sum_{n_2} \dots \sum_{n_j} \dots \sum_{n_m} J_{n_2 \dots n_j \dots n_m}^{(i)} X_2^{n_2} \dots X_j^{n_j} \dots X_m^{n_m}$$

(where j can take any value from 2 to m, and n_j any positive value including 0).

2. Nomenclature

Order of the Interaction Coefficients	Free Energy		Enthalpy		Entropy	
	X*	%*	X*	%*	X*	%*
Zeroth	$\ln \gamma_i^c$	0	$H_i^{E^\circ}$	0	$S_i^{E^\circ}$	0
First	$\epsilon_i^{(j)}$	$e_i^{(j)}$	$\sigma_i^{(j)}$	$h_i^{(j)}$	$\eta_i^{(j)}$	$s_i^{(j)}$
Second	$\rho_i^{(j,k)}$	$r_i^{(j,k)}$				
n th (with $\sum_{j=2}^m n_j = n$)	$k_{n_2 \dots n_m}^{(i)}$		$I_{n_2 \dots n_m}^{(i)}$		$J_{n_2 \dots n_m}^{(i)}$	

* The composition coordinate is either mole fraction (X) or weight percent (%).

3. Relations between Free Energy, Enthalpy and Entropy Interaction Coefficients

Composition coordinate:

Zeroth order: $\ln \gamma_i^c = \frac{H_i^{E^\circ}}{RT} - \frac{S_i^{E^\circ}}{R}$

First order: $\epsilon_i^{(j)} = \frac{n_i^{(j)}}{RT} - \frac{\sigma_i^{(j)}}{R}$ $e_i^{(j)} = \frac{h_i^{(j)}}{2.3RT} - \frac{s_i^{(j)}}{2.3R}$

nth order: $K_{n_2 \dots n_m}^{(i)} = \frac{I_{n_2 \dots n_m}^{(i)}}{RT} - \frac{J_{n_2 \dots n_m}^{(i)}}{R}$

4. Reciprocal Relationships

$$\epsilon_j^{(i)} = \epsilon_i^{(j)} = \epsilon_{i,j}$$

$$\rho_i^{(i,j)} + \epsilon_{i,j} = 2\rho_j^{(i)} + \epsilon_{i,i}$$

$$\rho_i^{(j,k)} + \epsilon_{j,k} = \rho_j^{(i,k)} + \epsilon_{i,k} = \rho_k^{(i,j)} + \epsilon_{i,j}$$

$$K_{n_2 \dots n_i \dots n_m}^{(i)} = K_{n_2 \dots n_i \dots n_m}^{(1)} - \frac{n_i + 1}{\sum_{j=2}^m n_j} K_{n_2 \dots n_i + 1 \dots n_m}^{(1)}$$

Identical relations can be written for the enthalpy and entropy interaction coefficients.

5. Conversion Relationships

$$\epsilon_i^{(j)} = 230 \frac{M_i}{M_1} e_i^{(j)} + \frac{M_1 - M_i}{M_1}$$

$$n_i^{(j)} = 100 \frac{M_i}{M_1} h_i^{(j)}$$

$$\sigma_i^{(j)} = 100 \frac{M_i}{M_1} s_i^{(j)} - R \frac{M_1 - M_i}{M_1}$$

$$\rho_i^{(j)} = \frac{230}{M_1^2} [M_j^2 r_i^{(j)} 10^2 + M_j (M_1 - M_j) e_i^{(j)}] + \frac{1}{2} \frac{(M_1 - M_i)^2}{M_1^2}$$

$$\rho_i^{(j,k)} = \frac{230}{M_1^2} [M_j M_k r_i^{(j,k)} 10^2 + M_j (M_1 - M_k) e_i^{(j)} + M_k (M_1 - M_j) e_j^{(k)}] + \frac{(M_1 - M_j)(M_1 - M_k)}{M_1^2}$$

APPENDIX BRECIPROCAL RELATIONSHIPS BETWEEN GENERALIZED INTERACTION COEFFICIENTS

To establish relation (III.8), we first seek the factor multiplying the general term $X_2^{n_2} \dots X_k^{n_k-1} \dots X_m^{n_m}$, and, for this purpose, analyse the contributions of the different terms in the general equation III.6. The contribution of:

$$\begin{aligned}
 1 \times \frac{\partial \ln \gamma_1}{\partial X_k} & \text{ is } n_k K_{n_2, \dots, n_k, \dots, n_m}^{(1)} \\
 -X_i \frac{\partial \ln \gamma_1}{\partial X_k} & : -n_k K_{n_2, \dots, n_{i-1}, \dots, n_m}^{(1)} \quad (i \neq k, \text{ but taking all other values from 2 to } m) \\
 -X_k \frac{\partial \ln \gamma_1}{\partial X_k} & : -(n_k - 1) K_{n_2, \dots, n_{k-1}, \dots, n_m}^{(1)} \\
 X_i \frac{\partial \ln \gamma_i}{\partial X_k} & : n_k K_{n_2, \dots, n_{i-1}, \dots, n_m}^{(i)} \quad (i \neq k, \text{ but taking all other values from 2 to } m) \\
 X_k \frac{\partial \ln \gamma_k}{\partial X_k} & : (n_k - 1) K_{n_2, \dots, n_{k-1}, \dots, n_m}^{(k)}
 \end{aligned}$$

The sum of these contributions must be null. For convenience, call:

$$A = K_{n_2, \dots, n_k, \dots, n_m}^{(1)} \quad B_i = K_{n_2, \dots, n_{i-1}, \dots, n_m}^{(i)} - K_{n_2, \dots, n_{i-1}, \dots, n_m}^{(1)} \quad (B.1)$$

Then:

$$n_k A + (n_k - 1)B_k + n_k \sum_{i \neq k} B_i = 0 \quad (\text{B.2})$$

or

$$A + \sum_{i=2}^m B_i = \frac{B_k}{n_k} \quad (\text{B.3})$$

But, k may take any value from 2 to m . Thus, the ratio $\frac{B_k}{n_k} = C$ is independent of k . Replacing the B_i by their values $n_i C$ in equation B.3,

$$A = \sum_{i=2}^m B_i = A + C \sum_{i=2}^m n_i = C \quad (\text{B.4})$$

or:

$$C = - \frac{A}{\left(\sum_{i=2}^m n_i \right) - 1} = \frac{B_i}{n_i} \quad (\text{B.5})$$

Hence:

$$B_i = - \frac{n_i}{\left(\sum_{i=2}^m n_i \right) - 1} A \quad (\text{B.6})$$

that may be rewritten:

$$B_{i+1} = \frac{n_{i+1}}{\sum_{i=2}^m n_i} A \quad (\text{B.7})$$

Therefore:

$$K_{n_2, \dots, n_i, \dots, n_m}^{(i)} = K_{n_2, \dots, n_i, \dots, n_m}^{(1)} - \frac{n_{i+1}}{n_i} K_{n_2, \dots, n_{i+1}, \dots, n_m}^{(1)} \quad (\text{B.8})$$

To establish relation (III.7), the $\ln \gamma_i$ are replaced by their expansion in equation III.3. Identifying the factor of the general term $X_2^{n_2} \dots X_k^{n_k} \dots X_m^{n_m}$ in both expressions III.1 and III.5 of F^E/RT , the following relation is readily obtained:

$$A + \sum_{i=2}^m B_i = \psi_{n_2, \dots, n_k, \dots, n_m} \quad (\text{B.9})$$

and comparing with equations B.3 and B.5:

$$\psi_{n_2, \dots, n_k, \dots, n_m} = C = - \frac{A}{\left(\sum_{i=2}^m n_i \right)^{-1}} \quad (\text{B.10})$$

or:

$$\psi_{n_2, \dots, n_k, \dots, n_m} = - \frac{K^{(1)}_{n_2, \dots, n_k, \dots, n_m}}{\left(\sum_{i=2}^m n_i \right) - 1} \quad (\text{B.11})$$

APPENDIX CCONVERSION RELATIONSHIP BETWEEN THE INTERACTION
COEFFICIENTS ϵ , ρ AND e , r

The activities and symbols used are defined in Table C.1.

TABLE C.1Nomenclature for Activities and Reference State

<u>Composition Coordinate</u>	<u>Activity</u>	<u>Activity Coefficient</u>	<u>Reference State</u>
wt. %	a_i'	f_i	Infinite dilution: $\lim_{\%i \rightarrow 0} f_i = 1$
atom fraction	a_i''	γ_i	Pure component: $\lim_{X_i \rightarrow 1} \gamma_i = 1$
atom fraction	a_i'''	ψ_i	Infinite dilution: $\lim_{X_i \rightarrow 0} \psi_i = 1$

Often, the value of $e_i^{(j)}$ is first determined experimentally and then the value of $\epsilon_i^{(j)}$ is computed for theoretical treatment of the data. The relationship for the conversion has been:

$$\epsilon_i^{(j)} = 230 \frac{M_j}{M_1} e_i^{(j)} \quad (C.1)$$

where M_j and M_1 are the atomic weights of solute (j) and solvent (1). Similarly, for the "self interaction" coefficient of component (2)

in a 1-2 binary system:

$$\epsilon_2^{(2)} = 230 \frac{M_2}{M_1} e_2^{(2)} \quad (C.2)$$

As will be demonstrated below, even in the limit where $i \rightarrow 0$, $j \rightarrow 0$, or $2 \rightarrow 0$, equations C.1 and C.2 should include an additional term which may be significant.

At a given temperature, the defining equation of any activity of solute i , relative to its partial molar free energy \bar{F}_i , is:

$$\frac{d\bar{F}_i}{RT} = d \ln a_i' = d \ln a_i'' = d \ln a_i''' \quad (C.3)$$

Hence:

$$d \ln \gamma_i X_i = d \ln f_i \%i$$

and

$$d \ln \gamma_i = d \ln f_i + d \ln (\%i/X_i) \quad (C.4)$$

The total differential equation (C.4) yields the following partial differential equation:

$$\frac{\partial \ln \gamma_i}{\partial X_j} = \sum_{\mu} \frac{\partial \ln f_i}{\partial \% \mu} \cdot \frac{\partial \% \mu}{\partial X_j} + \frac{\partial \ln (\%i/X_i)}{\partial X_j} \quad (C.5)$$

where μ is any solute ((2) to (m)). At infinite dilution, the term $\frac{\partial \% \mu}{\partial X_j} = 0$, except when $\mu = (j)$, for which it equals $100 \frac{M_1}{M_1}$. And, by definition of the interaction coefficients ϵ and e , equation C.5 yields:

$$\epsilon_i^{(j)} = \frac{230 M_i}{M_1} e_i^{(j)} + \frac{(M_1 - M_i)}{M_1} \quad (C.6)$$

The importance of the additional term $\frac{M_1 - M_j}{M_1}$ has been illustrated by Lupis and Elliott.⁽¹³⁾ Table C.2 lists recalculated values of ϵ and e coefficients for liquid iron alloys.

Re-deriving equation C.5, with respect to X_k , yields:

$$\frac{\partial^2 \ln \gamma_i}{\partial X_j \partial X_k} = \sum_{\mu} \sum_{\nu} \frac{\partial^2 \ln f}{\partial \%_{\mu} \partial \%_{\nu}} \cdot \frac{\partial \%_{\mu}}{\partial X_j} \cdot \frac{\partial \%_{\nu}}{\partial X_k} + \sum_{\mu} \frac{\partial \ln f}{\partial \%_{\mu}} \cdot \frac{\partial^2 \%_{\mu}}{\partial X_i \partial X_k} + \frac{\partial^2 \ln(\%_i / X_i)}{\partial X_j \partial X_k} \quad (C.7)$$

At infinite dilution, in the second member, the first summation contains only one non-zero term for $\mu = X_j$, with $\nu = X_k$. It equals:

$$2.3 \times 10^4 \frac{M_j M_k}{M_1^2} r_i^{(j,k)}$$

The second summation contains two non-zero terms for $\mu = X_j$ and for $\mu = X_k$:

$$\frac{2.3 \times 10^2}{M_1^2} \left\{ M_j (M_1 - M_k) e_i^{(j)} + M_k (M_1 - M_j) e_i^{(k)} \right\}$$

The last term is equal to:

$$\frac{(M_1 - M_j)(M_1 - M_k)}{M_1^2}$$

$$\rho_i^{(j,k)} = 2.3 \times 10^4 \frac{M_j M_k}{M_1^2} r_i^{(j,k)} + \frac{2.3 \times 10^2}{M_1^2} \left\{ M_j (M_1 - M_k) e_i^{(j)} + M_k (M_1 - M_j) e_i^{(k)} \right\} + \frac{(M_1 - M_j)(M_1 - M_k)}{M_1^2} \quad (C.8)$$

Combining equations C.6 and C.8, we can express r as a function of ρ and ϵ :

$$r_i^{(j,k)} = \frac{0.434 \times 10^{-4}}{M_j M_k} \left\{ M_1^2 \rho_i^{(j,k)} - M_1(M_1 - M_k) \epsilon_i^{(j)} - M_1(M_1 - M_j) \epsilon_i^{(k)} \right\} \\ + (M_1 - M_j)(M_1 - M_k) \quad (C.9)$$

Recalling the definitions of $\rho_i^{(j)}$ and $r_i^{(j)}$ (equations III.16 and III.24), the following results are immediately deduced from equations C.8 and C.9:

$$\rho_i^{(j)} = \frac{230 M_i}{M_1^2} [10^2 M_j r_i^{(j)} + (M_1 - M_j) \epsilon_i^{(j)}] + \frac{1}{2} \left(\frac{M_1 - M_i}{M_1} \right)^2 \quad (C.10)$$

$$r_i^{(j)} = \frac{0.434 \times 10^{-4}}{M_j^2} [M_1^2 \rho_i^{(j)} - M_1(M_1 - M_j) \epsilon_i^{(j)} + \frac{1}{2}(M_1 - M_j)^2] \quad (C.11)$$

TABLE C.2

INTERACTION COEFFICIENTS $\epsilon_i^{(j)}$ FOR DILUTE SOLUTIONS OF ELEMENTS DISSOLVED IN LIQUID IRON AT 1600 C*

Dissolved Element (i)	Added Element (j)													
	Al	As	B	C	Cb	Co	Cr	Cu	H	Mn	Mo	N		
Al	<u>5.3</u>			<u>5.3</u>					1.97					0.85
As														5.2
B														
C	5.3			<u>11.7</u>	<u>-23.7</u>	<u>2.9</u>	<u>-5.1</u>	<u>4.1</u>	3.1					7.2
Cb				<u>-23.7</u>					3.8					<u>-26.3</u>
Co				2.9					<u>-1.54</u>					2.6
Cr				-5.1					0.38					-9.6
Cu				4.1					-0.40					2.2
H			3.1						-0.01					
Mn	2.0			3.8		<u>0.38</u>	<u>-0.40</u>	<u>-0.01</u>	0.98					
Mo									<u>-0.30</u>					-4.5
N	<u>0.85</u>	<u>5.2</u>												-5.1
Ni														0.75
O									-0.05					2.4
P				<u>-5.6</u>	<u>-54.3</u>	<u>1.6</u>	<u>-8.7</u>	<u>-2.5</u>						2.6
S				12.3					1.85					7.0
Sb	<u>7.0</u>						<u>-4.65</u>	<u>-3.3</u>	1.5					2.2
Se														3.3
Si														0.4
Sn	7.0			13					3.6		0.0			5.9
Ta				14.4					1.5					2.3
Ti									-17.2					-27.6
V									-15.7					-124
W				-7.9										-21
				-4.6										-3.8

* Calculations based on values reported by Elliott, Gleiser and Ramakrishna (53).
 Note: Underlined numbers are deduced from experimental results and plain numbers from the relationship: $\epsilon_i^{(j)} = \epsilon_j^{(i)}$

TABLE C.2 (continued)

INTERACTION COEFFICIENTS $\epsilon_i^{(j)}$ FOR DILUTE SOLUTIONS OF ELEMENTS DISSOLVED
IN LIQUID IRON AT 1600 C*

Dissolved Element (i)	Added Element (j)													
	Ni	O	P	S	Sb	Sc	Si	Sn	Ta	Ti	V	W		
Al				7.0			7.0							
As														
B														
C	2.9	- 5.6		12.3			13				-7.9	-4.6		
Cb		-54.3												
Co		1.6												
Cr		- 8.7		- 4.65										
Cu		- 2.5		- 3.3										
H			1.85	1.5			0	1.5	-17.2	-15.7				
Mn		0		- 5.6										
Mo		0.67												
N		2.6	7.0	2.2	3.3	-0.4	5.9	2.3	-27.6	-124	-21	-3.8		
Ni	2.4	1.4		- 0.05			1.2							
O	-0.01		9.4	-11.6			-16.0	-1.1		-37.4	-56.6	3.8		
P	1.4	-12.5	9.4	6.2			11.4							
S	-0.05	9.4	6.2	- 3.3			8.1							
Sb		-11.6												
Se														
Si	1.2	-16.0	11.4	8.1			13							
Sn		- 1.1												
Ta														
Ti		-37.4												
V		-56.6												
W		3.8												

* Calculations based on values reported by Elliott, Gleiser and Ramakrishna (53).
Note: Underlined numbers are deduced from experimental results and plain numbers from the relationship: $\epsilon_i^{(j)} = \epsilon_j^{(i)}$

TABLE C.2

INTERACTION COEFFICIENTS $e_i^{(j)} \times 10^2$ * FOR DILUTE SOLUTIONS OF ELEMENTS DISSOLVED IN LIQUID IRON AT 1600 C**

Dissolved Element (i)	Added Element (j)												
	Al	As	B	C	Cb	Co	Cr	Cu	H	Mn	Mo	N	
Al	4.3			9.1					24				0.2
As													7.7
B									50				11.1
C	4.3			22	-6.0	1.2	-2.4	1.6	66.7		-0.9		-47
Cb				-49					-60.8				
Co				4.2					-14.4				3.2
Cr				-11.8					-33.3				-17.9
Cu				6.6				-2.1	-23.7				2.5
H	1.3		5.0	6.0	-0.23	0.18	0.22	0.05	0	-0.14			
Mn									-30.9				-9.1
Mo				-10.2									-10.1
N	0.3	1.8		13	-6.7	1.1	-4.5	0.9	-24.8	-2.0	-1.1		0
Ni				4.2									2.8
O				-13	-14	0.7	-4.1	-0.9		0	0.35		5.7
P	5.8			23.3			-2.2	-1.2	21				10.8
S									12	-2.5			2.4
Sb													4.5
Se													2.0
Si	5.8			24					63.5	0			9.0
Sn				28					63				2.7
Ta									-436				-49
Ti									-400				-215
V				-17.5									-37.5
W				-10.8									-7.9

$$* e_i^{(j)} = \frac{\delta \log f_i}{\delta \%_j} \frac{M_i}{M_j} = \frac{M_i}{M_j} e_i^{(j)} + 0.434 \times 10^{-2} \frac{M_i - M_j}{M_j}$$

** Calculations based on values reported by Elliott, Gleiser and Ramakrishna (63).
 Note: Underlined numbers are deduced from experimental results and plain numbers from the reciprocal relationship noted above.

TABLE C.2 (continued)

INTERACTION COEFFICIENTS $e_i^{(j)} \times 10^{2*}$ FOR DILUTE SOLUTIONS OF ELEMENTS DISSOLVED IN LIQUID IRON AT 1600 C**

Dissolved Element (i)	Added Element (j)												
	Ni	O	P	S	Sb	Se	Si	Sn	Ta	Ti	V	W	
Al				4.9			5.6						
As													
B													
C	<u>1.2</u>	-9.6		<u>2</u>			11				<u>-3.8</u>	<u>-0.3</u>	
Cb		-83.4											
Co		1.4		-3.84									
Cr		-14.3		-2.8									
Cu		-4.9											
H			<u>1.1</u>	0.8			<u>2.7</u>	<u>0.53</u>	<u>-2</u>	<u>-8</u>			
Mn		-1.1		-4.6			<u>0.96</u>						
Mo		-2.27											
N		5.0	<u>5.1</u>	1.3	0.9	0	4.7	0.7	-3.4	-63	-10	-0.2	
Ni	<u>1.0</u>	<u>1.04</u>		-0.36			-0.05						
O	<u>0.6</u>	-20	<u>7.0</u>	0.4	-9.1		-14	0		-19	-27	0.8	
P		<u>13.1</u>		<u>4.36</u>			<u>9.4</u>						
S		-18.7	<u>4.5</u>	-2.8			<u>6.6</u>						
Sb													
Se													
Si	<u>0.5</u>	-24.9	<u>86</u>	5.73			<u>11</u>						
Sn		-2.8											
Ta													
Ti		-58											
V		-86.9											
W		4.6											

$$* e_i^{(j)} = \frac{\delta \log f_i}{\delta \% j} \times 100 = \frac{M_i}{M_j} e_i^{(j)} + 0.434 \times 10^{-2} \frac{M_i - M_j}{M_j}$$

** Calculations based on values reported by Elliott, Gleiser and Ramakrishna (53).
 Note: Underlined numbers are deduced from experimental results and plain numbers from the reciprocal relationship noted above.

APPENDIX D

CALCULATIONS OF THE QUASI-CHEMICAL MODEL

1. Binary System

As mentioned in Chapter IV, no rigorous mathematical formula is available for $g(N_A, N_B, N_{AB})$. It was noted, however, that:

$$\Sigma g(N_A, N_B, N_{AB}) = \frac{(N_A + N_B)!}{N_A! N_B!} \quad (D.1)$$

Assuming that the number of configurations corresponding to a given value of N_{AB} may be calculated as if the various types of pairs do not interfere with one another would yield:

$$g_1(N_A, N_B, N_{AB}) = \frac{[\frac{1}{2} Z(N_A + N_B)]!}{N_{AA}! N_{BB}! [\frac{N_{AB}}{2}]!^2} \quad (D.2)$$

In the numerator, one finds the total number of pairs and, in the denominator, the different types of pairs. The factor $(N_{AB}/2)!$ is squared, in order to distinguish between the two modes of occupation AB and BA. Formula D.2 overestimates the value of g , because the different pairs do interfere with one another.⁽¹⁰⁾ Consequently, g is multiplied by a correction term, $h(N_A, N_B)$, and h is determined by the following procedure.

The maximum term, g , arises for N_{AB}^* corresponding to a random distribution. Thus:

$$g^* = \frac{(N_A + N_B)!}{N_A! N_B!} = h(N_A, N_B) \frac{[\frac{1}{2} Z(N_A + N_B)]!}{(\frac{1}{2} Z N_A - \frac{1}{2} N_{AB}^*)! (\frac{1}{2} Z N_B - \frac{1}{2} N_{AB}^*)! [\frac{1}{2} N_{AB}^*]!^2} \quad (D.3)$$

which fixes the value of $h(N_A, N_B)$. Replacing, now, h by its expression in $g = g_1 \cdot h$:

$$g(N_A, N_B, N_{AB}) = \frac{(N_A + N_B)!}{N_A! N_B!} \times \frac{(\frac{1}{2}ZN_A - \frac{1}{2}N_{AB}^*)! (\frac{1}{2}ZN_B - \frac{1}{2}N_{AB}^*)! [(\frac{1}{2}N_{AB}^*)!]^2}{(\frac{1}{2}ZN_A - \frac{1}{2}N_{AB}^*)! (\frac{1}{2}ZN_B - \frac{1}{2}N_{AB}^*)! [(\frac{1}{2}N_{AB}^*)!]^2} \quad (D.4)$$

To determine N_{AB}^* , it is noted that the probability of finding A on the site (i) is: $\frac{N_A}{N}$ (where $N = N_A + N_B$), and of finding B on the neighboring site (ii) is: $\frac{N_B}{N}$. Thus, the probability of finding A on (i) and B on (ii), or B on (i) and A on (ii) becomes $\frac{2N_A N_B}{N}$. Multiplying, now, this probability by the total number of neighboring sites $\frac{1}{2}Z(N_A + N_B)$, the total number of pairs AB, corresponding to a random distribution, is obtained:

$$N_{AB}^* = \frac{ZN_A N_B}{N} \quad (D.5)$$

The sum

$$\sum g(N_A, N_B, N_{AB}) e^{-\beta N_{AB} \omega_{AB}}$$

is now replaced by its maximum term: ⁽⁹⁾

$$\bar{g}(N_A, N_B, \bar{N}_{AB}) e^{-\beta \bar{N}_{AB} \omega_{AB}}$$

where \bar{N}_{AB} is determined by:

$$\frac{\partial}{\partial N_{AB}} \left[g(N_A, N_B, N_{AB}) e^{-\beta N_{AB} \omega_{AB}} \right] = 0 \quad (D.6)$$

which, by using Stirling's approximation ($\ln p! \approx p \ln p - p$), is found to be equivalent to:

$$\frac{\bar{N}_{AB}}{(ZN_A - \bar{N}_{AB})(ZN_B - \bar{N}_{AB})} = e^{-2\beta\omega_{AB}} = (1 + \lambda_{AB})^{-1} \quad (D.7)$$

an equation easily solved for \bar{N}_{ab} . And, as:

$$F^M = -kT \ln \bar{g} + \bar{N}_{AB} \omega_{AB} \quad (D.8)$$

replacing \bar{g} and \bar{N}_{AB} by their values, obtained from equations D.4, D.5 and D.7, leads to the quasi-chemical expression of the excess free energy in equation IV.13. The intermediate calculations are long, but straight forward, and do not need to be reproduced here. They also constitute a particular case of the more complex calculations of ternary systems that will be considered now.

2. Ternary System

A procedure, identical to the one followed in the study of the binary, leads to:

$$ZN_A = 2N_{AA} + N_{AB} + N_{AC} \quad (D.9a)$$

$$ZN_B = 2N_{BB} + N_{AB} + N_{BC} \quad (D.9b)$$

$$ZN_C = 2N_{CC} + N_{AC} + N_{BC} \quad (D.9c)$$

and

$$g = \frac{N!}{N_A! N_B! N_C!} \cdot \frac{N_{AA}^*! N_{BB}^*! N_{CC}^*! \left[\left(\frac{1}{2} N_{AB}^* \right)! \right]^2 \left[\left(\frac{1}{2} N_{AC}^* \right)! \right]^2 \left[\left(\frac{1}{2} N_{BC}^* \right)! \right]^2}{\bar{N}_{AA}! \bar{N}_{BB}! \bar{N}_{CC}! \left[\left(\frac{1}{2} \bar{N}_{AB} \right)! \right]^2 \left[\left(\frac{1}{2} \bar{N}_{AC} \right)! \right]^2 \left[\left(\frac{1}{2} \bar{N}_{BC} \right)! \right]^2} \quad (D.10)$$

where:

$$N_{ii}^* = \frac{1}{2}(ZN_i - N_{ij}^* - N_{ik}^*) \quad (D.11)$$

with:

$$N_{ij}^* = \frac{ZN_i N_j}{N} \quad (N = N_i + N_j + N_k = N_A + N_B + N_C) \quad (D.12)$$

and

$$\bar{N}_{ii} = \frac{1}{2}(ZN_i - \bar{N}_{ij} - \bar{N}_{ik}) \quad (D.13)$$

The \bar{N}_{ij} are given by:

$$\frac{\bar{N}_{ij}^2}{2\bar{N}_{ii} \times 2\bar{N}_{jj}} = e^{-2\beta\omega_{ij}} = (1 + \lambda_{ij})^{-1} \quad (D.14)$$

This time, however, the expression of \bar{N}_{ij} is much more difficult to find. The following system must be solved:

$$\bar{N}_{AB}^2 \lambda_{AB} + \bar{N}_{AB} [(ZN_A - \bar{N}_{AC}) + (ZN_B - \bar{N}_{BC})] - (ZN_A - \bar{N}_{AC})(ZN_B - \bar{N}_{BC}) = 0 \quad (D.15a)$$

$$\bar{N}_{BC}^2 \lambda_{BC} + \bar{N}_{BC} [(ZN_B - \bar{N}_{AB}) + (ZN_C - \bar{N}_{AC})] - (ZN_B - \bar{N}_{AB})(ZN_C - \bar{N}_{AC}) = 0 \quad (D.15b)$$

$$\bar{N}_{AC}^2 \lambda_{AC} + \bar{N}_{AC} [(ZN_A - \bar{N}_{AB}) + (ZN_C - \bar{N}_{BC})] - (ZN_A - \bar{N}_{AB})(ZN_C - \bar{N}_{BC}) = 0 \quad (D.15c)$$

There are no theoretical difficulties in solving this system of three equations with three unknowns ($\bar{N}_{AB}, \bar{N}_{AC}, \bar{N}_{BC}$). However, a direct calculation of these unknowns is not possible and, consequently, an interaction procedure is adopted.

Choosing X_B and X_C as infinitesimal variables of the same order and, recalling that N_{ij}^* is the value of \bar{N}_{ij} in a random solu-

tion, it is possible to write:

$$\frac{\bar{N}_{ij}}{N} = \frac{N_{ij}^*}{N} + a_{ij} + O(X^3) = ZX_i X_j + a_{ij} + O(X^3) \quad (D.16)$$

a_{ij} is a second order correcting term which accounts for the non-randomness of the solution. Equation D.15a then becomes:

$$a_{AB}[X_A^2 + X_B^2 + 2X_A X_B(1 + \lambda_{AB})] + a_{AC}X_B^2 + a_{BC}X_A^2 + Z\lambda_{AB}X_A^2 X_B^2 + \frac{1}{2}[\lambda_{AB}a_{AB}^2 - a_{AB}a_{AC} - a_{BC}a_{AB} - a_{AC}a_{BC}] = 0 \quad (D.17a)$$

Equations D.17b and D.17c correspond to D.15b and D.15c, and are obtained from D.17a by circular permutation of the indicies. In each of the equations D.17, only the terms of the lowest order must be retained. In equations D.17a and D.17c they are of the second order:

$$a_{AB} + a_{BC} + Z\lambda_{AB}X_B^2 = 0 \quad (D.18a)$$

$$a_{AC} + a_{BC} + Z\lambda_{AC}X_C^2 = 0 \quad (D.18c)$$

In equation D.17b, they are of the fourth order and, replacing a_{AB} and a_{AC} by their values obtained in equations D.18a and D.18c, yields:

$$a_{BC}^2 + 2a_{BC}ZX_B X_C - Z^2 X_B^2 X_C^2 \frac{(1 + \lambda_{AB})(1 + \lambda_{AC})}{(1 + \lambda_{BC})} - 1 = 0 \quad (D.18b)$$

or:

$$a_{BC}^2 + 2a_{BC}ZX_B X_C + Z^2 X_B^2 X_C^2 [1 - \exp 2\beta(\omega_{AB} + \omega_{AC} - \omega_{BC})] = 0$$

which yields:

$$a_{BC} = - Z X_B X_C [1 \pm \exp \beta(\omega_{AB} + \omega_{AC} - \omega_{BC})]$$

Only the value corresponding to the negative sign has a physical meaning since, when all the ω are null, a_{BC} must be null (complete randomness). Consequently:

$$a_{BC} = Z X_B X_C \mu \quad (D.19)$$

with

$$\mu = e^{\beta(\omega_{AB} + \omega_{AC} - \omega_{BC})} - 1 \quad (D.20)$$

Therefore, equations D.18a and D.18c yield:

$$a_{AB} = - Z X_B [\lambda_{AB} X_B + \mu X_C] \quad (D.21)$$

$$a_{AC} = - Z X_C [\lambda_{AC} X_C + \mu X_B] \quad (D.22)$$

The same procedure is now repeated. Equation D.16 is rewritten as:

$$\frac{\bar{N}_{ij}}{N} = \frac{N_{ij}^*}{N} + a_{ij} + b_{ij} + O(X^4) \quad (D.23)$$

and the b_{ij} coefficients are determined by replacing \bar{N}_{ij} by its new value in the system of equation D.15:

$$b_{AB} = 2Z X_B^2 (1 + \lambda_{AB}) (\lambda_{AB} X_B + \mu X_C) + Z X_B X_C (1 + \mu) [X_B (\lambda_{AB} + \mu) + X_C (\lambda_{AC} + \mu)] \quad (D.24a)$$

$$b_{BC} = - Z X_B X_C (1 + \mu) [X_B (\lambda_{AB} + \mu) + X_C (\lambda_{AC} + \mu)] \quad (D.24b)$$

$$b_{AC} = 2Z X_C^2 (1 + \lambda_{AC}) (\lambda_{AC} X_C + \mu X_B) + Z X_B X_C (1 + \mu) [X_B (\lambda_{AB} + \mu) + X_C (\lambda_{AC} + \mu)] \quad (D.24c)$$

The values of the different pairs \bar{N}_{ii} and \bar{N}_{ij} are thus known up to, and including, the third order term. Recalling that:

$$F^M = -kT \ln \bar{g} + \bar{N}_{AB} \omega_{AB} + \bar{N}_{BC} \omega_{BC} + \bar{N}_{AC} \omega_{AC} \quad (D.25)$$

all the elements needed to calculate F^M (or F^E) are seen to have been obtained. The calculations leading to equation IV.31 are straight forward, but very lengthy. We do not find it necessary to reproduce them here.

APPENDIX ETABLE E.1IDENTIFICATION OF THE EXPERIMENTAL POINTS IN FIG. IV.1

<u>Identification Number</u>	<u>Solvent</u> <u>1</u>	<u>Solute</u> <u>2</u>	<u>log γ_2^0</u>	<u>$\epsilon_{2,2}$</u>	<u>T °C</u>
1	Al	- Ag	-0.28	-3.1	1000
2	Ag	- Bi	-0.52	2.55	1000
3	Ag	- Al	-1.66	6.4	700
4	Ag	- Al	-1.56	5.6	800
5	Ag	- Al	-1.41	4.6	900
6	Ag	- Al	-0.96	4.22	1000
7	Ag	- Cd	-0.74	1.47	827
8	Ag	- Pb	0.30	-0.4	1000
9	Au	- Bi	-0.05	0.1	700
10	Au	- Pb	-0.85	5	600
11	Au	- Tl	-0.31	0.1	700
12	Bi	- Ag	0.41	-6.2	
13	Bi	- Au	-0.11	2.1	700
14	Bi	- Cd	0	-1.22	500
15	Bi	- Hg	-0.41	-0.33	321
16	Bi	- Mg	-2.26	0.85	700
17	Bi	- Pb	-0.34	1.44	500
18	Bi	- Pb	-0.28	0.75	665
19	Bi	- Sn	0.05	-0.06	330
20	Bi	- Tl	-1.40	3.22	270
21	Bi	- Tl	-0.85	2.14	480
22	Bi	- Zn	0.54	-3.3	600
23	Cd	- Bi	-0.08	-6.5	500
24	Cd	- Hg	-1	3.36	327
25	Cd	- Hg	-1.2	2.5	350
26	Cd	- Na	-2	15.8	395
27	Cd	- Pb	0.71	-4.56	500
28	Cd	- Sb	-0.57	-6.5	500
29	Cd	- Sn	0.28	-1.4	500
30	Cd	- Zn	0.45	-1.78	682
31	Cd	- Zn	-0.68	0.72	727

TABLE E.1 (continued)

IDENTIFICATION OF THE EXPERIMENTAL POINTS IN FIG. IV.1

<u>Identification Number</u>	<u>Solvent 1</u>	<u>Solute 2</u>	<u>log γ_2^0</u>	<u>$\epsilon_{2,2}$</u>	<u>T °C</u>
32	Fe	- Al	-1.20	5.3	1600
33	Fe	- C(gr)	-0.33	11	1600
34	Fe	- Cu	0.92	-5.5	1600
35	Fe	- Ni	-0.18	-0.01	1600
36	Fe	- Si	-2.96	13	1600
37	Hg	- Tl	-0.37	6.0	325
38	Pb	- Ag	0.18	-0.92	1000
39	Pb	- Au	-0.60	3.2	600
40	Pb	- Bi	-0.31	2.6	500
41	Pb	- Cd	0.51	-2.6	500
42	Pb	- Mg	-1.20	0.6	833
43	Pb	- Na	-2.66	3.6	400
44	Pb	- Zn	1.04	-5.3	653
45	Sb	- Cd	-0.60	1.5	500
46	Sb	- Pb	-0.14	0.59	500
47	Sb	- Sn	-0.40	2.2	905
48	Sn	- Zn	0.42	-1.0	437
49	Tl	- Au	-0.51	2.6	700
50	Tl	- Sn	0.45	-1.7	325
51	Sn	- Au	-2.22	5.8	600
52	Sn	- Pb	0.36	-0.65	500
53	Sn	- Tl	0.46	-3.2	352
54	Sn	- Tl	0.38	-1.78	414
55	Zn	- Cd	0.54	-3.33	682

Most values of $\log \gamma_2^0$ and $\epsilon_{2,2}$ are reported by Dealy and Pehlke (), Exceptions occur for the silver-bismuth system reported by Hultgren, Orr, Anderson and Kelly (), for the iron alloys (numbered 32 to 36) reported by Elliott, Gleiser and Ramakrishna (), and for the value of $\epsilon_{Si, Si}$ in iron, which is based on Schroeder and Chipman's results. ()

APPENDIX F
CALCULATION OF THE "FREE VOLUME"

In Chapter V, the movement of an atom within its cell was accounted for by the following expression of the free volume:

$$v_f = \int_{\text{cell}} e^{-[\psi(r) - \psi(0)]/kT} dr \quad (\text{F.1})$$

The Z nearest neighbors are treated as uniformly "smeared" over a spherical surface of radius a, where a is the distance between the centers of nearest neighbor cells. In Fig. F.1, the central atom is at P, a distance r from the center O of the cell. The area of the ring, shown on the surface of the sphere, is $2\pi a^2 \sin\theta d\theta$. The numbers of "smeared" nearest neighbors in this area are:

$$Z \frac{2\pi a^2 \sin\theta}{4\pi a^2} d\theta = \frac{Z}{2} \sin\theta d\theta$$

and the potential energy of interaction between the atom, at P, and the neighbors in the ring is:

$$u(R) \frac{Z}{2} \sin\theta d\theta$$

where

$$R^2 = r^2 + a^2 - 2ar \cos\theta \quad (\text{F.2})$$

and $u(R)$ is the potential of the bonding force between two neighbors. Hence, the total energy of interaction between the atom at P and all of its nearest neighbors is:

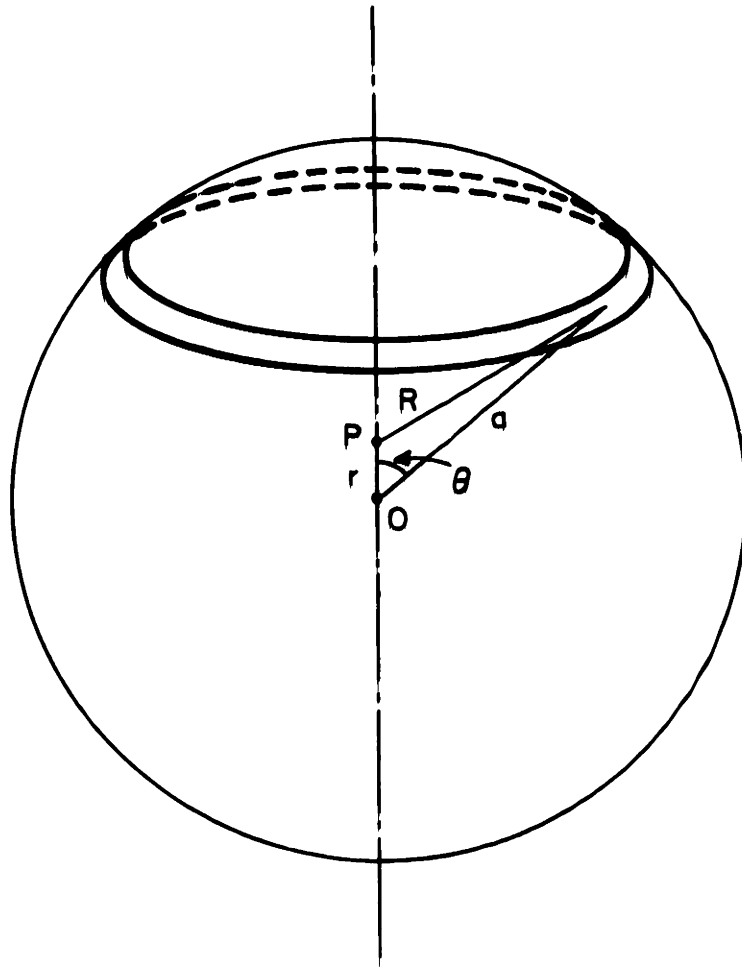


FIG. F 1. CELL GEOMETRY FOR THE "FREE VOLUME" MODEL

$$\psi(r) = \frac{Z}{2} \int_0^\pi u(R) \sin\theta \, d\theta \quad (\text{F.3})$$

$u(R)$ may be expressed as a Taylor's series, with respect to the distance $R - a_0$, where a_0 is the distance corresponding to the minimum of $u(R)$:

$$u(R) = u(a_0) + A(R - a_0)^2 + O(R^3) \quad (\text{F.4})$$

with:

$$A = \left(\frac{\partial^2 u}{\partial R^2} \right)_{R=a_0} \quad (\text{F.5})$$

Terms of the third order and higher orders, are neglected for simplicity. Equation F.3 then becomes:

$$\psi(r) = \frac{Z}{2} \int_0^\pi u(a_0) + A[(r^2 + a^2 - 2ar \cos\theta)^{1/2} - a_0]^2 \sin\theta \, d\theta \quad (\text{F.6})$$

Carrying out the integration yields:

$$\psi(r) = Zu(a_0) + ZA[(a - a_0)^2 + r^2(1 - \frac{2a_0}{3a})] \quad (\text{F.7})$$

Consequently:

$$\psi(r) - \psi(0) = ZAr^2(1 - \frac{2a_0}{3a}) \quad (\text{F.8})$$

and

$$v_f = 4\pi \int_{\text{cell}} e^{-ZAr^2(1 - \frac{2a_0}{3a})/kT} r^2 dr \quad (\text{F.9})$$

Since A is a positive quantity, it is possible to write:

$$\frac{1}{\sigma^2} = \frac{ZA(1 - \frac{2a_e}{3a})}{kT} \quad (\text{F.10})$$

Therefore:

$$v_f = 4\pi \int_0^a e^{-\frac{r^2}{\sigma^2}} r^2 dr \quad (\text{F.11})$$

Integrating by part yields:

$$v_f = -2\pi\sigma^2 a \exp(-a^2/\sigma^2) + (\pi\sigma^2)^{3/2} \text{erf}(a/\sigma) \quad (\text{F.12})$$

It may be seen that a/σ is usually a large number. For a 6-12 Lennard-Jones potential, and a temperature of about 1000°K , a/σ is, roughly, equal to 20. Consequently:

$$\exp(-\frac{a^2}{\sigma^2}) \approx 0 \quad \text{and} \quad \text{erf}(\frac{a}{\sigma}) \approx 1 \quad (\text{F.13})$$

The value of v_f is, then:

$$v_f = (\pi\sigma^2)^{3/2} = \frac{ZA(1 - \frac{2a_e}{3a})}{\pi kT} \quad (\text{F.14})$$

or

$$v_f = \left\{ \frac{1}{2\pi kT} \left(\frac{\partial^2 \psi}{\partial r^2} \right) \right\}^{-3/2} \quad (\text{F.15})$$

APPENDIX G

TABLE G.1
IDENTIFICATION OF THE EXPERIMENTAL POINTS IN FIG. V.1

<u>Solvent</u> <u>1</u>	<u>Solute</u> <u>2</u>	<u>H₂^{E°}</u> <u>(Kcal.)</u>	<u>S₂^{E°}</u> <u>(cal. °K⁻¹)</u>	<u>T°K</u>	<u>State</u>
Ag	- Au	- 4.85	-1.38	800	solid
Ag	- Au	- 4.66	-1.30	1350	liquid
Ag	- Bi	- 2.40	2.31	1000	liquid
Ag	- Cd	- 6.00	0.74	673	solid
Ag	- Cu	6.00	0.29	1052	solid
Ag	- Cu	5.26	1.33	1400	liquid
Ag	- Zn	- 3.60	-0.60	873	solid
Al	- Sn	8.50	4.75	1000	liquid
Al	- Zn	3.14	0.70	625	solid
Al	- Zn	3.25	2	750	liquid
Au	- Ag	- 4.05	-1.38	800	solid
Au	- Ag	- 3.86	-1.38	1350	liquid
Au	- Cd	-16.47	-5.0	700	solid
Au	- Cu	- 2.84	-0.0	720	solid
Au	- Fe	5.08	4.52	1123	solid
Au	- Hg	2.50	4.3	550	solid
Au	- Ni	6.15	2.35	1150	solid
Au	- Sn	-16.0	1.72	873	liquid
Au	- Tl	- 0.57	0.85	973	liquid
Bi	- Ag	9.94	1.06	1000	liquid
Bi	- Cd	0.78	1.01	594	liquid
Bi	- Mg	-11.6	-0.2	973	liquid
Bi	- Pb	- 0.85	0.34	700	liquid
Bi	- Sn	2.8	1.6	412	solid
Bi	- Tl	- 2.95	1.42	732	liquid
Bi	- Zn	3.68	2.10	873	liquid
Cd	- Bi	2.30	2.74	773	liquid
Cd	- Cu	- 1.56	-2.61	875	liquid
Cd	- Ga	3.54	0.72	700	liquid
Cd	- In	1.85	0.55	723	liquid
Cd	- Pb	3.72	1.56	773	liquid
Cd	- Sb	2.27	5.4	773	liquid
Cd	- Sn	2.33	1.71	773	liquid
Cd	- Tl	3.25	1.68	673	liquid
Cd	- Zn	2.25	0	800	liquid

TABLE G.1 (continued)

IDENTIFICATION OF THE EXPERIMENTAL POINTS IN FIG. V.1

<u>Solvent</u> <u>1</u>	<u>Solute</u> <u>2</u>	<u>H₂^{E°}</u> <u>(Kcal.)</u>	<u>S₂^{E°}</u> <u>(cal. °K⁻¹)</u>	<u>T °K</u>	<u>State</u>
Ce	- Hg	- 31.7	- 21.5	298	liquid
Cu	- Ag	9.0	1.9	1052	solid
Cu	- Ag	3.73	0.32	1400	liquid
Cu	- Mg	- 11.15	- 2.8	1150	liquid
Cu	- Pd	- 12	- 3.73	1000	solid
Cu	- Pt	- 12	- 1.5	923	solid
Cu	- Zn	- 7.8	- 1.7	773	solid
Cu	- Zn	- 7.1	- 1.5	1300	liquid
Fe	- C	9.86	3.6	1426	solid
Ga	- Cd	3.08	0.07	700	liquid
Ga	- Zn	1.21	0.75	723	liquid
Hg	- In	- 2.15	- 0.36	433	liquid
Hg	- K	- 24.9	- 9.7	600	liquid
Hg	- Na	- 19.8	- 7	648	liquid
Hg	- Sn	1.47	- 1.32	433	liquid
Hg	- Tl	- 1.78	- 1.29	293	liquid
Hg	- Zn	0.7	- 0.26	608	liquid
In	- Cd	1.13	0.28	723	liquid
In	- Pb	0.96	0.31	673	liquid
In	- Sb	- 2.93	1.17	973	liquid
In	- Sn	- 0.58	1.34	773	liquid
In	- Tl	2.6	1.0	700	liquid
K	- Pb	- 13.74	- 7.03	848	liquid
K	- Hg	- 14.2	- 15.6	600	liquid
Mg	- Cu	- 11.65	- 6.79	1150	liquid
Mg	- Pb	- 13.50	- 4.20	833	liquid
Na	- Hg	- 11.8	- 5.22	648	liquid
Na	- Pb	- 20	- 12.5	698	liquid
Na	- Sn	- 14	- 4	773	liquid
Na	- Tl	- 11.1	- 9.3	648	liquid
Pb	- Cd	2.32	0.6	773	liquid
Pb	- Na	- 8.75	- 0.0		
Pb	- Tl	- 0.66	- 0.85	773	liquid
Pb	- Zn	5.75	1.97	926	liquid
Pd	- Cu	- 9.6	- 5.4	1000	solid
Pt	- Cu	- 2.10	1.3	923	solid

TABLE G.1 (continued)

IDENTIFICATION OF THE EXPERIMENTAL POINTS IN FIG. V.1

<u>Solvent</u> <u>1</u>	<u>Solute</u> <u>2</u>	H_2^E (Kcal.)	S_2^E (cal. °K ⁻¹)	<u>T °K</u>	<u>State</u>
Sb	- Zn	0.76	1.51	823	liquid
Sn	- Al	3.50	2.05	1000	liquid
Sn	- Au	7.6	1.17	873	liquid
Sn	- Cd	1.52	0.91	773	liquid
Sn	- Na	-14.6	-7.9	773	liquid
Sn	- Zn	2.22	1.55	700	liquid
Tl	- Bi	- 5.31	-0.03	772	liquid
Tl	- Cd	1.76	0.46	673	liquid
Tl	- In	4.3	1.24	700	liquid
Tl	- Na	-19.5	17.4	648	liquid
Tl	- Zn	4.12	0.5	1099	liquid
Zn	- Al	3.25	2	750	liquid
Zn	- Bi	8.43	2.10	873	liquid
Zn	- Cu	- 7.1	-1.5	1300	liquid
Zn	- Ga	2.2	1.45	723	liquid
Zn	- Pb	12.08	5.65	926	liquid
Zn	- Sb	2.6	2.8	823	liquid
Zn	- Sn	5.47	3.77	700	liquid
Zn	- Tl	7.12	0.5	1099	liquid

All values listed are reported by Hultgren, Orr, Anderson and Kelly. (52)

APPENDIX H
EXPERIMENTAL DATA

All runs and corresponding data are listed chronologically in the following pages. However, it was felt to be more convenient to give the measurements of the "hot volume" separately. It must be noted that a comparison of the hot volume in different runs is not strictly possible, because the experimental set up was usually different in each run (different reaction bulbs, water-cooling or air-cooling, etc.).

"Hot Volume" Data

Run 3923

Run 3114

P Argon	$10^3/T \text{ } ^\circ\text{K}^{-1}$	$r = \frac{\text{cc Argon (STP)}}{P \text{ Argon}} \cdot 10^2$	P Argon	$10^3/T \text{ } ^\circ\text{K}^{-1}$	$r = \frac{\text{cc Argon (STP)}}{P \text{ Argon}} \cdot 10^2$
126.4	0.770	8.307	168.3	0.7775	9.620
144.4	0.7821	8.490	293.3	0.7775	9.860
344.6	0.7867	8.633	398.3	0.7784	9.910
473.9	0.7867	8.649	478.5	0.7793	9.964
597.6	0.7873	8.678	576	0.7785	9.983
677.4	0.7873	8.704	654	0.7785	10.018
771.9	0.7872	8.711	523	0.7790	9.961
771.9	0.7227	8.401	764	0.7790	10.060
771.9	0.7448	8.592			
771.9	0.7213	8.390			
771.9	0.7633	8.568			
771.9	0.7652	8.592			

$$\frac{\partial r}{\partial (10^3/T)} = 5.0$$

$$\frac{\partial r}{\partial p} = 1.8 \times 10^{-4}$$

m = 181.549 g of silver

$$\frac{\partial r}{\partial (10^3/T)} = \text{undetermined}$$

$$\frac{\partial r}{\partial p} = 4.0 \times 10^{-4}$$

m = 221.147 g of silver

"Hot Volume" Data

Run 4019

Run 4120

P_{Argon}	$10^3/T \text{ } ^\circ\text{K}^{-1}$	$r = \frac{\text{cc Argon (STP)}}{P_{\text{Argon}}} \cdot 10^2$	P_{Argon}	$10^3/T \text{ } ^\circ\text{K}^{-1}$	$r = \frac{\text{cc Argon (STP)}}{P_{\text{Argon}}} \cdot 10^2$
61.5	0.7733	9.691	17	0.7076	11.284
62.1	0.7418	9.597	60.5	0.7501	10.909
118	0.7390	9.681	67.5	0.7558	10.857
117	0.7910	9.966	162	0.7558	10.988
213	0.7917	10.075	329	0.7009	11.732
218.5	0.7390	9.822	520.5	0.7760	11.220
351.8	0.7390	9.957	765	0.7760	11.294
350.2	0.7401	10.003	778.7	0.7204	11.095
347.4	0.7955	10.083			
474	0.7955	10.405			
575	0.7955	10.289			
584	0.7385	10.130			
748	0.7385	10.214			

$$\frac{\partial r}{\partial (10^3/T)} = 3.0$$

$$\frac{\partial r}{\partial p} = 5.5$$

$$\frac{\partial r}{\partial (10^3/T)} = 3$$

m = 172.297 g of silver

m = 138.759 g of silver

"Hot Volume" Data

Run 4510

Run 4531

P Argon	$10^3/T \text{ } ^\circ\text{K}^{-1}$	$r = \frac{\text{cc Argon (STP)}}{P \text{ Argon}} \cdot 10^2$	P Argon	$10^3/T \text{ } ^\circ\text{K}^{-1}$	$r = \frac{\text{cc Argon (STP)}}{P \text{ Argon}} \cdot 10^2$
39	0.7342	8.128	36.5	0.7892	9.397
165.5	0.7775	7.813	106	0.7880	9.575
275.7	0.7797	9.848	213	0.7812	9.765
279.3	0.7243	9.721	419.3	0.7812	9.874
403	0.7257	9.789	557.3	0.7812	9.905
396.5	0.7958	9.950	765.5	0.7797	9.950
401	0.7598	9.863	772.5	0.7465	9.860
658.6	0.7592	9.968	780.8	0.7209	9.755
754	0.7592	9.967	764.5	0.7923	9.963
748.4	0.7955	10.041	767.5	0.7920	10.887*
761	0.7251	9.875	781.6	0.7220	10.690*
			699.3	0.7920	10.892*

* The "hot volume" includes the additions reservoir.

$$\frac{\partial r}{\partial(10^3/T)} = 2.3 \quad \frac{\partial r}{\partial p} = 3.6$$

m = 191.001 g of silver

$$\frac{\partial r}{\partial(10^3/T)} = 2.8 \quad \frac{\partial r}{\partial p} = 2.2$$

m = 208.151 g of silver

"Hot Volume" Data

Run 4624

Run 4711

P_{Argon}	$10^3/T \text{ } ^\circ\text{K}^{-1}$	$r = \frac{\text{cc Argon (STP)}}{P_{\text{Argon}}} \cdot 10^2$	P_{Argon}	$10^3/T \text{ } ^\circ\text{K}^{-1}$	$r = \frac{\text{cc Argon (STP)}}{P_{\text{Argon}}} \cdot 10^2$
88.7	0.7569	9.729	111.5	0.7449	9.543
238	0.7572	9.769	342.3	0.7462	9.863
463.4	0.7572	9.870	346	0.7087	9.749
758	0.7569	9.960	341.9	0.7739	9.866
758	0.7948	10.078	754.2	0.7747	10.106
758	0.7261	9.935	756.8	0.7102	9.940
758	0.7575	10.053	760.0	0.749	10.021
694.4	0.7647	10.973*	752.5	0.7992	10.129
758	0.7647	11.001*	761.2	0.7396	10.013
758	0.7175	10.860*			
758	0.7879	11.078*			
771	0.7246	10.891*			

* The "hot volume" includes the additions reservoir.

$$\frac{\partial r}{\partial(10^3/T)} = 3.1$$

$$\frac{\partial r}{\partial p} = 3.4 \times 10^{-4}$$

m = 182.204 g of silver

$$\frac{\partial r}{\partial(10^3/T)} = 2.2$$

$$\frac{\partial r}{\partial p} = 4.3 \times 10^{-4}$$

m = 180.025 g of silver

"Hot Volume" Data

Run 4729

Run 4809

P Argon	$10^3/T \text{ } ^\circ\text{K}^{-1}$	$r = \frac{\text{cc ARGON (STP)}}{P \text{ Argon}} \cdot 10^2$	P Argon	$10^3/T \text{ } ^\circ\text{K}^{-1}$	$r = \frac{\text{cc ARGON (STP)}}{P \text{ Argon}} \cdot 10^2$
252.5	0.7559	9.101	137.5	0.7855	9.149
602.9	0.7559	9.199	229.6	0.7855	9.162
732.2	0.7559	9.213	308.3	0.7855	9.137
740.3	0.7152	9.112	391.6	0.7855	9.173
726.2	0.7876	9.289	474.1	0.7855	9.190
735.3	0.7392	9.175	564.6	0.7855	9.205
724.2	0.8030	9.315	642.6	0.7855	9.223
741.3	0.6960	9.100	708.8	0.7855	9.227
731.9	0.7570	9.217	762.9	0.7855	9.215
661.6	0.7572	10.196*	604	0.7855	9.197
665.6	0.7289	10.135*	743.8	0.7855	9.228
668.7	0.7072	10.088*	751.8	0.7390	9.130
659.0	0.7824	10.237*	758.6	0.7168	9.048
655.9	0.8041	10.285*	749.2	0.7633	9.162
660.2	0.7638	10.218*	742.2	0.8031	9.248
			744.7	0.7855	9.227
			668.1	0.7855	10.274*
			673.9	0.7393	10.185*
			677.9	0.7168	10.125*
			673	0.7633	10.199*

* The "hot volume" includes the additions reservoir.

$$\frac{\partial r}{\partial (10^3/T)} = 2.3 \quad \frac{\partial r}{\partial p} = 2.5 \times 10^{-4}$$

m = 167.949 g of silver

$$\frac{\partial r}{\partial (10^3/T)} = 2.4 \quad \frac{\partial r}{\partial p} = 1.6 \times 10^{-4}$$

m = 166.807 g of silver

"Hot Volume" Data

Run 4826		Run 4917	
P Argon	$10^3/T \text{ } ^\circ\text{K}^{-1}$	$r = \frac{\text{cc ARGON (STP)}}{\text{P ARGON}} \cdot 10^2$	$r = \frac{\text{cc ARGON (STP)}}{\text{P ARGON}} \cdot 10^2$
132.8	0.7743	7.651	83.2
265.4	0.7743	7.743	82.5
347.9	0.7743	7.761	232.7
353.0	0.7383	7.649	240.2
356.4	0.7115	7.576	238.2
346.8	0.8015	7.785	234.6
349.3	0.7747	7.730	459
465.3	0.7747	7.767	456
590.5	0.7747	7.883	465
721.4	0.7747	7.922	471.5
733.4	0.7383	7.792	460.6
743.7	0.7115	7.685	459
715.2	0.8015	7.991	764.5
720.4	0.7747	7.933	780.3
722.6	0.7747	7.909	790.2
639.3	0.7747	8.939*	760.5
646.3	0.7383	8.843*	766.5
653.6	0.7115	8.744*	675
636.1	0.8015	8.984*	767.5
640.2	0.7747	8.927*	785.2
			779.2
			761.4
			768.4
			0.739
			0.8031
			0.8012
			0.7127
			0.7389
			0.7747
			0.7747
			0.8012
			0.7385
			0.7117
			0.7747
			0.7775
			0.7748
			0.7386
			0.7117
			0.8012
			0.7748
			0.7748
			0.7748
			0.7117
			0.7385
			0.8012
			0.8012
			0.7748
			7.849
			7.915
			7.856
			7.610
			7.674
			7.792
			7.867
			7.919
			7.766
			7.659
			7.840
			7.867
			7.923
			7.762
			7.665
			7.964
			7.902
			8.973*
			8.995*
			8.793*
			8.860*
			9.068*
			8.985*

* The "hot volume" includes the additions reservoir.

$$\frac{\partial r}{\partial (10^3/T)} = 2.3 \quad \frac{\partial r}{\partial p} = 4.6 \times 10^{-4}$$

m = 171.335 g of silver

$$\frac{\partial r}{\partial (10^3/T)} = 3.1 \quad \frac{\partial r}{\partial p} = 2.4 \times 10^{-4}$$

m = 187.954 g of silver

EXPERIMENTAL RESULTS FROM RUN 3923

No.	P _{O₂}	10 ³ /T °K ⁻¹	hot volume	total no. of cc (STP)	% O ₂	1 + log K'
1	13	0.7972	1.1	50.4	0.0388	
2	26	0.7935	2.2	73.7	0.0561	0.4822
3	46.8	0.7836	4.0	99.0	0.0746	0.4782
4	64.2	0.7880	5.5	114.9	0.0860	0.4709
5	100.6	0.7861	8.6	145.1	0.1073	0.4695
6	140.4	0.7830	12.1	171.3	0.1251	0.4639
7	340.2	0.7840	29.3	275.0	0.1928	0.4582
8	461.5	0.7876	39.9	325.1	0.2238	0.4582
9	596	0.7844	51.7	371.4	0.2508	0.4521
10	692.4	0.7843	60.1	401.6	0.2678	0.4481
11	739	0.7836	64.3	416.7	0.2765	0.4477
12	806	0.7326	68.5	405.1	0.2641	0.4089
13	749	0.7622	64.5	405.1	0.2672	0.4300
14	694.5	0.7850	60.4	405.1	0.2704	0.4516
15	665	0.7997	58.1	405.1	0.2722	0.4638
16	766.8	0.7513	65.7	405.1	0.2663	0.4234

EXPERIMENTAL RESULTS FROM RUN 3114

No.	P _{O₂}	10 ³ /T °K ⁻¹	hot volume	total no. of cc (STP)	% O ₂	1 + log K ^o	% Cu
1	171.5	0.7733	16.7	226	0.1349	0.4534	0.000
2	523.3	0.7358	51.4	392.7	0.2198	0.4231	0.000
3	458.4	0.7812	45.6	392.7	0.2236	0.4592	0.000
4	630	0.7791	63.0	466.3	0.2597	0.4552	0.000
5	682	0.7550	67.8	466.3	0.2566	0.4328	0.000
6	711.7	0.7390	70.5	466.3	0.2549	0.4204	0.000
7	604.8	0.7958	60.7	466.3	0.2512	0.4666	0.000
8	653.8	0.7936	65.7	485.4	0.2702	0.4644	0.000
9	679	0.7812	68.0	485.4	0.2687	0.4538	0.000
10	671.2	0.7787	66.9	481.6	0.2670	0.4535	0.000
11	615	0.7799	61.2	481.6	0.2705	0.4781	0.060
12	678.3	0.7787	67.6	506.1	0.2821	0.4751	0.060
13	724	0.7754	72.3	523.3	0.2902	0.4732	0.060
14	611.8	0.7774	60.8	523.3	0.2971	0.5201	0.181
15	691	0.7769	68.9	556.8	0.3134	0.5168	0.181
16	734.4	0.7763	73.3	574.4	0.3219	0.5151	0.181
17	710.7	0.7799	71.0	570.3	0.3207	0.5207	0.181
18	646.2	0.7799	64.4	570.3	0.3247	0.5467	0.255
19	720.2	0.7772	71.9	600.7	0.3394	0.5424	0.255
20	768.7	0.7558	76.4	600.7	0.3365	0.5245	0.255
21	680.5	0.7936	68.2	600.7	0.3418	0.5577	0.255
22	528.9	0.7787	52.4	600.7	0.3510	0.6240	0.493
23	599.4	0.7769	59.5	635.7	0.3688	0.6183	0.493
24	669.2	0.7772	66.7	673.0	0.3880	0.6164	0.493

EXPERIMENTAL RESULTS FROM RUN 3114 (continued)

No.	P _{O₂}	10 ³ /T °K ⁻¹	hot volume	total no. of cc (STP)	% O ₂	1 + log K'	% Cu
25	713.7	0.7766	71.2	673.0	0.3851	0.5992	0.493
26	656.7	0.7967	65.8	673.0	0.3886	0.6212	0.493
27	741.6	0.7671	73.9	673.0	0.3834	0.5890	0.493
28	685	0.7839	68.4	668.8	0.3842	0.6071	0.493
29	542	0.7799	53.8	668.8	0.3927	0.6675	0.695
30	628.3	0.7781	62.5	712.5	0.4150	0.6593	0.695
31	724.8	0.7754	72.3	758.3	0.4379	0.6516	0.695
32	597.8	0.7745	59.4	758.3	0.4453	0.7008	0.874

Note: Temperatures are in error. The melting point of pure silver was not well determined, but indicated that the true temperature was well above the apparent one (may be by 20 to 30°C).

EXPERIMENTAL RESULTS FROM RUN 4019

No.	P _{O₂}	10 ³ /T °K ⁻¹	hot volume	total no. of cc (SIP)	Z ₀	1 + log K'	Z _{Cu}
1	699.3	0.7451	75.9	382.0	0.2530	0.4210	0.000
2	753.0	0.7145	81.4	382.0	0.2485	0.3973	0.000
3	620.2	0.7923	67.9	382.0	0.2596	0.4384	0.000
4	577.0	0.7951	63.0	382.0	0.2635	0.4806	0.044
5	727.5	0.7102	78.4	382.0	0.2508	0.4089	0.044
6	651.3	0.7527	70.7	382.0	0.2572	0.4438	0.044
7	608.1	0.7781	66.3	382.0	0.2609	0.4648	0.044
8	550.5	0.8129	60.2	382.0	0.2658	0.4946	0.044
9	611.5	0.8169	67.1	402.3	0.2769	0.4895	0.044
10	729	0.7509	79.4	402.3	0.2673	0.4360	0.044
11	792	0.7183	85.9	402.3	0.2614	0.4084	0.044
12	672.6	0.7787	73.5	402.3	0.2716	0.4604	0.044
13	724.8	0.7775	79.5	417.9	0.2795	0.4567	0.044
14	688.8	0.7775	75.4	417.9	0.2828	0.4728	0.082
15	821	0.7134	89.0	417.9	0.2715	0.4170	0.082
16	616	0.8152	67.8	417.9	0.2890	0.5065	0.082
17	481.8	0.8122	52.6	417.9	0.3008	0.5772	0.342
18	642	0.7099	68.9	417.9	0.2874	0.4952	0.342
19	531.8	0.7612	57.4	417.9	0.2968	0.5500	0.342
20	643.9	0.7586	69.9	456.6	0.3183	0.5389	0.342
21	777.3	0.7079	84.0	456.6	0.3068	0.4820	0.342
22	565.7	0.7993	61.8	456.6	0.3250	0.5760	0.342
23	568.7	0.7993	62.2	456.6	0.3247	0.5745	0.342
24	633.2	0.7736	69.0	456.6	0.3191	0.5436	0.342
25	787	0.7081	85.3	456.6	0.3057	0.4772	0.342

EXPERIMENTAL RESULTS FROM RUN 4120

No.	P _{O₂}	10 ³ /T °K ⁻¹	hot volume	total no. of cc (STP)	Z _O	1 + log K'	Z _{Cu}
1	43	0.8044	4.8	71.8	0.0690	0.4624	0.000
2	50.8	0.7509	5.5	71.8	0.0682	0.4210	0.000
3	50.1	0.7519	5.8	71.8	0.0679	0.4225	0.000
4	43.1	0.8044	5.0	71.8	0.0687	0.4601	0.000
5	34	0.8031	4.0	71.8	0.0697	0.5178	0.140
6	40.9	0.7458	4.7	71.8	0.0690	0.4728	0.140
7	52	0.7509	6.0	81.9	0.0779	0.4741	0.140
8	42.2	0.8031	4.9	81.9	0.0790	0.5255	0.140
9	38.5	0.8012	4.5	81.9	0.0794	0.5477	0.199
10	48	0.7535	5.5	81.9	0.0784	0.4938	0.199
11	56.2	0.7147	6.4	81.9	0.0775	0.4545	0.199
12	61	0.7147	7.0	85.5	0.0806	0.4540	0.199
13	43	0.8002	5.0	85.5	0.0826	0.5408	0.199
14	50.9	0.7586	5.9	85.5	0.0817	0.4993	0.199

EXPERIMENTAL RESULTS FROM RUN 4510

No.	P _{O2}	10 ³ /T °K ⁻¹	hot volume	total no. of cc (STP)	% O ₂	1 + log P ₁
1	10	0.7873	1.0	42.0	0.0307	0.4273
2	26	0.7886	2.6	71.5	0.0515	0.4447
3	31.2	0.7277	3.0	71.5	0.0512	0.4024
4	69	0.7293	6.7	111.0	0.0779	0.4126
5	116	0.7283	11.2	146.5	0.1010	0.4135
6	105	0.7707	10.3	146.5	0.1017	0.4372
7	95	0.8044	9.4	146.5	0.1024	0.4619
8	113	0.7468	11.0	146.5	0.1012	0.4188
9	178.5	0.7440	17.5	186.7	0.1279	0.4213
10	290	0.7396	28.3	245.4	0.1620	0.4187
11	260.8	0.7768	25.7	245.4	0.1639	0.4469
12	236.3	0.8077	23.4	245.4	0.1656	0.4728
13	304	0.7220	29.6	245.4	0.1610	0.4058
14	434.7	0.7163	42.4	296.6	0.1896	0.3991
15	595.5	0.7178	58.5	354.6	0.2209	0.3971
16	491.6	0.7858	48.9	354.6	0.2280	0.4526
17	549.7	0.7451	54.2	354.6	0.2240	0.4207
18	618.3	0.7426	61.1	377.1	0.2357	0.4171
19	738	0.7396	73.1	414.4	0.2544	0.4119

EXPERIMENTAL RESULTS FROM RUN 4531

No.	P _{O₂}	10 ³ /T °K ⁻¹	net volume	Total no. of cc (SJP)	% O ₂	i + log K'
1	157.7	0.7824	15.5	209.3	0.1327	0.4645
2	241.4	0.7833	23.8	265.3	0.1654	0.4677
3	325	0.7830	32.0	311.4	0.1912	0.4660
4	426.5	0.7800	42.1	359.5	0.2172	0.4624
5	534	0.7827	52.9	407.9	0.2429	0.4621
6	631.8	0.7833	62.7	447.6	0.2633	0.4606
7	721.3	0.7839	71.7	481.5	0.2803	0.4589
8	698.7	0.7854	76.0	481.5	0.2774	0.4613
9	838.5	0.7177	89.7	481.5	0.2680	0.4067
10	776.3	0.7479	83.7	481.5	0.2721	0.4301
11	690.5	0.7892	75.3	481.5	0.2778	0.4645
12	651.5	0.8082	71.2	481.5	0.2806	0.4816
13	736.0	0.7662	79.7	481.5	0.2748	0.4460
14	795.3	0.7369	85.5	481.5	0.2709	0.4229
15	674.6	0.7973	73.6	481.5	0.2790	0.4715

EXPERIMENTAL RESULTS FROM RUN 4624

No.	P_{O_2}	$10^3/T \text{ } ^\circ K^{-1}$	log volume	total no. of cc (SIP)	γ_0	$1 + \log K^0$	% Au
1	153.5	0.7440	19.2	170.3	0.0217	0.4327	0.000
2	245.9	0.7429	24.4	219.4	0.1530	0.4297	0.000
3	273	0.7094	26.8	219.4	0.1511	0.4014	0.000
4	382.5	0.7089	37.5	264.2	0.1779	0.3992	0.000
5	502.7	0.7071	49.3	307.2	0.2021	0.3953	0.000
6	401	0.7848	40.3	307.2	0.2091	0.4590	0.000
7	528	0.7848	53.0	354.0	0.2357	0.4514	0.000
8	549	0.7643	54.8	354.0	0.2343	0.4404	0.000
9	648.7	0.7697	64.7	387.8	0.2529	0.4372	0.000
10	695	0.7259	75.6	387.8	0.2444	0.4075	0.000
11	960.2	0.7251	82.7	407.5	0.2544	0.4053	0.000
12	694.7	0.7251	75.6	388.2	0.2448	0.4083	0.000
13	562.2	0.8012	62.5	388.2	0.2550	0.4720	0.000
14	619.8	0.7665	68.6	388.2	0.2503	0.4428	0.000
15	637	0.7663	69.8	388.2	0.2473	0.4315	0.647
16	737.2	0.7112	79.8	388.2	0.2395	0.3859	0.647
17	694.1	0.7365	75.6	388.2	0.2420	0.4035	0.647
18	597.6	0.7925	65.9	388.2	0.2495	0.4493	0.647
19	640.9	0.7606	70.3	388.2	0.2461	0.4281	0.647
20	660.4	0.7669	72.5	388.2	0.2426	0.4154	1.379
21	682.6	0.7669	75.0	388.2	0.2387	0.4012	2.204
22	662.5	0.7665	72.7	381.4	0.2353	0.4014	2.204
23	639.2	0.7668	70.1	374.0	0.2316	0.4023	2.204
24	608	0.7670	66.6	364.2	0.2268	0.4040	2.204
25	670.9	0.7291	72.9	364.2	0.2220	0.3734	2.204

EXPERIMENTAL RESULTS FROM RUN 4624 (continued)

No.	P _{O2}	10 ³ /T °K ⁻¹	hot volume	Total vol. of cc (STP)	% O ₂	1 + log K ^o	% Au
26	705.5	0.7092	76.3	364.2	0.2194	0.3574	2.204
27	638.6	0.7473	69.6	364.2	0.2245	0.3890	2.204
28	569.8	0.7930	62.8	364.2	0.2297	0.4237	2.204
29	550.9	0.7944	60.7	358.4	0.2269	0.4256	2.204
30	591.8	0.7674	64.8	358.4	0.2237	0.4040	2.204
31	613.4	0.7672	67.2	358.4	0.2201	0.3892	2.994
32	635.3	0.7671	69.7	358.4	0.2165	0.3743	3.778
33	655.2	0.7675	71.9	358.4	0.2133	0.3612	4.468
34	651.2	0.7704	71.5	358.4	0.2136	0.3631	4.468
35	752.4	0.7097	81.5	358.4	0.2061	0.3163	4.468
36	624	0.7883	68.8	358.4	0.2156	0.3764	4.468
37	702.6	0.7388	76.6	358.4	0.2098	0.3388	4.468
38	677.3	0.7547	74.1	358.4	0.2116	0.3506	4.468
39	664	0.7635	72.8	358.4	0.2126	0.3569	4.468

EXPERIMENTAL RESULTS FROM RUN 4711

No.	P _{O₂}	10 ³ /T °K ⁻¹	hot volume	total no. of cc (STP)	% O ₂	1 + log K'
1	121.7	0.7427	11.9	148.9	0.1085	0.4333
2	107.3	0.7843	10.6	148.9	0.1096	0.4648
3	137.5	0.7059	13.3	148.9	0.1074	0.4021
4	101.6	0.8052	10.0	148.9	0.1100	0.4783
5	115.7	0.7631	11.3	148.9	0.1090	0.4460
6	129.9	0.7275	12.6	148.9	0.1079	0.4167
7	936.5	0.7127	73.2	383.3	0.2453	0.3965
8	593.1	0.7925	59.6	383.3	0.2560	0.4621
9	666.5	0.7505	66.6	383.3	0.2505	0.4273
10	661.5	0.7554	66.2	383.3	0.2509	0.4296
11	582.2	0.8012	58.6	383.3	0.2568	0.4675
12	913.8	0.7267	70.9	383.3	0.2471	0.4066
13	621.1	0.7783	62.3	383.3	0.2539	0.4485

EXPERIMENTAL RESULTS FROM KUN 4729

No.	P _{O₂}	10 ³ /T °K ⁻¹	hot volume	total no. of cc (STP)	% O ₂	1 + log K'
1	7	0.7618	0.6	24.0	0.0199	0.4580
2	85.7	0.7618	7.8	119.7	0.0950	0.4517
3	179.2	0.7618	16.3	178.6	0.1379	0.4533
4	347	0.7618	31.7	256.1	0.1904	0.4409
5	468.6	0.7618	43.0	301.9	0.2196	0.4467
6	718.9	0.7618	66.4	382.6	0.2681	0.4403
7	690.9	0.7618	70.6	382.6	0.2646	0.4432
8	749.6	0.7324	76.2	382.6	0.2598	0.4174
9	622.4	0.8021	64.0	382.6	0.2701	0.4748
10	684.6	0.7695	70.0	382.6	0.2650	0.4458
11	997.6	0.7112	80.8	382.6	0.2559	0.3975
12	742.7	0.7332	75.7	382.6	0.2602	0.4202

EXPERIMENTAL RESULTS FROM RUN 4809

No.	P _{O2}	10 ⁵ /T °K ⁻¹	hot volume	total no. of cc (STP)	% O ₂	1 + log K'
1	2.6	0.7855	0.2	21.0	0.0177	0.4847
2	6.7	0.7855	0.6	33.6	0.0282	0.4775
3	11.2	0.7855	1.0	41.3	0.0344	0.4523
4	17.6	0.7855	1.6	52.5	0.0436	0.4566
5	27.7	0.7855	2.5	67.7	0.0558	0.4655
6	36.6	0.7855	3.3	77.9	0.0637	0.4630
7	51.1	0.7855	4.7	93.4	0.0759	0.4663
8	68.7	0.7855	6.3	109.4	0.0881	0.4671
9	96.8	0.7855	8.8	131.5	0.1048	0.4679
10	115.6	0.7855	10.6	144.6	0.1146	0.4680
11	146.0	0.7855	13.3	163.9	0.1287	0.4678
12	200.8	0.7855	18.4	184.1	0.1502	0.4655
13	235.5	0.7855	21.6	211.1	0.1619	0.4638
14	296.4	0.7855	27.2	239.1	0.1810	0.4622
15	324.5	0.7558	29.5	239.1	0.1791	0.4379
16	282.5	0.8025	25.9	239.1	0.1821	0.4751
17	350.2	0.7314	31.6	239.1	0.1773	0.4169
18	374.9	0.7076	33.6	239.1	0.1755	0.3978
19	300.6	0.7855	27.5	239.1	0.1807	0.4584
20	357.1	0.7855	32.8	261.8	0.1956	0.4555
21	409	0.7855	37.6	281.7	0.2085	0.4537
22	496.5	0.7855	45.7	313.4	0.2286	0.4515
23	585.8	0.7855	53.9	343.3	0.2471	0.4494

EXPERIMENTAL RESULTS FROM RUN 4809 (continued)

No.	P _{O₂}	10 ³ /T °K ⁻¹	hot volume	total no. of cc (STP)	Z ₀	1 + log K'
24	657.2	0.7855	60.6	365.9	0.2606	0.4475
25	745.7	0.7855	68.9	392.6	0.2763	0.4455
26	637.3	0.7855	58.7	362.3	0.2591	0.4517
27	791.4	0.7855	73.1	406.8	0.2848	0.4457
28	788.6	0.7855	72.9	406.8	0.2850	0.4468
29	759.9	0.7855	98.2	406.8	0.2805	0.4477
30	667.6	0.7855	68.6	379.9	0.2657	0.4524
31	757.1	0.7390	77.1	379.9	0.2585	0.4132
32	799.3	0.7178	80.9	379.9	0.2552	0.3959
33	713.5	0.7615	73.0	379.9	0.2619	0.4318
34	633.8	0.8044	65.5	379.9	0.2683	0.4681
35	820.0	0.7076	82.9	379.9	0.2535	0.3875
36	669.2	0.7855	68.7	379.9	0.2656	0.4518

EXPERIMENTAL RESULTS FROM RUN 4628

No.	P _{O₂}	10 ³ /T °K ⁻¹	hot volume	total no. of cc (STP)	Z ₀	1 + log K'
1	5	0.7745	0.4	29.2	0.0240	0.4708
2	13	0.7745	1.0	45.5	0.0370	0.4521
3	20.5	0.7745	1.6	57.1	0.0463	0.4494
4	42	0.7745	3.2	83.7	0.0671	0.4553
5	65.5	0.7745	5.0	106.6	0.0846	0.4599
6	129.5	0.7745	9.9	152.6	0.1188	0.4590
7	130.8	0.7747	10.0	152.6	0.1187	0.4566
8	163.1	0.7051	12.2	152.6	0.1168	0.4017
9	148	0.7383	11.2	152.6	0.1177	0.4259
10	200.2	0.8015	15.4	201.9	0.1551	0.4802
11	269.5	0.7115	20.4	201.9	0.1510	0.4041
12	365.1	0.7115	27.7	238.0	0.1749	0.4020
13	274	0.8015	21.2	238.0	0.1802	0.4774
14	400.2	0.7383	30.7	262.0	0.1924	0.4234
15	327.5	0.8015	25.5	262.0	0.1067	0.4766
16	434.4	0.7116	33.0	262.0	0.1904	0.4012
17	357.6	0.7746	27.7	262.0	0.1948	0.4533
18	499.5	0.8015	39.3	330.0	0.2416	0.4743
19	544.3	0.7747	42.7	330.0	0.2389	0.4506
20	606.2	0.7383	46.9	330.0	0.2353	0.4208
21	655.5	0.7115	50.2	330.0	0.2326	0.3988
22	746.4	0.7115	57.4	354.2	0.2467	0.3962
23	568.1	0.8015	45.0	354.2	0.2570	0.4731
24	743.6	0.7115	57.1	354.2	0.2469	0.3973
25	618.6	0.7747	48.7	354.2	0.2539	0.4494

EXPERIMENTAL RESULTS FROM RUN 4828 (continued)

No.	P _{O₂}	10 ³ /T °K ⁻¹	hot volume	total no. of cc (STP)	% O ₂	1 + log K'	% Pt
26	688.7	0.7383	53.5	354.2	0.2499	0.4192	
27	650	0.7581	50.9	354.2	0.2521	0.4356	
28	626.7	0.7581	55.7	354.2	0.2481	0.4365	0.000
29	552.9	0.8015	49.3	354.2	0.2534	0.4729	0.000
30	622.4	0.7636	55.4	354.2	0.2484	0.4385	0.000
31	618.8	0.7644	55.1	354.2	0.2486	0.4402	0.000
32	554	0.8018	49.4	354.2	0.2533	0.4723	0.000
33	717.3	0.7115	63.1	354.2	0.2420	0.3964	0.000
34	646.3	0.7495	57.3	354.2	0.2468	0.4276	0.000
35	601	0.7745	53.7	354.2	0.2500	0.4489	0.000
36	665	0.7383	58.8	354.2	0.2456	0.4191	0.000
37	717.9	0.7115	63.1	354.2	0.2420	0.3962	0.000
38	735.3	0.7115	64.7	354.2	0.2395	0.3864	0.500
39	570.9	0.8015	51.0	354.2	0.2508	0.4614	0.500
40	753.0	0.7115	66.3	354.2	0.2369	0.3766	1.040
41	588.8	0.8015	52.6	354.2	0.2481	0.4501	1.040
42	635	0.7748	56.8	354.2	0.2447	0.4276	1.040
43	700.8	0.7383	62.1	354.2	0.2403	0.3983	1.040
44	741.4	0.7383	66.0	354.2	0.2344	0.3763	2.190
45	626.3	0.8015	56.2	354.2	0.2423	0.4264	2.190
46	706.3	0.7577	63.0	354.2	0.2367	0.3901	2.190
47	676.2	0.7751	60.7	354.2	0.2386	0.4031	2.190
48	795.5	0.7115	70.2	354.2	0.2309	0.3535	2.190
49	763.3	0.7115	67.1	346.2	0.2269	0.3549	2.190
50	712.6	0.7385	63.2	346.2	0.2301	0.3758	2.190

EXPERIMENTAL RESULTS FROM RUN 4828 (continued)

No.	P _{O2}	10 ³ /T °K ⁻¹	hot volume	total no. of cc (STP)	% O ₂	l + log K'	% Pt
51	602.1	0.8015	54.0	346.2	0.2376	0.4263	2.190
52	647.9	0.7745	57.9	346.2	0.2344	0.4045	2.190
53	679.0	0.7573	60.4	346.2	0.2324	0.3906	2.190
54	696	0.7573	62.0	346.2	0.2299	0.3805	2.698
55	619.2	0.8015	55.6	346.2	0.2350	0.4155	2.698
56	781.3	0.7115	68.8	346.2	0.2243	0.3448	2.698
57	736	0.7573	65.8	346.2	0.2243	0.3577	3.769
58	672.8	0.8015	60.7	346.2	0.2284	0.3851	3.769
59	736.1	0.7575	65.8	346.2	0.2243	0.3577	3.769
60	704.7	0.7749	63.2	346.2	0.2264	0.3711	3.769
61	681.7	0.7881	61.3	346.2	0.2279	0.3813	3.769
62	770.2	0.7385	68.7	346.2	0.2220	0.3434	3.769
63	677.2	0.7936	61.0	346.2	0.2281	0.3832	3.769
64	696	0.7877	62.6	346.2	0.2269	0.3749	3.769
65	809.3	0.7225	71.7	346.2	0.2195	0.3278	3.769
66	695.1	0.7839	62.5	346.2	0.2269	0.3752	3.769
67	684.7	0.7904	61.6	346.2	0.2276	0.3798	3.769
68	830	0.7115	73.4	346.2	0.2182	0.3198	3.769
69	801	0.7282	71.1	346.2	0.2200	0.3310	3.769
70	684.3	0.7748	61.2	338.6	0.2219	0.3688	3.769
71	712	0.7748	63.8	338.6	0.2179	0.3524	4.574
72	741.1	0.7748	66.6	338.6	0.2138	0.3354	5.432
73	627.1	0.7376	49.0	287.4	0.1874	0.3144	5.434
74	631.4	0.7368	49.4	287.4	0.1871	0.3123	5.434
75	540.8	0.7385	41.7	264.6	0.1752	0.3173	5.434
76	577.8	0.7117	44.1	264.6	0.1743	0.2983	5.434

EXPERIMENTAL RESULTS FROM RUN 4828 (continued)

No.	P _{O2}	10 ³ /T °K ⁻¹	hot volume	total no. of cc (STP)	Z ₀	1 + log K'	% Pt	% Cu
77	491.8	0.7748	38.4	264.6	0.1778	0.3444	5.434	
78	517	0.7558	40.2	264.6	0.1768	0.3302	5.434	
79	43.5	0.7117	3.3	62.3	0.0465	0.2883	5.441	
80	35	0.7748	2.7	62.3	0.0469	0.3398	5.441	
81	92.7	0.7748	7.1	102.9	0.0754	0.3341	5.440	
82	110.8	0.7117	8.3	102.9	0.0744	0.2897	5.440	
83	283.6	0.7117	21.4	172.0	0.1185	0.2876	5.437	
84	239.9	0.7748	18.5	172.0	0.1208	0.3324	5.437	
85	252.6	0.7558	19.3	172.0	0.1201	0.3188	5.437	
86	263.8	0.7385	20.1	172.0	0.1195	0.3072	5.437	
87	537	0.7117	40.9	246.8	0.1619	0.3846	5.435	
88	458.8	0.7748	35.8	246.8	0.1659	0.3295	5.435	
89	771.8	0.7117	59.4	304.2	0.1926	0.3812	5.433	
90	749	0.7251	58.0	304.2	0.1936	0.2902	5.433	
91	662.5	0.7757	52.3	304.2	0.1981	0.3267	5.433	
92	689.7	0.7584	54.1	304.2	0.1967	0.3148	5.433	
93	725.4	0.7390	56.5	304.2	0.1948	0.2998	5.433	
94	664.9	0.7748	52.5	304.2	0.1979	0.3256	5.433	
95	638.3	0.7748	57.0	304.2	0.1944	0.3266	5.433	
96	570.3	0.7748	50.7	304.2	0.1992	0.3617	5.433	0.0000
97	433.7	0.7748	38.3	304.2	0.2085	0.4410	5.433	0.0834
98	331.7	0.7748	29.1	304.2	0.2153	0.5130	5.433	0.2839
99	364.7	0.7559	31.8	304.2	0.2132	0.4881	5.433	0.4808
100	448.6	0.7117	38.8	304.2	0.2077	0.4320	5.433	0.4808
101	405.6	0.7336	35.3	304.2	0.2105	0.4596	5.433	0.4808
102	412.7	0.7304	35.9	304.2	0.2100	0.4548	5.433	0.4808

EXPERIMENTAL RESULTS FROM RUN 4917

No.	P _{O₂}	10 ³ /T °K ⁻¹	hot volume	total no. of cc (STP)	% O ₂	1 + log K'
1	5.2	0.7751	0.4	34.7	0.0245	0.4734
2	14.4	0.7751	1.1	54.3	0.0404	0.4668
3	31.8	0.7551	2.4	80.2	0.0590	0.4600
4	59.1	0.7751	4.6	111.8	0.0814	0.4653
5	73.8	0.7117	5.6	111.8	0.0806	0.4129
6	67.6	0.7385	5.2	111.8	0.0810	0.4336
7	54.5	0.7999	4.3	111.8	0.0817	0.4841
8	61.4	0.7715	4.7	111.8	0.0813	0.4562
9	143.1	0.7751	11.1	176.7	0.1257	0.4617
10	177	0.7117	13.5	176.7	0.1239	0.4094
11	276	0.7117	21.0	223.5	0.1536	0.4062
12	203	0.8027	16.0	223.5	0.1574	0.4836
13	223	0.7751	17.3	223.5	0.1563	0.4603
14	252.2	0.7387	19.4	223.5	0.1548	0.4293
15	342.6	0.7751	26.8	280.0	0.1920	0.4563
16	418.7	0.7117	32.0	280.0	0.1880	0.4036
17	565.6	0.7117	43.4	329.3	0.2167	0.4000
18	465	0.7751	36.5	329.3	0.2219	0.4528
19	508	0.7472	39.5	329.3	0.2196	0.4292
20	427.5	0.8012	33.9	329.3	0.2239	0.4750
21	520.9	0.7385	40.3	329.3	0.2190	0.4224
22	735.2	0.7385	57.2	395.8	0.2566	0.4164
23	658.9	0.7751	51.9	395.8	0.2605	0.4468
24	794.6	0.7117	61.1	395.8	0.2536	0.3944
25	605.9	0.8012	48.2	395.8	0.2633	0.4696

EXPERIMENTAL RESULTS FROM RUN 4917 (continued)

No.	P _{O2}	$10^3/T$ °K ⁻¹	hot volume	total no. of cc (STP)	% O ₂	1 + log K'	% Pd
26	684.7	0.7612	53.7	395.8	0.2592	0.4362	
27	682.7	0.7630	53.6	395.8	0.2592	0.4370	
28	635.1	0.7749	57.0	395.8	0.2567	0.4484	
29	705.0	0.7385	62.6	395.8	0.2525	0.4186	
30	586.9	0.8012	53.2	395.8	0.2596	0.4704	
31	761.6	0.7117	67.0	395.8	0.2492	0.3960	
32	672.8	0.7557	60.1	395.8	0.2544	0.4320	
33	682.6	0.7558	61.0	395.8	0.2532	0.4268	
34	689.2	0.7558	61.6	395.8	0.2524	0.4234	
35	691.7	0.7558	61.8	395.8	0.2522	0.4223	
36	779.4	0.7117	68.6	395.8	0.2472	0.3675	
37	605.1	0.8012	54.9	395.8	0.2575	0.4602	
38	653.9	0.7751	58.8	395.8	0.2545	0.4384	
39	724.8	0.7385	64.4	395.8	0.2503	0.4089	
40	733.6	0.7385	65.2	395.8	0.2494	0.4046	
41	700.4	0.7558	62.6	395.8	0.2513	0.4180	
42	616.1	0.8012	55.9	395.8	0.2563	0.4544	
43	700.4	0.7558	62.6	395.8	0.2513	0.4180	
44	664.8	0.7751	60.0	395.8	0.2536	0.4332	
45	791.9	0.7117	69.7	395.8	0.2460	0.3819	
46	800.9	0.7117	70.5	395.8	0.2450	0.3777	
47	800.4	0.7117	70.4	395.8	0.2450	0.3780	
48	747.1	0.7385	66.4	395.8	0.2481	0.3982	
49	625.1	0.8012	56.7	395.8	0.2555	0.4495	
50	674.9	0.7751	60.7	395.8	0.2523	0.4278	

EXPERIMENTAL RESULTS FROM RUN 4917 (continued)

No.	P _{O2}	10 ³ /T °K ⁻¹	hot volume	total no. of cc (STP)	% O ₂	1 + log K ¹	% Pd
51	712.3	0.7558	63.7	395.8	0.2501	0.4122	0.625
52	24	0.7739	1.0	65.0	0.0475	0.4279	1.022
53	30	0.7117	2.3	65.0	0.0472	0.3759	1.022
54	87.5	0.7117	6.6	112.7	0.0798	0.3714	1.022
55	71.8	0.7751	5.6	112.7	0.0806	0.4186	1.022
56	176	0.7751	13.7	181.8	0.1265	0.4196	1.021
57	198.7	0.7385	15.3	181.8	0.1253	0.3891	1.021
58	216.6	0.7116	16.5	181.8	0.1244	0.3673	1.021
59	162.9	0.8012	12.8	181.8	0.1271	0.4387	1.021
60	388.9	0.7117	29.7	249.0	0.1649	0.3626	1.021
61	320.5	0.7748	25.0	249.0	0.1684	0.4137	1.021
62	525.3	0.7748	41.3	324.3	0.2126	0.4078	1.020
63	628.8	0.7117	48.3	324.3	0.2074	0.3580	1.020
64	754.7	0.7117	58.0	358.5	0.2257	0.3551	1.020
65	722.9	0.7117	63.6	358.5	0.2216	0.3563	1.020
66	753.7	0.7117	66.3	366.8	0.2257	0.3554	1.020
67	586.7	0.8012	53.2	366.8	0.2356	0.4283	1.020
68	634.2	0.7751	57.0	366.8	0.2327	0.4061	1.020
69	701.6	0.7385	62.3	366.8	0.2287	0.3767	1.020
70	670.9	0.7558	59.9	366.8	0.2305	0.3898	1.020
71	675.9	0.7558	60.4	366.8	0.2299	0.3869	1.140
72	688.4	0.7558	61.5	366.8	0.2286	0.3806	1.297
73	695.8	0.7558	62.2	366.8	0.2279	0.3769	1.391
74	702.8	0.7558	62.8	366.8	0.2272	0.3734	1.491
75	716.9	0.7558	64.1	366.8	0.2257	0.3662	1.724

EXPERIMENTAL RESULTS FROM RUN 4917 (continued)

No.	P _{O₂}	10 ³ /T °K ⁻¹	hot volume	total no. of cc (STP)	% O ₂	1 + log K'	% Pd
76	717.6	0.7558	64.2	366.8	0.2257	0.3659	1.724
77	801.4	0.7117	70.6	366.8	0.2209	0.3327	1.724
78	794.2	0.7117	69.9	366.8	0.2214	0.3356	1.724
79	676.4	0.7751	60.0	366.8	0.2281	0.3835	1.724
80	716.6	0.7546	64.1	366.8	0.2257	0.3663	1.724
81	746.5	0.7385	66.3	366.8	0.2240	0.3542	1.724
82	802.5	0.7117	70.7	366.8	0.2209	0.3323	1.724
83	801.1	0.7117	70.5	366.8	0.2209	0.3328	1.724
84	638	0.8012	57.9	366.8	0.2303	0.4003	1.724
85	18.8	0.7948	1.5	58.0	0.0408	0.4189	1.724
86	24.8	0.7117	1.9	58.0	0.0405	0.3553	1.724
87	49.3	0.7117	3.7	81.5	0.0567	0.3511	1.724
88	110.6	0.7117	8.4	123.7	0.0847	0.3486	1.724
89	251.5	0.7117	19.1	190.5	0.1267	0.3439	1.724
90	208.6	0.7751	16.1	190.5	0.1288	0.3919	1.724
91	366.4	0.7754	38.6	254.4	0.1686	0.3652	1.724
92	438.0	0.7117	33.4	354.4	0.1650	0.3371	1.724
93	407.5	0.7385	31.4	254.4	0.1665	0.3566	1.724
94	388.1	0.7558	30.1	254.4	0.1674	0.3698	1.724
95	340.2	0.8012	26.8	254.4	0.1699	0.4047	1.724
96	594.9	0.7751	46.7	330.7	0.2119	0.3792	1.724
97	704.1	0.7117	53.9	330.7	0.2064	0.3317	1.724
98	745.5	0.7117	57.2	341.2	0.2119	0.3299	1.724
99	714.0	0.7117	62.16	341.2	0.2078	0.3313	1.724
100	745.8	0.7117	65.4	349.4	0.2118	0.3300	1.724

EXPERIMENTAL RESULTS FROM RUN 4917 (continued)

No.	P _{O₂}	10 ³ /T °K ⁻¹	hot volume	total no. of cc (STP)	% O ₂	1 + log K'	% Pd	% Cu
101	639.8	0.7751	57.4	349.4	0.2178	0.3755	1.724	0.000
102	596.7	0.8012	54.0	349.4	0.2203	0.3956	1.724	0.000
103	697	0.7385	61.7	349.4	0.2145	0.3503	1.724	0.000
104	669.6	0.7558	59.7	349.4	0.2161	0.3621	1.724	0.000
105	684.9	0.7558	61.1	349.4	0.2144	0.3538	2.011	0.000
106	702.4	0.7558	62.7	349.4	0.2126	0.3447	2.279	0.000
107	677.8	0.7751	60.9	349.4	0.2140	0.3552	2.279	0.000
108	781.5	0.7117	68.7	349.4	0.2082	0.3124	2.279	0.000
109	733.7	0.7385	65.1	349.4	0.2109	0.3316	2.279	0.000
110	703.8	0.7558	62.8	349.4	0.2125	0.3441	2.279	0.000
111	723.7	0.7558	64.7	349.4	0.2105	0.3339	2.585	0.000
112	742.7	0.7117	65.3	335.1	0.1996	0.3051	2.585	0.000
113	670.7	0.7558	59.9	335.1	0.2035	0.3358	2.585	0.000
114	686.9	0.7558	61.4	335.1	0.2016	0.3264	2.994	0.000
115	713.1	0.7385	63.3	335.1	0.2004	0.3158	2.994	0.000
116	758.6	0.7117	66.7	335.1	0.1976	0.2963	2.994	0.000
117	735.8	0.7256	65.0	335.1	0.1989	0.3056	2.994	0.000
118	758.6	0.7117	66.7	335.1	0.1976	0.2963	2.994	0.000
119	726.3	0.7117	63.7	327.0	0.1946	0.2990	2.994	0.000
120	760.0	0.7117	66.7	335.3	0.1978	0.2962	2.994	0.000
121	711.4	0.7117	62.4	335.3	0.2008	0.3172	2.992	0.061
122	666.2	0.7117	58.4	335.3	0.2037	0.3375	2.990	0.123
123	761.0	0.7117	66.8	361.8	0.2170	0.3361	2.990	0.123

EXPERIMENTAL RESULTS FROM RUN 4917 (continued)

No.	P _{O₂}	10 ³ /T °K ⁻¹	hot volume	total no. of cc (STP)	% O ₂	1 + log K'	% Pd	% Cu
124	671.6	0.7558	59.8	361.8	0.2221	0.3733	2.990	0.123
125	705.2	0.7385	62.4	361.8	0.2202	9.3590	2.990	0.123
126	733.3	0.7256	64.6	361.8	0.2186	0.3473	2.990	0.123
127	762.1	0.7117	66.9	361.8	0.2169	0.3356	2.990	0.123
128	698.3	0.7117	61.2	361.8	0.2208	0.3625	2.988	0.205
129	634.9	0.7117	55.6	361.8	0.2248	0.3908	2.985	0.293
130	758.9	0.7117	66.6	399.1	0.2440	0.3877	2.985	0.293
131	647.8	0.7558	57.7	399.1	0.2505	0.4335	2.985	0.293
132	722.0	0.7256	63.6	399.1	0.2462	0.4023	2.985	0.293
133	690.5	0.7385	61.1	399.1	0.2480	0.4153	2.985	0.293

BIOGRAPHICAL NOTE

The author is a Greek citizen, and was born on March 5, 1938, in Alexandria, Egypt. He attended the College St. Marc of Alexandria where he received the Baccalaureat in 1955.

He pursued his studies in Paris, France, with a program of "Mathematiques Superieures" at the Lycée Louis-le-Grand, from 1955 to 1956, and "Mathematiques Spéciales" at the Lycée St. Louis, from 1956 to 1958. In 1958, he was admitted to the Ecole Nationale Superieure des Mines de Paris, after an entrance examination in which he ranked first among the foreign candidates (over one hundred). In 1961, he obtained the degree of "Ingenieur Civil des Mines," ranking in the upper 10% part of his class. While pursuing his studies, and specializing in Metallurgy at the Ecole des Mines, he obtained a "Licence ès Sciences" from the University of Paris in 1959, and a diploma from the Institut d'Administration des Entreprises in 1960.

In September, 1961, he entered the Department of Metallurgy at the Massachusetts Institute of Technology as a research assistant to Professor John F. Elliott. From 1962 to 1964, he was, in addition, a teaching assistant to Professor Harold Freeman in the Department of Economics at the Massachusetts Institute of Technology.

He is a member of Sigma Xi and Tau Beta Pi, and is a student member of the American Society of Metals and the Metallurgical Society of the AIME.

Professor John F. Elliott and the author are co-authors of two technical notes which are to be published in the Transactions of the Metallurgical Society of the AIME. The first note concerns "The Relationship between the Interaction Coefficients ϵ and e ," and the second "Free Energy, Entropy and Enthalpy Interaction Coefficients."

